
**Numerical modelling of the migration direction
of offshore sand waves using Delft3D**
Including underlying seabed topography



Sjoerd Leenders

Delft University of Technology



The work in this thesis was supported by Deltares. Their cooperation is hereby gratefully acknowledged.



Copyright © department Hydraulic Engineering
All rights reserved.

Numerical modelling of the migration direction of
offshore sand waves using Delft3D
Including underlying seabed topography

a Master thesis

by
Sjoerd Leenders

in partial fulfilment of the requirements for the degree of

Master of Science
in Civil Engineering

at the Delft University of Technology

to be defended publicly on Tuesday June 26th, 2018 at 11:00 AM (UTC+01:00),
in Lecture Hall G of the faculty of Civil Engineering & Geosciences of the TU Delft.

Graduation Committee

Prof.dr.ir. S.G.J. Aarninkhof	Delft University of Technology
Dr.ir. M. Zijlema	Delft University of Technology
Dr.ir. D.J.R. Walstra	Delft University of Technology / Deltares
Ir. J.J. Schouten	Deltares
Ir. R. Hoekstra	Deltares
Dr.ir. B.W. Borsje	University of Twente

(An electronic version of this thesis is available at <http://repository.tudelft.nl/>)

Preface

With this thesis report, I conclude my Master of Science in Hydraulic Engineering at the faculty of Civil Engineering and Geosciences of the Technical University Delft.

I want to thank my graduation committee for their knowledge and guidance throughout my thesis. Special thanks to Jan-Joost Schouten, Roderik Hoekstra and Bas Borsje. Jan-Joost and Roderik from Deltares, who always had time to give advise on how to approach my thesis work, and always had a positive and enthusiastic attitude, which reflected on my motivation for the project. Bas, despite the distance between Enschede and Delft, the countless hours calling explaining all there is to known about sand waves, really helped me with the more theoretical aspects regarding my thesis work.

This thesis was conducted at the research institute Deltares, which was a great place to graduate. Employees and fellow student always had an open and helpful attitude towards each other, which made it a very good learning environment. Specialists on all kind of subjects related to my thesis helped to make the thesis a success. To this matter, I want to thank Tom Roetert and Erik de Goede. Tom, your knowledge on data-driven analysis really helped understanding the practical side of sand wave research. To cope with the *Domain Decomposition* model technique difficulties, Erik always made time to guide me in the right direction.

Finally I want to thank my friends and family. The support and good times really helped me to keep motivated during my study and final thesis. Thank you!

Sjoerd Leenders
Delft, June 2018

Summary

Introduction The growth of the offshore wind industry results in intensive usage of the sandy seabed in the North Sea, currently and in the coming decades. Large-scale bed forms are present in shallow seas with sandy beds such as the North Sea. The most dynamic bed forms are sand waves. Due to their dynamic behaviour, sand waves can interact within offshore human developments and together with their dimensions pose a threat; e.g. decrease in navigation depth, exposure of submarine cables, interaction with foundations of offshore wind turbines and destabilization of bed protections. A thorough understanding of the dynamics can result in less risks for the offshore wind sector and therefore bring down the levelized cost of electricity from offshore wind.

Currently, sand wave field dynamics are investigated by data-driven analyses. These analyses are based on seabed surveys over preferable more than 10 years and are considered most reliable at the moment. However, these surveys are very costly and/or often not available. Complex numerical models may provide an approach to analyse sand wave dynamics in a cost and time efficient way, though two aspects have to be considered. Not all relevant processes regarding sand wave dynamics are yet understood. Furthermore, due to the large scale of sand wave fields in combination with the fine grid resolution required to model sand waves, large computational efforts form a difficulty for numerical modelling of sand wave fields. Previous numerical studies focused on reproducing the length and height of sand waves. The migration direction is the next step towards the full prediction of sand wave fields and the subject of this research.

Objective Recent data-driven analyses showed migration directions of sand waves in opposite direction over small spatial scale, possibly related to underlying seabed topography. Understanding the governing processes of the migration direction of sand waves including underlying seabed topography is the focus of this research using the numerical process-based model Delft3D.

In part I idealized models are used to investigate the migration direction of sand waves. In Fig. S.1, an overview is presented of the migration directions of the idealized model cases considered in this thesis, and discussed below. Case 1, 2 and 3 are based on existing literature to look into migration over horizontal underlying seabed topography. The main focus of the thesis is represented by case 4,5 and 6, including underlying seabed topography represented by a tidal sand bank in the model. Part II, investigates the migration of sand waves in a more realistic model of the North Sea.

Part I

Before including underlying seabed topography, an existing 2DV model (Borsje et al., 2014) is used to show the capability of the process-based model Delft3D to reproduce the hydrodynamic and morphodynamic processes responsible for the existence of sand waves. Known migration situations from literature showed two important migration phenomena of sand waves over horizontal underlying seabed topography. Adding a residual current on top of a symmetrical tidal forcing showed sand wave migration in the direction of the residual current (Case 2). Sand wave migration in the direction of the asymmetrical tidal forcing is observed when adding an extra tidal constituent with a certain phase shift (Case 3).

Underlying seabed topography: Tidal sand bank To investigate the effect of underlying seabed topography on the migration direction of sand waves, the 2DV idealized model was extended to 3D. The bed form considered is the tidal sand bank, and mimicked as a tidal sand bank of infinite extent (Roos & Hulscher, 2003). Infinite far horizontal boundaries and the inclusion of the Coriolis effect were essential for the correct implementation of the tidal sand bank. To investigate the influence of the tidal sand bank solely, the model was first tested with symmetrical tidal boundary conditions. The recirculating cells of the sand waves are disturbed towards the top

of the tidal sand bank due to the tide-averaged flow caused by the presence of the tidal sand bank. Migration of sand waves on both flanks of the tidal sand bank towards the top of the tidal sand bank is observed. Increasing the height of the tidal sand bank, from 2 to 10 meters, resulted in an order higher migration magnitude. Decreasing the sediment grain size from $350 \mu\text{m}$ to $200 \mu\text{m}$ doubled the migration magnitude. In all cases migration towards the top is observed (Case 4).

Adding a residual current disturbed the horizontal tide-averaged flow pattern around the tidal sand bank, in the direction of the residual current. On the scale of sand waves, the tide-averaged flow on both flanks of the tidal sand bank is in the direction of the residual current. Sand wave migration on both flanks in the direction of the residual current is the result. The migration magnitude is larger compared with the symmetrical case, on the flank with an orientation towards the top similar as the direction of the residual current (Case 5).

In the case of including the S_4 -tide constituent, the tide-averaged flow pattern around the tidal sand bank is not altered. However, the migration direction is influenced by the asymmetrical tidal velocity signal. Due to the asymmetry, the horizontal tidal velocities in one direction are larger. The nonlinear relation between the flow velocity and the sediment transport enhances the sediment transports in that direction. On the flank of the tidal sand bank with the direction towards the top similar as the direction of the enlarged velocity, the migration of sand waves is larger compared with the symmetrical case. The migration magnitude is lower compared with the symmetrical case, but still towards the top, for the sand wave on the flank for which the larger horizontal velocity is in the opposite direction as the direction towards the top of the tidal sand bank (Case 6).

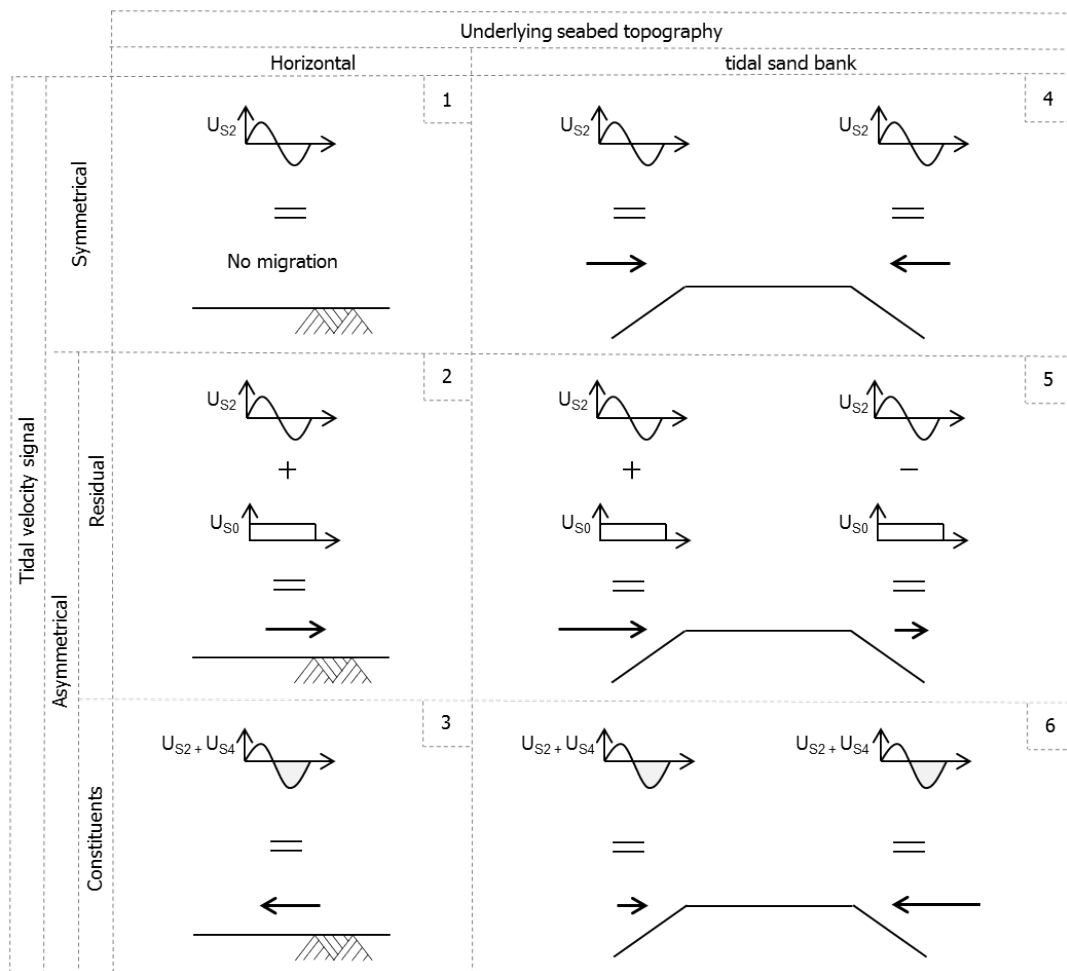


Figure S.1.: schematized migration direction idealized models

Part II

Comparing idealized with field case Data-driven analyses of bed surveys from Borssele Wind Farm Zone (hereafter: BWFZ), indicated a transition in migration direction over tidal sand banks. In the final part of this thesis it was investigated if this transition can be obtained in a more realistic model of BWFZ. The tidal sand bank presented in Fig. S.2a is observed.

In general the interaction between the flood flow, ebb flow and the tidal sand bank result in tide-averaged flow velocities in the direction of ebb flow. Based on the idealized model, migration in the direction of the residual flow is expected. However apart from the tide-averaged flow velocities in the ebb direction, the tidal velocity signal is asymmetrical in the flood direction. Together with the presence of the tidal sand bank, this results in areas in which the ebb flow is dominantly present and areas in which the flood flow is dominantly present. Areas with a dominant ebb flow show tide-averaged sediment transports in the ebb direction, indicating migration towards the South-West. In areas for which the flood flow is dominantly present, tide-averaged sediment transports are directed in the flood direction. This indicates migration towards the North-East (fig. S.2b). The migration directions from the model results and migration direction from data show a comparable transition over the tidal sand bank.

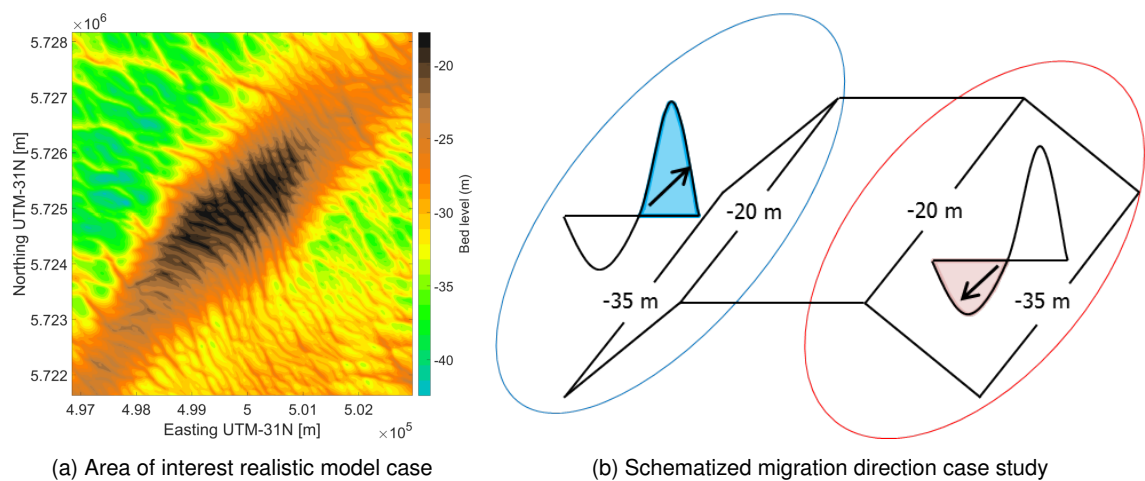


Figure S.2.

Concluding, the transition of the indicative migration direction of offshore sand waves from the model results can be linked to the presence of the tidal sand bank in the domain as seen for the idealized model including underlying seabed topography. The presence of the tidal sand bank influences the hydrodynamics during ebb and flood flow. This results in areas in which the tide-averaged sediment transport in the ebb direction are enhanced and areas in which the tide-averaged sediment transports in the flood direction are enhanced. In this way a transition in the migration direction over the tidal sand bank is observed.

The idealized model including underlying tidal sand bank provided insight in the possibility of a transition in the migration direction over the tidal sand bank. The step towards a more realistic model, showed that also here the transition is observed. However, the more complex configuration of the underlying seabed topography results in three dimensional hydrodynamic processes. To determine the migration direction at a certain location, it is recommended to look at the longer term migration direction. For this matter alternative modelling techniques, like Delft3D Flexible Mesh, might be necessary to limit the computational effort. Furthermore a post-processing technique similar to the data-driven analyses is required to make an accurate comparison between the migration direction from model results and the migration direction from data-driven analyses.

Contents

Preface	5
Summary	7
1. Introduction	13
1.1. Introduction	13
1.2. Problem definition	14
1.3. Research objectives and questions	15
1.4. Research approach	15
1.4.1. Idealized modelling	15
1.4.2. Case study Borssele	15
1.5. Research structure	16
2. Literature study	17
2.1. Processes governing sand waves	17
2.1.1. Tide	17
2.1.2. Residual current	18
2.1.3. Sediment transport	19
2.1.4. Surface gravity waves	20
2.1.5. Underlying seabed topography	20
2.2. Modelling sand waves	21
2.2.1. Data analyses	21
2.2.2. Stability analyses	21
2.2.3. Complex Numerical models	22
2.2.4. Comparison data analyses and modelling sand waves	23
2.3. Parameter study	23
3. Idealized model: Horizontal underlying seabed topography	25
3.1. Introduction	25
3.2. Methods	25
3.2.1. Model description	25
3.2.2. Model setup	25
3.2.3. Fast-Fourier transformation	27
3.3. Results	27
3.3.1. Hydrodynamic processes	27
3.3.2. Sediment transports	28
3.3.3. Migration direction	30
4. Idealized model: Tidal sand bank as underlying seabed topography	31
4.1. Introduction	31
4.2. Methods	31
4.2.1. Model modification	31
4.2.2. Model set-up	33
4.2.3. Fast-Fourier Transform	33

4.3. Results	34
4.3.1. Symmetrical boundary conditions	34
4.3.2. Residual current	38
4.3.3. Higher order tidal constituent	40
5. Case study Borssele	43
5.1. Introduction	43
5.2. Methods	43
5.2.1. Model description	43
5.2.2. Model modification	44
5.2.3. Model set-up	44
5.2.4. Migration direction derived from model results	46
5.2.5. Migration direction derived from data-driven analyses	46
5.3. Results	48
5.3.1. Model modification	48
5.3.2. Hydrodynamic processes	49
5.3.3. Sediment transports	50
5.3.4. Migration direction	51
6. Discussion	53
6.1. Assumptions and inaccuracy idealized model including underlying seabed topography	53
6.2. The step from idealized modelling to a field case	54
6.3. The domain decomposition model as engineering tool	56
7. Conclusions	57
7.1. Migration direction over horizontal underlying seabed topography	57
7.2. Migration direction over underlying seabed topography	57
7.3. Borssele migration direction	58
8. Recommendations	59
8.1. Idealized model underlying seabed topography	59
8.2. Modelling sand wave migration direction in practice	59
8.3. Future Research	60
References	61
Appendices	64
A. Grid study tidal sand bank	65
B. Hydrodynamics Case I,II,III and IV	67
B.1. Case I	67
B.2. Case II	68
B.3. Case III	69
B.4. Case IV	70
C. Discussion Domain Decomposition	71
D. Results other locations	75
E. Domain decomposition model as engineering tool	85

1 | Introduction

In this research the migration direction of offshore sand waves is investigated in idealized and realistic numerical models. This chapter starts with an introduction on sand wave research and the current state of modelling sand waves. This resulted in the problem definition followed by the research objectives and research questions. Finally the approach to accomplish the objectives is described and visually presented.

1.1. Introduction

Rhythmic large-scale bed forms are present in shallow seas with sandy beds. Depending on the length, height, propagation speed and formation timescale a spatial and temporal distinction can be made between these large-scale rhythmic forms.

On the largest scale, tidal sandbanks have a wavelength in the order of 5-10 km and can have heights up to half of the local water depth (Hulscher, 1996). Tidal sandbanks are nearly static and with reference to the principal tidal current their orientation is rotated 10-30 degrees anticlockwise (in the northern hemisphere) (Hulscher, 1996). Sand waves represent the subsequent scale with lengths in the order of hundreds of meters (Besio et al., 2008), and heights up to 20% of the water depth (Knaapen et al., 2001). The orientation of sand waves is almost perpendicular to the main tidal direction (Besio et al., 2008) and can migrate in the order of tens of meters per year (Blondeaux & Vittori, 2016a). On the smallest scale (mega) sand ripples are present with a wavelength up to 10 m and heights in the order of 0.01-0.1 m. The migration rate of (mega) ripples is in the order of 100 meters per year. An overview is presented in table 1.1.

Bed form	Length [m]	Height [m]	Migration speed	Timescale
(Mega) Ripples	(1-10)	(0.01-0.1)	100 m/year	Days
Sand Waves	(100-1000)	(1-10)	10 m/year	Decades
Tidal sand banks	(5000-10.000)	(10-30)	(0-1) m/year	Centuries

Table 1.1.: Characteristics of offshore sand bed forms Morelissen et al. (2003); Dodd et al. (2003).

Despite the large scale, tidal sand banks are not very relevant for engineering purposes because they are nearly static. Sand ripples have too small heights to pose a threat. Sand waves due to their dynamic behavior can interact with human offshore activities and together with their dimensions are relevant for engineering and research purposes. Sand waves are observed worldwide in shallow sandy seas, an overview is given in Blondeaux and Vittori (2016a). Important to point out is that sand waves are only observed in seas with strong tidal currents (Hulscher, 1996).

The North Sea, in which tidal currents are present, is also a sea with many functions and human activities. The Dutch government set a goal for 16 % renewable energy in 2023 (Netherlands Enterprise Agency, 2015). In the period of 2023-2030 this will further increase to 24%. The share of renewable electricity in 2023 will be about half of the total electricity production and by 2030 about two third of the total electricity will be renewable (Energieonderzoek Centrum Nederland, 2017). This transition towards renewable energy and electricity will mainly be provided by offshore wind energy in the North Sea.

The growth of the offshore wind industry results in intensive usage of the sandy seabed in the North Sea; e.g. foundations of structures in the seabed, seabed protections, submarine cables between windmills and towards main land. Sand waves can interact within these developments and pose a threat. Decrease in navigation depth, exposure of submarine cables, interaction with foundation of mono piles and destabilization of bed protections. A thorough understanding of the dynamics can result in less risks for the offshore wind sector and therefore bring down the levelized cost of electricity from offshore wind.

The investigation of sand waves can be divided into two segments. Data analyses and modelling of sand waves. Data analyses are based on seabed surveys over preferable more than 10 years and are considered most reliable at the moment but costly. During the operation of offshore wind farms additional surveys have to be made to monitor the predicted sand wave dynamics. Modelling sand waves is relevant when limited or no data is available and useful to gain understanding in dependencies on governing processes and parameters of sand waves.

Sand wave modelling started with linear models examining properties and processes relevant to the initial stage of sand waves formation (Hulscher, 1996). Including non-linear effects in models resulted in more knowledge on possible equilibrium shapes of sand wave (van den Berg et al., 2012). Recently complex numerical models including many processes in a sophisticated way are developed to gain more knowledge on sand waves dynamics and the equilibrium of sand waves.

Complex numerical models so far have been used to investigate the general behaviour regarding sand waves by means of studying an artificial sand wave (Tonnon et al., 2007). The formation stage of sand waves is studied regarding the turbulence model used (Borsje et al., 2013) and the inclusion of suspended sediment (Borsje et al., 2014). The equilibrium height has been modelled beginning with a sinusoidal bed with very small amplitude sand waves (Choy, 2015; Van Gerwen, 2016).

The development in the offshore wind industry demands knowledge on sand wave dynamics and the prediction of the morphodynamics of wind farm seabeds. Since the execution of bed surveys is very costly, modelling sand wave field dynamics becomes relevant for the offshore wind industry. The ultimate goal is to predict sand wave field dynamics using complex numerical models.

Complex numerical models may provide a way to look cost and time efficiently at sand wave dynamics, however not all the relevant processes regarding sand wave dynamics are understood. For the determination of sand wave field dynamics during the lifetime of an offshore wind farm the properties height, length, migration rate and the migration direction are important. The sand wave length is studied by Borsje et al. (2014) and the sand wave height by Choy (2015); Van Gerwen (2016) using complex numerical models. The migration direction is the subsequent step towards the full prediction of sand wave fields and the subject of this research.

1.2. Problem definition

The prediction of sand wave fields over the life time of an offshore wind farm (OWF) is relevant with the extensive usage of the North Sea seabed currently and in the future. Complex numerical models may provide an approach to analyse sand wave dynamics in a cost and time efficient way. However sand wave dynamics are not yet fully understood. Numerous linear and non-linear stability models are made and give insight in important processes regarding the initial sand wave behaviour and equilibrium characteristics respectively. More recently complex numerical models allow for including many processes in an advanced way to gain a better understanding regarding sand wave behaviour, dynamics and equilibrium characteristics. With these models progression is made towards predicting sand wave fields fully over a lifetime of OWF's, however this is not yet accomplished. To add a step in determining full sand wave field development the migration direction of sand wave is essential. Understanding the governing processes of the migration direction of sand waves including underlying seabed topography is the focus of this research.

1.3. Research objectives and questions

According to the literature study and problem definition the following objective of this research is defined:

“Understanding the hydro- and morphodynamic processes regarding the migration direction of offshore sand waves including underlying seabed topography using the model Delft3D”

The objective stated above resulted in the research question:

“What are the hydro- and morphodynamic processes determining the migration direction of offshore sand waves including underlying seabed topography?”

This research question is answered by three sub-questions:

- How do the strength, direction and phase shift of different tidal constituents relate to the migration direction of sand waves over a horizontal underlying bottom?
- What is the influence of underlying seabed topography on the migration direction of sand waves?
- How can the migration direction of sand waves observed in Borssele Wind Farm Zone be explained, using the case study of Borssele?

1.4. Research approach

This thesis comprises three parts. The first part includes a literature study to introduce the important processes governing sand waves and state of the art models to investigate sand waves. In addition a parameter study is executed to derive parameter scenarios representative for North Sea areas in which sand waves are observed. The second part contains the modelling of the migration direction of sand waves in idealized models. In the third part a step is made towards a more realistic representation of sand wave migration to verify the findings of part two. Finally a discussion and the conclusions on the entire research are presented.

1.4.1. Idealized modelling

The migration direction is investigated with respect to prominent processes regarding the existence and migration of sand waves; The tide, sediment transport mode and the influence of seabed topography. Since the influence of the tide and sediment is present for both situations with a horizontal underlying bottom and the inclusion of underlying bottom forms, both are tested separately. For the horizontal underlying bottom (chapter 3), an existing model is used (van Gerwen et al., 2018). The horizontal bottom model is extended in the third dimension, since modelling the migration direction required a 3-D approach. Known processes are reproduced to show that the model is capable of reproducing the most important processes governing sand waves in two and three dimensions. Subsequently the model was modified to test the influence of underlying seabed topography in (chapter 4). The bed form influencing the migration direction of sand waves is the tidal sand bank. The tidal sand bank is modelled as a tidal sand bank of infinite extent. Infinite far boundaries in both horizontal directions and the inclusion of the Coriolis effect are characteristic in modelling an infinite long tidal sand bank (Roos & Hulscher, 2003). Again the processes regarding the tide and sediment transport mode are tested with respect to the migration direction of sand waves.

1.4.2. Case study Borssele

The obtained knowledge from the idealized models is used in chapter 5 to compare sand wave migration observed within Borssele Wind Farm Zone in the Netherlands (BWFZ) with sand wave migration computed by a model of the same area. Migration directions of sand waves vary significantly over small spatial scales in BWFZ. These migration directions are derived from the comparison of two data surveys from 2010 and 2015. A model is set-up to test if the found results show the influence of underlying seabed topography on the migration direction of sand waves. The research approach is visually presented in the research structure in section 1.5.

1.5. Research structure

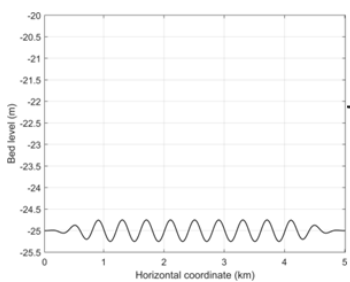
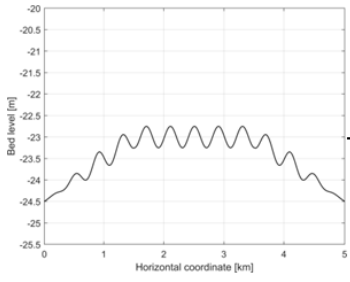
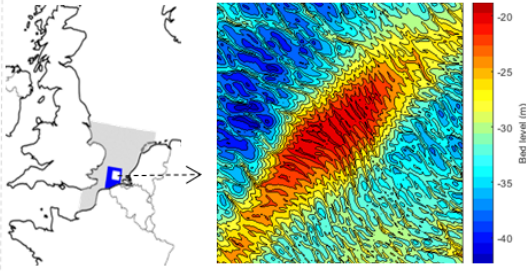
	Chapter	Content	Goal
Part I: Literature study	2	<p>Literature study</p> <ul style="list-style-type: none"> Processes governing sand waves State of the art models sand waves <ul style="list-style-type: none"> North Sea model situations 	<p>Provide theoretical background on processes and modelling of sand waves</p> <p>Derive parameter settings for idealized models based on North Sea data (Borsje et. Al 2009)</p>
	3	<p>Model Delft3D</p> <p>2DV + 3D</p> 	<p>Show model capability of representing relevant processes in 2DV and 3D</p>
Part II: Idealized modelling	4	<p>3D</p> <p>Seabed topography</p> 	<p>Investigate influence of underlying seabed topography on migration direction sand waves</p>
	5	<p>Case study Borssele</p> <p>Domain Decomposition</p> 	<p>Apply gained knowledge part II in realistic model of sand wave field with underlying bed forms and compare with migration data</p>
Part III: North Sea model	6	Discussion	Discuss and conclude on entire research
	7 & 8	Conclusion & recommendations	

Figure 1.1.: Report structure

2 | Literature study

The literature study consists of three parts. First the most important processes regarding the formation of sand waves are discussed. Secondly the investigation on sand wave modelling is presented until the current state of the art models. Finally a parameter study is performed to derive representative North Sea parameters used in the idealized models. In figure 2.1 an overview is given of definitions regarding a sand wave.

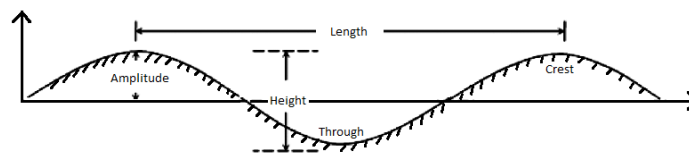


Figure 2.1.: Sand wave properties

2.1. Processes governing sand waves

The tide, residual currents, sediment transport, surface gravity waves and seabed topography are important processes relating to the presence and behaviour of sand waves. In the following subsections the processes are separately discussed.

2.1.1. Tide

Hulscher (1996) explained that the formation of sand waves is governed by the tidal motion in combination with the wavy seabed. Vertical recirculating cells are the result of the interaction of an oscillatory tidal current interacting with a sinusoidal bottom (fig. 2.2). Near the bottom a balance between the residual current generated sediment transport from the trough to the crest and the gravity generated sediment transport from the crest to the trough determines the development of the sand wave. When the net sediment transport is towards the crest a growing sand wave will be the result. Opposite a decay of the sand wave is gained when the net sediment transport is towards the trough.

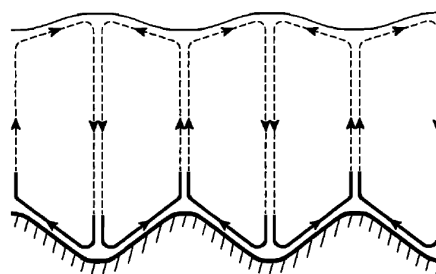


Figure 2.2.: Recirculating cells sand wave formation(Hulscher, 1996)

The recirculating cells can be explained by a residual current caused by the oscillatory tidal motion over the seabed. When looking unidirectional the tidal velocity profile adjusts near the bed when moving over a sand wave. From the flat bottom towards the crest of the sand wave the velocity increases due to a decreasing water depth. A decrease holds for the velocity profile moving from the crest towards the flat bottom, an increasing water depth results in a decreasing velocity near the bottom (fig. 2.3a).

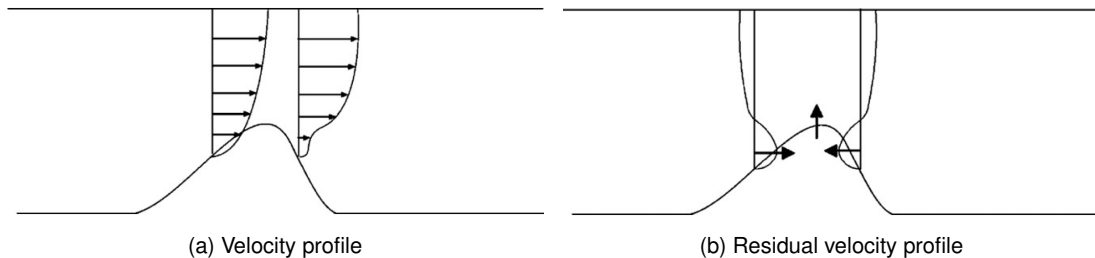


Figure 2.3.: Tidal velocity profiles over sand wave (Tonnon et al., 2007)

Averaged over a tidal cycle a flow in both directions over the sand wave occurs. When looking at the time averaged flow, known as residual flow, both velocity profiles at both sides of the sand wave crest can be added resulting in the residual velocity profile of the tidal motion over a sand wave (fig. 2.3b). This process generates the recirculating cells responsible for the formation stage of a sand wave.

Apart from the formation stage, tidal motion determines the migration of sand waves due to multiple tidal constituents. When only including a M_2 tide constituent the tidal velocity signal is time averaged zero resulting in a static sand wave. Adding a residual current Z_0 induces an asymmetrical tidal velocity signal which is not zero averaged over time. Including a residual tidal current therefore results always in migrating sand waves in the direction of this residual component (e.g. Z_0) (Besio et al., 2003b).

Migration of sand waves is not always in the direction of the residual current, adding a M_2 and M_4 tide constituent together with a residual current Z_0 result in sand waves migrating in the opposite direction compared to the residual current (Besio et al., 2003b, 2004). Important to note is that the upstream migration was observed with a certain phase difference between the M_2 and M_4 tide constituents. For models including a residual current Z_0 and the M_2 and M_4 tide constituent, positive and negative migration of sand wave was observed due to different phase shifts between the constituents. This indicates the importance of the phase difference between tidal constituents. The model with a M_2 and M_4 tide constituent only, without a tidal residual current, shows a time average velocity signal of zero. However migration was observed, this can be explained by a non linear relationship between fluid velocity and sediment transport (Besio et al., 2004).

Besio et al. (2004) further points out that the model presented is a 2DV model in which the tidal constituents used are projected unidirectional along the horizontal axis of the 2DV model. In the related case study in the research this was showed appropriate due to relative small angle differences between the normative tidal constituents. However it is stressed that the influence of transverse tidal constituent can be important. This is the case when there are multiple tidal constituents with significant angles and magnitudes.

There may be more tidal constituents apart from the Z_0 , M_2 and M_4 given a location. Depending on their strength, direction and phase shift they can influence the migration direction of sand waves as described above. As tidal currents are side specific a harmonic analysis should provide the tidal constituents present at a location.

2.1.2. Residual current

In a similar reasoning as for the tidal residual currents, residual currents are related to the migration properties of sand wave behaviour because an asymmetrical horizontal velocity profile is present. Residual currents, driven by the wind or pressure gradients, result in migration of the sand wave in the direction of the residual current (A. A. Németh et al., 2002).

2.1.3. Sediment transport

Sediment transport is caused by bed shear stresses resulting from the flow over the bed particles and can be distinguished in two transport modes, bed load transport and suspended load transport. Above a certain critical bed shear stress for a certain bed configuration bed load is initiated. When the bed shear stresses increases further a second threshold can be exceeded and suspended load transport is present. The transport modes have different effects on the behaviour of sand waves. Both are discussed in the next paragraphs.

Bed load transport Bed load transport is related to sliding and rolling of sediment particles near the bottom. The tide average recirculating cells explained in section 2.1.1 showed that the near bottom sediment flux towards the crest of the sand wave is responsible for the formation of sand waves. Bed load transport is therefore associated with the growth of sand waves (Hulscher, 1996; Borsje et al., 2014). The sediment flux from the crest towards the trough caused by bed slopes reduces the growth of sand waves by slope-induced bed load transport due to gravity. Bed slope effects are often taken into account in the bed load transport formulas to account for the slope-induced bed load transport (Bagnold, 1956; Walstra et al., 2007).

Suspended load transport Suspended load transport is related to transport of bed particles higher in the water column. According to the recirculating cells related to the tidal motion, suspended load is transported away from the sand wave crest. Borsje et al. (2014) showed the absence of sand waves on the Dutch continental shelf when suspended load transport is the dominant transport mode and studied the influence of suspended load transport on the formation stage of sand waves. The influence of suspended sediment transport is twofold. Including suspended load transport result in longer sand waves for relatively large grain sizes, for relative small grain sizes no sand wave growth is observed. Furthermore including suspended load transport resulted in a finite wave length and suppression of very long sand waves. The suppression of very long sand waves resulted in a finite range of sand wave lengths which experienced growth. Depending on flow velocity and grain size critical conditions were found for the existence of sand waves. According to the findings of Borsje et al. (2014), three dominant sediment transport mechanisms determine the formation process of sand waves (fig. 2.4). The net damping effect is caused by suspended transport and slope-induced transport. The growing net effect is causing by bed load transport. The interplay of the three mechanisms determine the existence and the dimensions of sand wave formation. van Gerwen et al. (2018) studied the influence of suspended sediment on the equilibrium height of sand waves. Identical as for the formation stage a dampening effect is caused by inclusion of suspended sediment load.

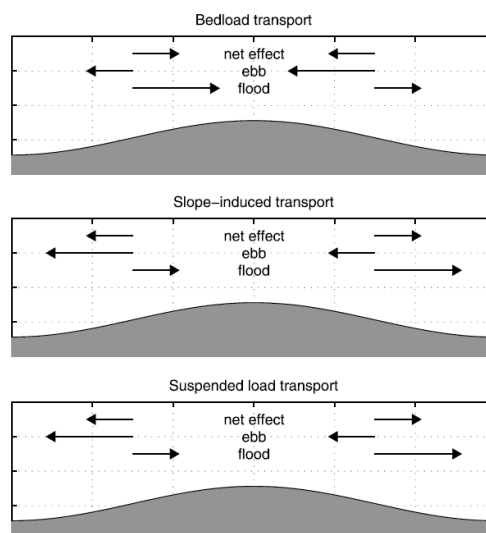


Figure 2.4.: Schematic overview dominant processes in sand wave formation (fluxes and sand wave dimensions not to scale)(Borsje et al., 2014)

2.1.4. Surface gravity waves

Surface gravity waves are generated by the friction opposed by the wind on the free surface of the ocean. In general the effect of surface waves have larger effects when the water depth is smaller and have a reducing effect on the crest height of sand waves (Tonnon et al., 2007). This can be explained by the fact that waves stir up sediment and increase the suspended load transport. The sediment in suspension is transported away from the crest by the recirculating cells.

Sterlini-van der Meer (2009) showed that surface gravity waves can influence the shape and migration of sand waves. In general a decreased sand wave height and a migration in the direction of the surface gravity waves are observed. The shape adjusts to a broader crest, milder slopes and smaller trough. The lowering of the crest height due to larger surface waves is higher compared with smaller waves. However due to the low frequency of occurring of large waves, smaller more frequent waves are more important.

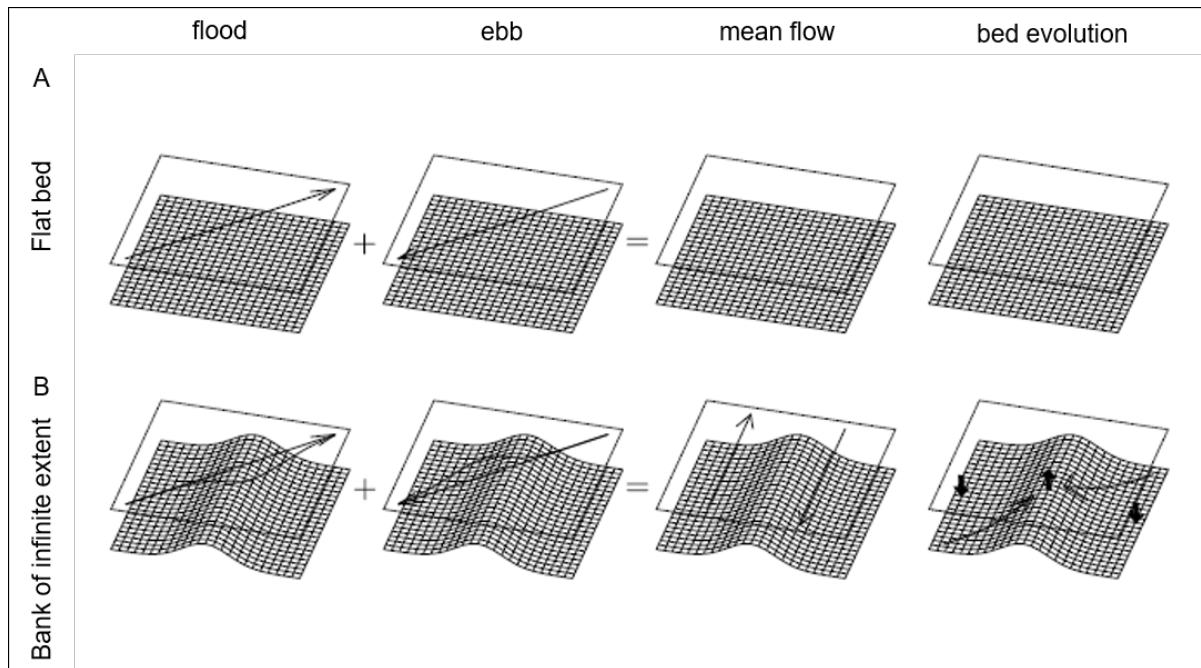


Figure 2.5.: Hydrodynamics and sediment transports around tidal sand bank of infinite extent (Roos & Hulscher, 2003)

2.1.5. Underlying seabed topography

A close relation between bottom current characteristics and seabed topography is shown by Wen-Bin and Mian (2011); Wen-Bin et al. (2014) for short sand waves in the northern part of the South China Sea. The bilateral reverse migration of sand waves in a field was predicted, meaning that sand wave migrated in other directions at opposite sides of a sand ridge. The seabed topography was considered as an crucial aspect to take into account next to temperature, salinity and the tide. Although the research of Wen-Bin et al. (2014) is on short sand waves, it indicates the influence of underlying bed forms on the bottom currents and thereby migration of bed forms.

As tidal sand banks are present under sand wave fields in the North Sea, an influence on the migration direction of sand waves might be present. Figure 2.5 show the flow alteration by the presence of a tidal sand bank of infinite extent (Roos & Hulscher, 2003). A symmetrical tidal signal over a flat bottom is shown as reference and result in a mean flow of zero (fig. 2.5 a). Tide averaged flow parallel to the flanks of the tidal sand bank is generated due to the presence of the tidal sand bank (fig. 2.5 b). This can be explained by three deflection mechanism of the flow. First, continuity result in acceleration of the cross-bank component. A decreased water depth additionally result in increased friction and deceleration of the along-bank component. Lastly the Coriolis effect increases flow to the right (On the Northern Hemisphere). The flow alteration result in sediment transport towards the top of the tidal sand bank and bed evolution as shown in the last column of Fig. 2.5 b.

2.2. Modelling sand waves

Two types of investigation regarding sand waves can be distinguished; data analyses and sand wave modelling. Data analyses of sand wave fields are currently the most used tool to predict seabed morphodynamics and therefore discussed in subsection 2.2.1. Subsequently the two model techniques, stability analyses and complex numerical models, are discussed in subsection 2.2.2 and 2.2.3. Subsection 2.2.4 gives a comparison between data analyses and the different model techniques and conclude on the relevance regarding this research.

2.2.1. Data analyses

Currently the most important technique to investigate sand wave dynamics is by means of morphodynamic analyses based on data from seabed surveys. These type of analyses are suitable when seabed surveys are available over a long period of time and are considered most reliable at the moment. Several studies within Deltares have focussed on the prediction of seabed morphodynamics during the lifetime of offshore wind farm zones (Deltares, 2008, 2015a, 2016b). Data of seabed surveys are used to predict wave lengths, wave heights, migration rates and migration directions. Fourier analyses are applied to determine the spatial characteristics such as height and length of the sand waves. Transects are analysed for the migration speed of sand waves and a cross correlation technique for the migration direction. Based on these morphodynamic analyses a best estimate bathymetry, a lowest seabed level and a highest seabed level are determined for the duration of the lifetime of an offshore wind farm zone. After the prediction of sand wave fields based on surveys also surveys are required when wind farms are in operation because a uncertainty exist in the prediction obtained by the analyses. The data analyses are considered most reliable at the moment, but not cost and time efficient. The execution of offshore bed surveys is very expensive, and the time period of the bed surveys prior to wind farm operation preferably over 10 to 15 years. During operation of wind farms, which is about 20-25 years, maintenance surveys are required with a return period in the order of years.

2.2.2. Stability analyses

The first group of models on sand waves are stability analyses. Stability analyses are often used for the prediction and understanding of rhythmic morphological features. They consider separate phenomena or features of bed forms using simplified geometry and model conditions (Dodd et al., 2003). Distinction is made between linear and non-linear stability analyses, looking at the initial formation stage and at the long term equilibrium profile respectively.

Linear stability analyses

Linear stability analyses assume initially small perturbations on a flat bottom to allow for a linear approach. The spatial components develop independent in time and the perturbation with the largest growth rate will provide the fastest growing mode which will prevail. Due to the small perturbation assumption, linear models are only suitable for the initial formation stage of sand waves and provide a specific wave length, an orientation and a migration speed of the fastest growing mode (Besio et al., 2008).

The first model of a shallow sea in which a dynamically coupled system describes tidal sand banks was made by (Huthnance, 1982). Regarding the hydrodynamics, depth-integrated shallow water equations were used. Conservation of sediment and a bed load transport parameterization defined the morphological processes. The wave length and orientation of the fastest growing mode showed a comparison with observations for sand banks. This model has been extended by several authors (see Hulscher (1996) for overview). The main short coming of these models was that only tidal sand bank could be predicted. In a three-dimensional shallow water model by Hulscher (1996) the occurrence of sand waves was described for the first time. The model of Huthnance (1982) was depth-average and thereby not able to describe the origin of sand waves, which is a steady circulation cell in the vertical direction caused by the bottom waviness. The model used a constant eddy viscosity and partial slip condition at the bottom to describe the turbulent stresses by the tidal currents. By assuming a height- and flow- dependent model for the eddy viscosity, (Komarova & Hulscher, 2000) extended the model. Gerkema (2000) and Besio et al. (2003a) further adjust the model by looking at the hydrodynamic solution method.

The model of [Hulscher \(1996\)](#) used a symmetrical tide resulting in static sand waves. Keeping the constant eddy viscosity and no slip condition at the bed the migration of sand waves was analyzed by [A. A. Németh et al. \(2002\)](#) and [Besio et al. \(2004\)](#), including a residual current and asymmetrical tide respectively.

The constant vertical eddy viscosity and partial slip condition were changed by a depth dependent eddy viscosity and a no slip condition at the bed by [Blondeaux and Vittori \(2005a, 2005b\)](#) and ([Besio et al., 2006](#)), both bed and suspended load transport were included in the model. Based on the model of [Besio et al. \(2006\)](#) [Cherlet et al. \(2007\)](#) showed that the model could predict sand wave length at different location on the Belgian Continental Shelf. [Van Oyen and Blondeaux \(2009a, 2009b\)](#) improved the morphodynamic module of the model by including an in homogeneous bed sediment configuration. Additional linear stability analysis studies considered the influence of biota ([Borsje et al., 2009](#)), non-erodible layers ([Blondeaux et al., 2016b](#)) and storms ([Campmans et al., 2017](#)).

Non-linear stability analyses

All the previous described linear stability analyses focus only on the formation stage of sand wave required by the small amplitude assumption. When sand waves grow further from the initial stage non-linear effects becomes important and non-linear stability analyses are necessary.

In non-linear stability analyses numerical approaches of idealized models are used to determine the equilibrium profile of sand waves ([Blondeaux & Vittori, 2016a](#)). The first non-linear model was made by [A. Németh et al. \(2006\)](#), which was adapted by [Sterlini-van der Meer \(2009\)](#). The most recent non-linear model by [van den Berg et al. \(2012\)](#) was based on the model of [A. Németh et al. \(2006\)](#) and is able to model sand waves from initial small bed perturbations up to their full grown shape in short time duration (order minutes to tens of minutes). The model used a constant eddy viscosity and partial slip condition at the bed. The domain length was 440 m, equal to one wave length. An equilibrium height of 22 m was found which was extremely large compared to the water depth of 30 m. Furthermore running the model for a long period resulted in one long wave over the domain because the model is not able to suppress very long wave length formation.

2.2.3. Complex Numerical models

The second group of models are complex numerical models. Complex numerical modelling allows including a lot of relevant processes in an advanced approach. A related point to consider is that due to high spatial and temporal resolution required, modelling sand waves demand large computational effort ([Borsje et al., 2013](#)).

An artificial sand wave was modelled by [Tonnon et al. \(2007\)](#) using Delft3D to study the behaviour of tidal sand waves and effects of tides, waves, sediment size, bed roughness and turbulence model. Another sand wave behaviour study in Delft3D was executed by [Matthieu and Raaijmakers \(2012\)](#), who looked at the interaction between migrating sand waves and offshore pipelines.

The first to model the formation stage of sand waves using Delft3D was the model by [Borsje et al. \(2013\)](#). Using a spatially and temporal varying model for the vertical eddy viscosity (k-epsilon model) they successfully reproduced the formation stage. A subsequent model showed that the in cooperation of suspended sediment load suppressed long sand waves which was a short coming of the model by [van den Berg et al. \(2012\)](#) ([Borsje et al., 2014](#)). Besides the behaviour of sand wave and the initial formation stage [Choy \(2015\)](#) and [van Gerwen et al. \(2018\)](#) looked into using complex numerical modelling to predict the equilibrium of sand wave with respect to the height. [van Gerwen et al. \(2018\)](#) showed that suspended load transport and tidal asymmetry both had a significant damping effect on the equilibrium wave height of sand waves and found equilibrium heights in the same range of field observations.

bed configuration

In complex numerical models discussed above an initial sand wave is assumed in the model. This initial bed configuration is based on the assumption that sand waves are self organizational phenomenon under a certain forcing with a prevailing characteristic length scale known as the fastest growing mode. To show the legitimacy of this assumption this is modeled starting with an unique randomized initial bathymetry instead of an assumed initial bed configuration ([Matthieu et al., 2013](#)). It is shown that the fastest growing mode emerges from the initial randomized bottom by a consolidating process. Very short and long wave lengths are dampened out over time leaving the fastest growing mode in the model. Depended on the initial deviation from the fastest growing mode and the randomized bathymetry the timescale is up to 80 years. Because of the long computational time

to model this phenomena this self organizational property is mimicked by running models with the same forcing but many different initial sand wave lengths. Models for varying wave lengths and a equal sand wave height, water depth and tidal velocity show after one tidal cycle a certain growth rate. The wave length with the largest growth rate after one tidal cycle is assumed the fastest growing mode. This method show good comparison with field measurements and the randomized initial bed method described above (Borsje et al., 2014).

2.2.4. Comparison data analyses and modelling sand waves

The first technique to investigate sand waves are data analyses. Data analyses provide an engineering tool to predict and monitor seabed morphodynamics and is currently the most used because it is the most reliable technique. Little knowledge however is gained about the processes governing sand wave dynamics with these analysis in academic research sense. Furthermore as mentioned seabed surveys are expensive to execute.

Research on sand waves started by modelling sand waves using stability analyses. Stability analyses consider isolated processes under the influence of idealized forcing and geometries referred to as idealized models. Long term modelling without large computational times can provide knowledge into processes governing the initial and long term sand wave behaviour by linear and non linear stability models respectively.

The other kind of modelling is that of complex numerical modelling. These models are based on the physical equations of conservation of mass and momentum, and include many of the important processes in coastal seas such as: waves, currents, sediment transport, bed level changes and the dynamic coupling between the bottom and the water motion (Dodd et al., 2003). Research with these kind of models focusses on the understanding of sand wave formation and behaviour including relevant processes in an advanced approach.

Numerical modelling may provide an engineering tool when all processes regarding sand wave dynamics can be modelled. However not all processes are fully understood to model sand wave field dynamics for engineering purposes. Wave height, wave length, migration direction and migration rate are necessary to understand when modelling seabed morphodynamics for offshore wind farms. So far mainly 2DV models have been used in complex numerical modelling because a requirement of high spatial and temporal resolution demands large computational efforts.

2.3. Parameter study

Prior to the idealized models, parameter ranges are derived from field data to set up these models. The domain considered is the entire Dutch part of the North Sea where sand waves are present. The offshore wind farm Borssele is located in the Dutch part of the North Sea, therefore the data used represent the case study performed in this research. Water depth, seabed topography, sediment grain size and tidal velocity are parameters relevant to set up the idealized models. The data source used to determine the parameter ranges is the study by Borsje et al. (2009), which gives parameter ranges for the entire Dutch Continental Shelf.

A distinction between area's with sand waves, sand banks and sand waves and sand banks together is made in the data study by Borsje et al. (2009). Sand waves are the subject of this research, therefore area's containing sand waves and area's containing sand waves and sand banks together are considered. Area's containing solely sand banks are left out of consideration. The Dutch part of the North Sea covers an area of about 57.000 [km²] (fig. 2.6 (left)). The data is collected using a grid with a resolution of 2*2 [km²] giving parameter information for almost 15.000 grid cells for the Dutch part of the North Sea (Borsje et al., 2009).

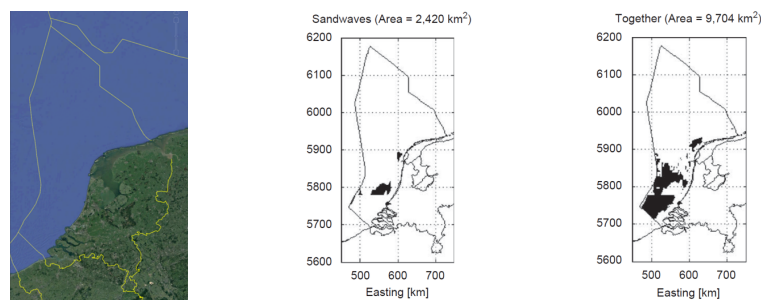


Figure 2.6.: Dutch Shelf (left), location sand waves North Sea (middle) and location sand waves and sand banks together North Sea (right) (Borsje et al., 2009)

Sand waves are not present everywhere on the Dutch Continental Shelf. In Fig. 2.6 the locations of sand waves (middle) and the location of sand waves together with sand banks (right) are shown. In Fig. 2.7 the parameter ranges are presented. Note that the category banks, which represents tidal sand banks, is not relevant as explained at the beginning of the section.

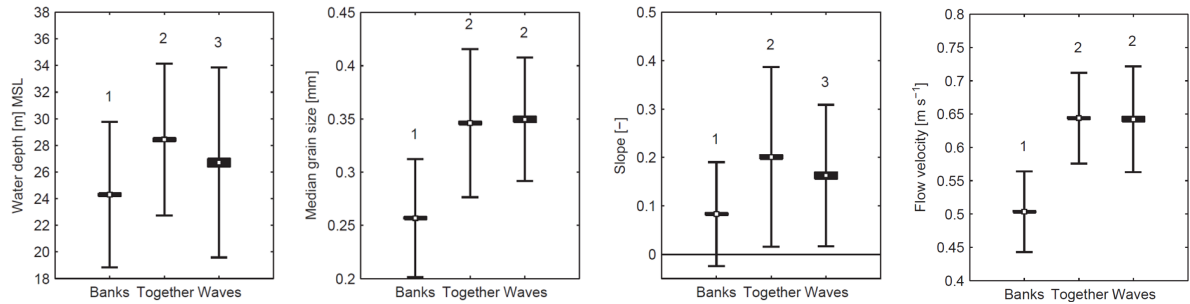


Figure 2.7.: Physical parameters sand waves in the Dutch part of the North Sea (Borsje et al., 2009)

For the idealized model the mean values in table 2.1 present the values used for the parameters to set up the idealized model. The values are based on the parameter histograms derived in (Borsje et al., 2009) shown in Fig. 2.8 which represent the parameter ranges in Fig. 2.7. The parameter configuration is representative for the occurrence of sand waves over the whole Dutch Continental Shelf and thus also for the Borssele Wind Farm Zone. When the model is set up other scenarios are presented to test the migration direction of sand waves.

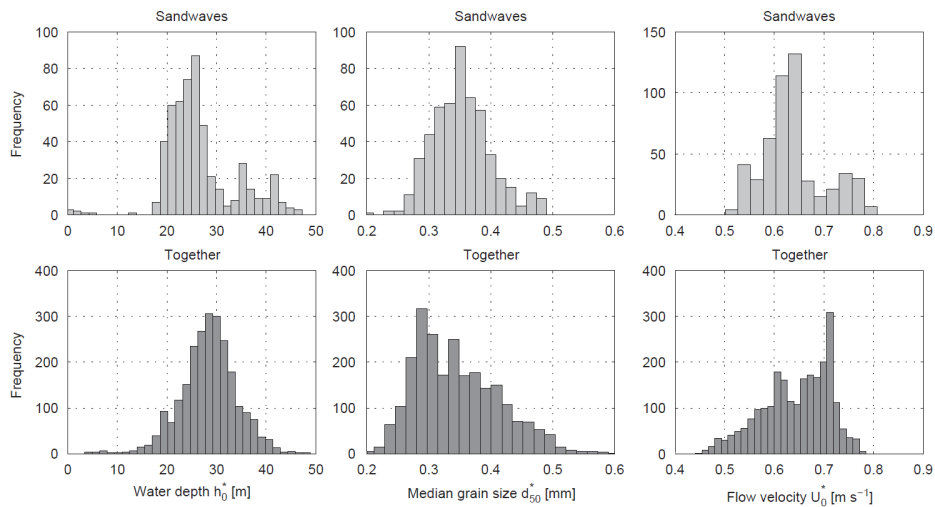


Figure 2.8.: Histograms plots for water depth, median grain size and flow velocity (Borsje et al., 2009).

Parameter	Parameter ranges		
	Mean	Min	Max
Water depth (m)	25	20	40
Median grain size (mm)	0.35	0.2	0.5
Flow velocity (m s^{-1})	0.65	0.5	0.8

Table 2.1.: Parameter settings used to set up idealized model

3 | Idealized model: Horizontal underlying seabed topography

3.1. Introduction

In this chapter the idealized model equations and the setup of the idealized model with a horizontal underlying seabed topography are described. In addition the Fast-Fourier Transform is presented, being the method to derive the migration direction from the model results. The model is tested in two dimensions and three dimensions. When the idealized model represent the hydrodynamic and morphological processes correctly, the model can be extended to investigate the influence of underlying seabed topography on the migration direction of sand waves.

3.2. Methods

3.2.1. Model description

3.2.1.1. Hydrodynamics

The process based model Delft3D is used for the idealized model (Lesser et al., 2004). The system of equations include the horizontal momentum equations, the continuity equation, the transport equation, and a turbulence closure model. The vertical momentum equation is reduced to the hydrostatic pressure relation as vertical accelerations are assumed to be small compared to gravitational acceleration and are not taken into account. For more detail the reader is referred to the Delft3D-FLOW manual (Deltares, 2017).

3.2.1.2. Sediment transport and morphology

Bed load transport is calculated by Van Rijn et al. (2004) with the correction parameter for slope effects according to Sekine and Parker (1992). Suspended load transport is taken into account in the model according to van Rijn (2007). The relevant parameters are discussed in the model setup.

3.2.2. Model setup

The first idealized model is the model by (van Gerwen et al., 2018). The model is run in two-dimensional (2DV) mode, including flow and variations in the x and z -direction only. The computational grid has a horizontal dimension of 50.000 m. The horizontal grid size is variable, with a minimal value of 10 m covering 5 km in the center of the computational grid. Outside of the center the horizontal grid size increases exponentially to 1500 m at the lateral boundaries. In the vertical dimension the computational grid consists of 60 σ layers with more refinement at the bed. The initial bed consist of a sinusoidal sand waves with a length of 400 m, equal to the fastest growing mode representative for a North Sea situation including suspended sediment load (Borsje et al., 2014). The initial profile is present in the center 5 km of the model. For the whole domain the underlying bed form consists of a flat bed. An envelope function is applied for a gradual increase of the wave height from the flat bed towards the center of the model domain (fig. 3.1). The height of the initial sand waves is 0.5 m. At the lateral boundaries Riemann boundaries are applied (Verboom & Slob, 1984). With these boundaries incoming waves are not reflected at the lateral boundaries, in this way the recirculating cells are not disturbed. The hydrodynamic time step is set to 12 seconds. The water depth is 25 m. For the boundary condition, the

model is forced with a semi-diurnal S_2 tidal signal. A tidal velocity amplitude of $U_{S_2} = 0.65$ m/s and a tidal period of 12 hours. The tidal velocity amplitude represents a typical North Sea situation, in which the M_2 -tide constituent is dominant. However, a tidal period of 12 hours according to the S_2 -tide constituent is chosen for post processing of the idealized model results.

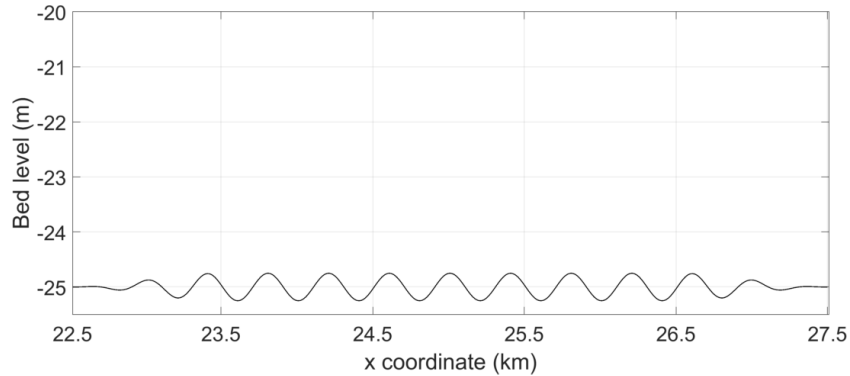


Figure 3.1.: Initial bed profile

The model is run for two tidal cycles. The first tidal cycle is used for spin-up and the second for morphological development. The bed slope correction parameter α_{bs} is set to 3, which corresponds to an angle of response of sand of 19 degrees. The Chézy roughness is $75 \text{ m}^{1/2}/\text{s}^2$. The physical parameters in the setup of the idealized model represent typical North Sea conditions where sand waves are observed (Borsje et al., 2009).

Table 3.1 gives an overview of the parameters used. Furthermore the model conditions of the cases considered are presented. In addition to the symmetrical boundary conditions of case I and II, case III and IV represent asymmetrical boundary conditions. In case III a residual current is added to the S_2 -tide constituent. To test the effect of more tidal constituents, case IV includes the S_4 -tide constituent next to the S_2 -tide constituent.

To investigate the migration direction of sand waves a three-dimensional approach is required. To test if the idealized model represent the recirculating cells, the 2DV model is expanded in the y-direction from 1 computational cell to 10 computation cells with a width of 10 m. Different widths are tested for the behaviour in three-dimensions.

Table 3.1.: Parameter overview

Parameter description	Symbol	Values	Dimension			
Mean water depth	H_0	25	m			
Initial wave amplitude	A_0	0.25	m			
Initial wave length	L_{FGM}	400	m			
Time step	Δt	12	s			
Median grain size	D_{50}	0.35	mm			
Chézy roughness	C	75	$\text{m}^{1/2} \text{s}^{-2}$			
Tidal velocity amplitude	U_{S_2}	0.65	m s^{-1}			
Tidal period	T_{S_2}	12	hours			
Bed slope correction parameter	α_{bs}	3.0	-			
Model conditions		Case I	Case II	Case III	Case IV	
Amplitude of horizontal S_2 tidal velocity	U_{S_2}	0.65	0.65	0.65	0.65	m s^{-1}
Amplitude of residual current	U_{S_0}	0	0	0.05	0	m s^{-1}
Amplitude of horizontal S_4 tidal velocity	U_{S_4}	0	0	0	0.05	m s^{-1}
Phase lag between S_2 and S_4	Φ	0	0	0	120	degrees
Include sediment (Y)es/(N)o	-	N	Y	Y	Y	-

3.2.3. Fast-Fourier transformation

The model updates the bottom in the second tidal cycle of the computation. In this way the amplitude at the beginning of the tidal cycle (A_0) and the amplitude at the end of the tidal cycle (A_1) can be compared. Exponential growth of the sand wave can be assumed for small amplitude waves and for sand wave migration A_1 is a complex value (Besio et al., 2008). Both (A_0) and (A_1) can be determined by a Fast-Fourier Transform¹ and the migration of sand waves is then defined as (Borsje et al., 2013)

$$\gamma_I = \frac{-1}{kT} \text{Im} \left\{ \log \left(\frac{A_1}{A_0} \right) \right\} \quad (3.1)$$

In which k is the topographic wave number $2\pi/L$ and T the tidal period. A distinction in the results is made between positive and negative migration in the x -direction.

3.3. Results

3.3.1. Hydrodynamic processes

The results of the idealized model show the capability of the process based model Delft3D to reproduce the morphological development of sand waves which is governed by the interaction between the sand wave topography and the tidal flow. Case I represents a symmetrical tidal forcing, which results in an equal tidal velocity profile on the sand wave crest during maximum flood and ebb flow (fig. 3.2a). When looking at the tidal flow pass over a sand wave, the flow velocity increases from the trough towards the crest due to a decreasing water depth. Moving over the sand wave the flow velocity decreases due to a increasing water depth. Tide averaged, the velocity profiles at both sides of the sand wave crest are as displayed in Fig. 3.2b. Over a full flood-ebb cycle each side of the sand wave is subject to both the accelerated and decelerated flows. This generates the recirculating cell (fig. 3.2c) responsible for the formation of sand waves.

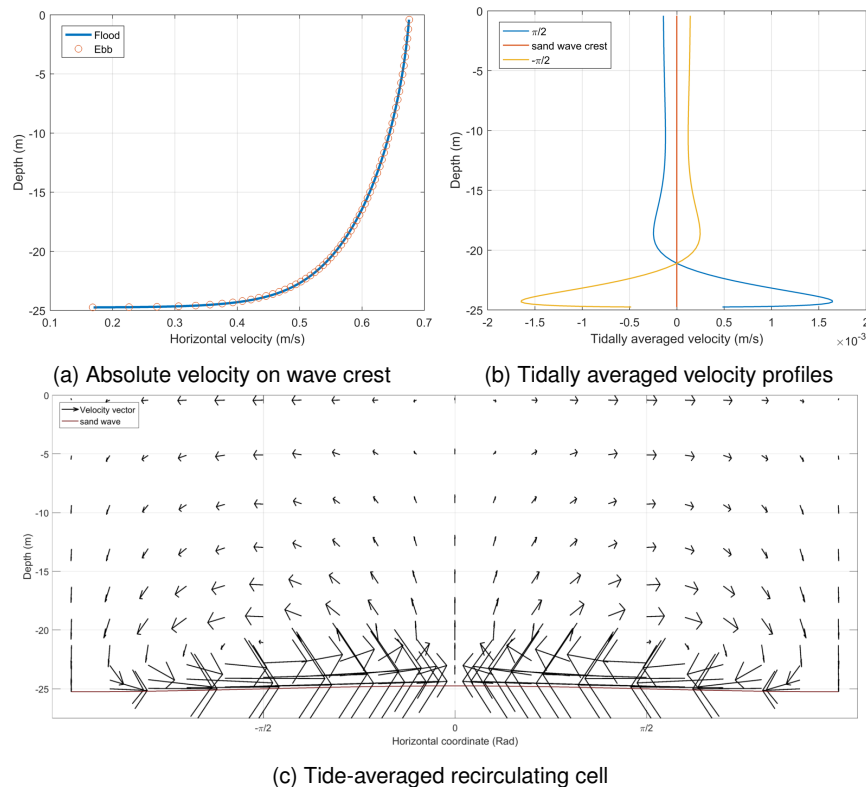


Figure 3.2.: Hydrodynamic processes

¹FFT is a Matlab module which determines the complex amplitude of the sinusoidal wave form

In addition to Case I, models are run with a larger initial sand wave amplitude. The tide-averaged flows and the recirculating cells observed are qualitatively similar but larger in magnitude (figs. 3.3 and 3.4).

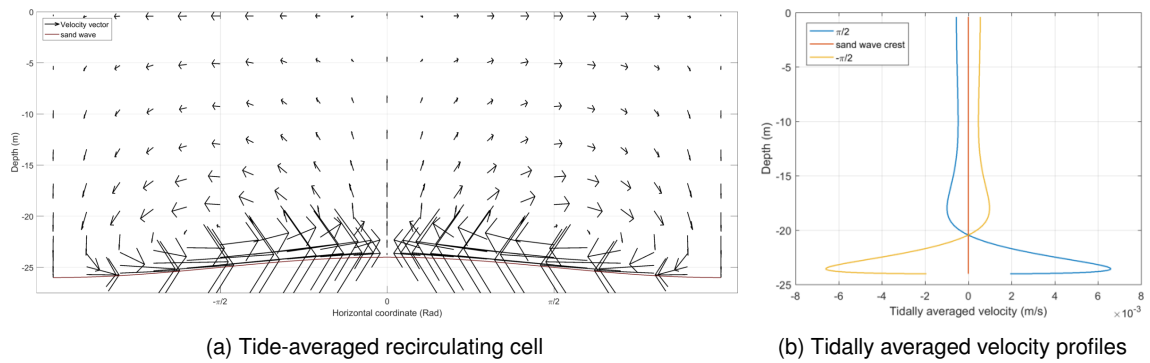


Figure 3.3.: Hydrodynamics sand wave amplitude 1 m

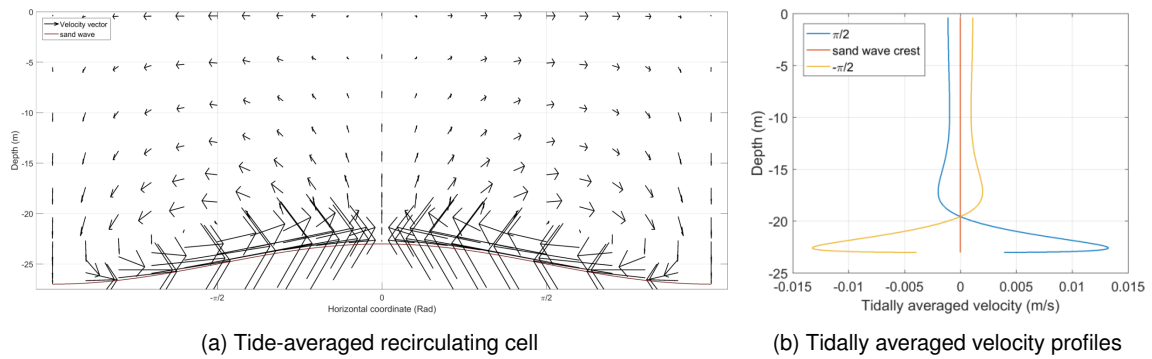


Figure 3.4.: Hydrodynamics sand wave amplitude 2 m

The expansion of the idealized model in the y -direction produced the same results. With a symmetrical tidal flow as boundary condition the recirculating cells are uniform in the y -direction, comparable to Fig. 3.2 . For brevity the results are not shown.

3.3.2. Sediment transports

Case II represent the implementation of sediment in the idealized model keeping the tidal forcing symmetrical. The tide-averaged concentrations and the concentration during maximum flood flow are shown (figs. 3.5 and 3.6). Together with the hydrodynamics, the concentrations result in the transport loads which are shown subsequently (fig. 3.7). Considering the tide-averaged concentration, higher concentrations are observed on top of the sand wave compared to the trough for both grain sizes. This can be explained by a higher flow velocity due to a decreased water depth on top of the sand wave. For a smaller grain size the tide-averaged concentrations are higher compared to a larger grain size (fig. 3.5b).

During maximum flood flow from left to right two important features can be observed regarding the role of suspended sediment in the model. Firstly the location of the suspended sediment concentration maxima over the vertical show a downstream shift with respect to the sand wave. Secondly the magnitudes of the maxima over the vertical decrease higher in the water column (fig. 3.6). The downstream shift in the suspended sediment concentrations during flood is larger for smaller grain sizes (fig. 3.6b). This same features can be observed during maximum ebb flow only with opposite direction.

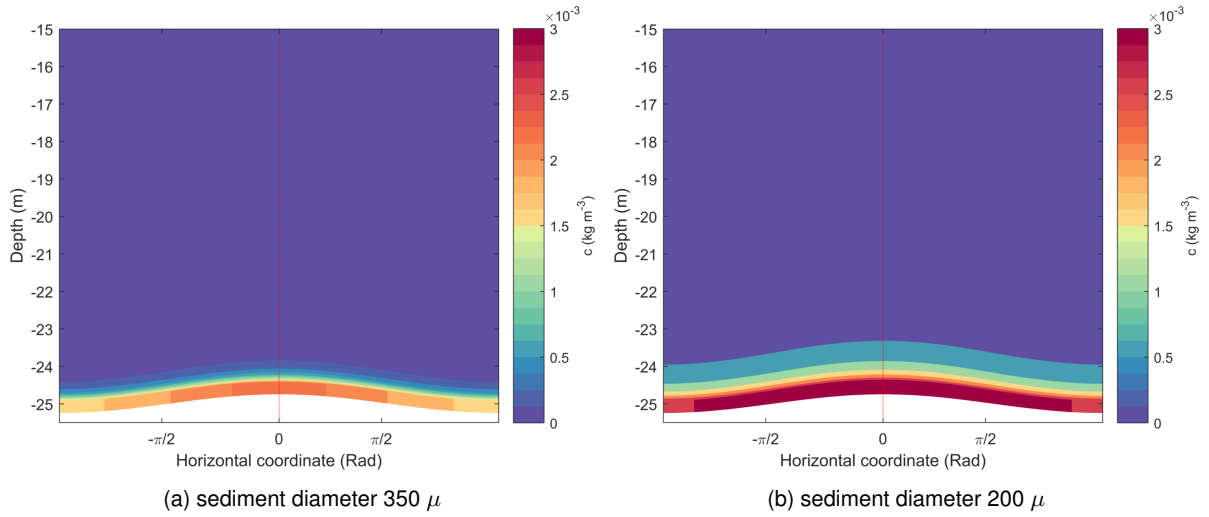


Figure 3.5.: Tide-averaged suspended sediment concentrations

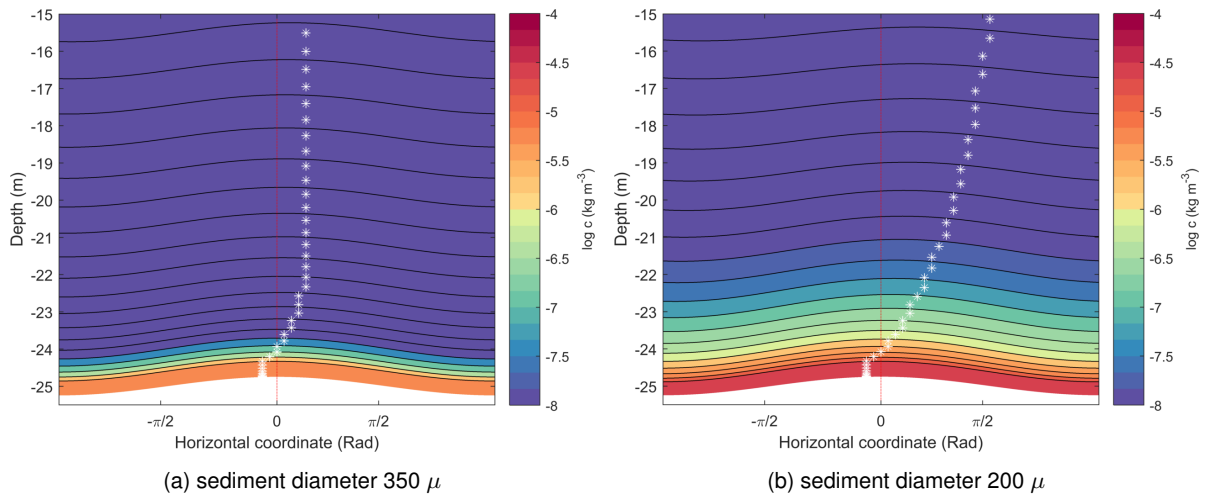


Figure 3.6.: Suspended sediment concentrations $\log c$ (kg m^{-3}) during maximum flood flow from left to right

Combining the hydrodynamics and sediment concentrations the sediment transport loads are calculated by the model (fig. 3.7). For a smaller grain size the tide-averaged bed load transport rate is opposite in sign compared to the tide-averaged suspended load transport rate (fig. 3.7b). The growth and decay of a sand wave is determined by the convergence and divergence of the sediment transport rates. Because the tide-averaged transport rates have opposite signs, they also have an opposite effect on the growth of sand waves. Bed load transport is related to the growth of sand waves, and suspended load transport is related to the damping of sand waves. For the larger grain size this effect is not observed, and both bed and suspended load transport provide the sand wave to grow. This is because the sediment concentration of the larger grain size are located close to the bed and initially suspended load transport has the same mechanism as bed load. If the sand wave height increases further this growing effect of the suspended transport load change in the damping effect described for the smaller grain size (van Gerwen et al., 2018).

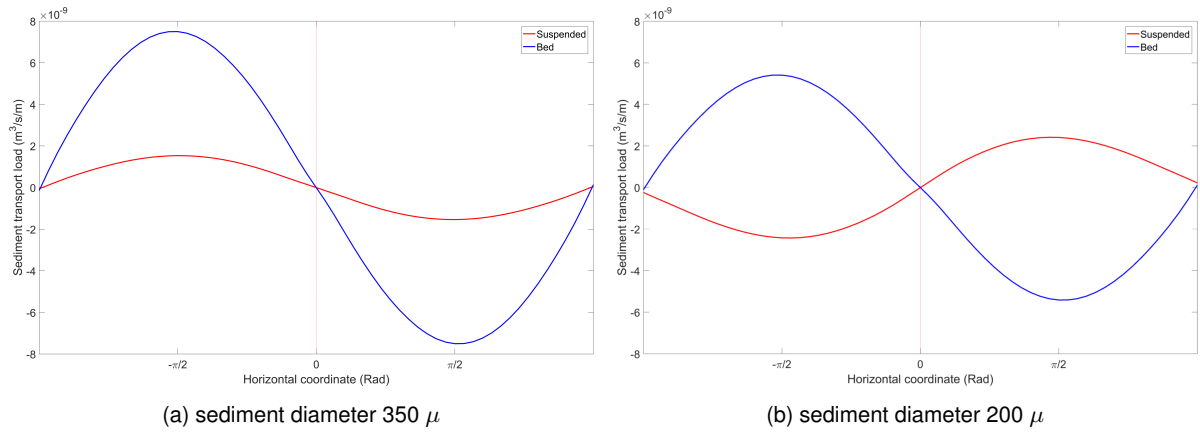


Figure 3.7.: Tide-averaged sediment transports rates ($\text{m}^3 \text{s}^{-1} \text{m}^{-1}$)

3.3.3. Migration direction

The tidal velocity signal in Case I and II is symmetrical, therefore the sand waves in these models do not migrate. Including a residual current or an additional tidal constituent result in migration as explained in subsection 2.1.2 and 2.1.1 respectively. Case III represents the situation in which a residual current is present in addition to the S_2 -tide-averaged constituent. Case IV represents the inclusion of the S_4 -tide constituent in addition to the S_2 -tide constituent.

For Case III the value of γ_I is positive which means that the sand wave migrates downstream. This can be explained by the fact that the recirculating cell is disturbed by the residual current and tide-averaged velocities are all in the same downstream direction. Case IV result in negative value for γ_I . The sand wave migration is therefore to the left. The combination of the S_2 and S_4 -tide constituents result in an asymmetrical tidal velocity signal enhancing the negative sediment transport loads.

4 | Idealized model: Tidal sand bank as underlying seabed topography

4.1. Introduction

The underlying seabed topography in the idealized model in the previous chapter is assumed horizontal. However, the bottom of sandy seas consist of different forms with smaller and bigger scales compared to sand waves (table 1.1). Mega ripples which are the small-scale bed forms are not considered since it is assumed that they do not influence the migration direction of sand waves. Large-scale bed forms known as tidal sand banks influence the local hydrodynamics and thereby it is possible that the migration direction of sand waves is affected. The bed form considered in this chapter is therefore the tidal sand bank. Tidal sand banks are nearly static and have a wave length of 5-10 km, and with reference to the principal tidal current their orientation is rotated 10-30 degrees anticlockwise (in the northern hemisphere) (Hulscher, 1996). To investigate the influence of underlying tidal sand banks, the idealized model is extended to be able to include tidal sand banks and the relevant processes governing these tidal sand banks. This is explained in section 4.2. Additionally, the Fast-Fourier Transform (FFT) is discussed in the methods, since the usage is different compared to the flat bottom model (subsection 4.2.3). Finally the results are presented in section 4.3.

4.2. Methods

The model of van Gerwen et al. (2018) (2DV) is used as starting point for the modification. The black line in Fig. 4.2 represent this model. The cell sizes are too small compared with the other cell sizes and therefore appear as grey areas in the figure.

4.2.1. Model modification

A tidal sand bank of infinite extent (Roos & Hulscher, 2003) is mimicked under a sand wave field. Figure 4.1a gives an overview of the definitions used in the idealized model regarding the tidal sand bank. The orientation

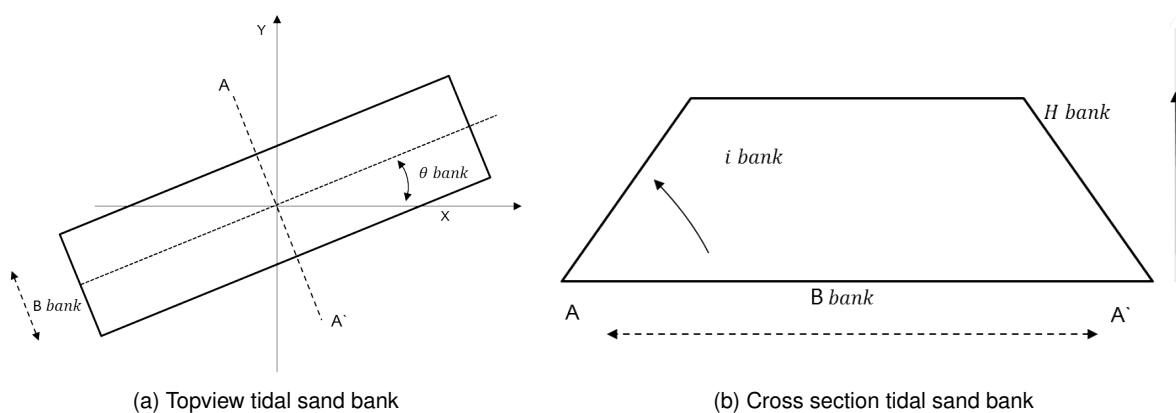


Figure 4.1.: illustrative orientation and shape tidal sand bank

of the tide is in the x -direction. The angle between the tidal current and the tidal sand bank is assumed 30 degrees anticlockwise, representing a typical North Sea situation. The cross section of the tidal sand bank without overlaying sand waves is displayed in Fig. 4.1b. Sand waves are assumed on top of the tidal sand bank with orientation perpendicular to the x -direction, so perpendicular to the direction of the tide (Besio et al., 2008). Characteristic for modelling infinite tidal sand banks are boundary conditions which are infinitely far from the area considered and the inclusion of the Coriolis effect (Roos & Hulscher, 2003). The model of (van Gerwen et al., 2018) includes a horizontal x -dimension of 50 km to exclude influences of boundary conditions in the longitudinal direction. The initial modification in the lateral direction considered additional refined cells in the y -direction between 22,5 km and 23,5 km. However, the flow still is influenced by the lateral boundaries of the model in that case. The idealized model is therefore expanded in the y -direction outside of the refined area, represented by the blue square in Fig. 4.2. To look at the flow around the tidal sand bank within the refined area the red rectangle is defined and showed enlarged in Fig. 4.2. A sensitivity study on the computational grid is performed to investigate from what distance the boundaries in the y -direction can be assumed infinite far from the red rectangle. The computational grid study showed that the expansion of the grid with 22,5 km is sufficient for the correct implementation of infinite far boundaries in the lateral direction. The second requirement is the inclusion of the Coriolis effect. The Coriolis effect is tested for different tidal sand bank lengths before sand waves were taken into account in the model. Again the length was increased until the effect became constant. The details of these two tests are presented in Appendix A.

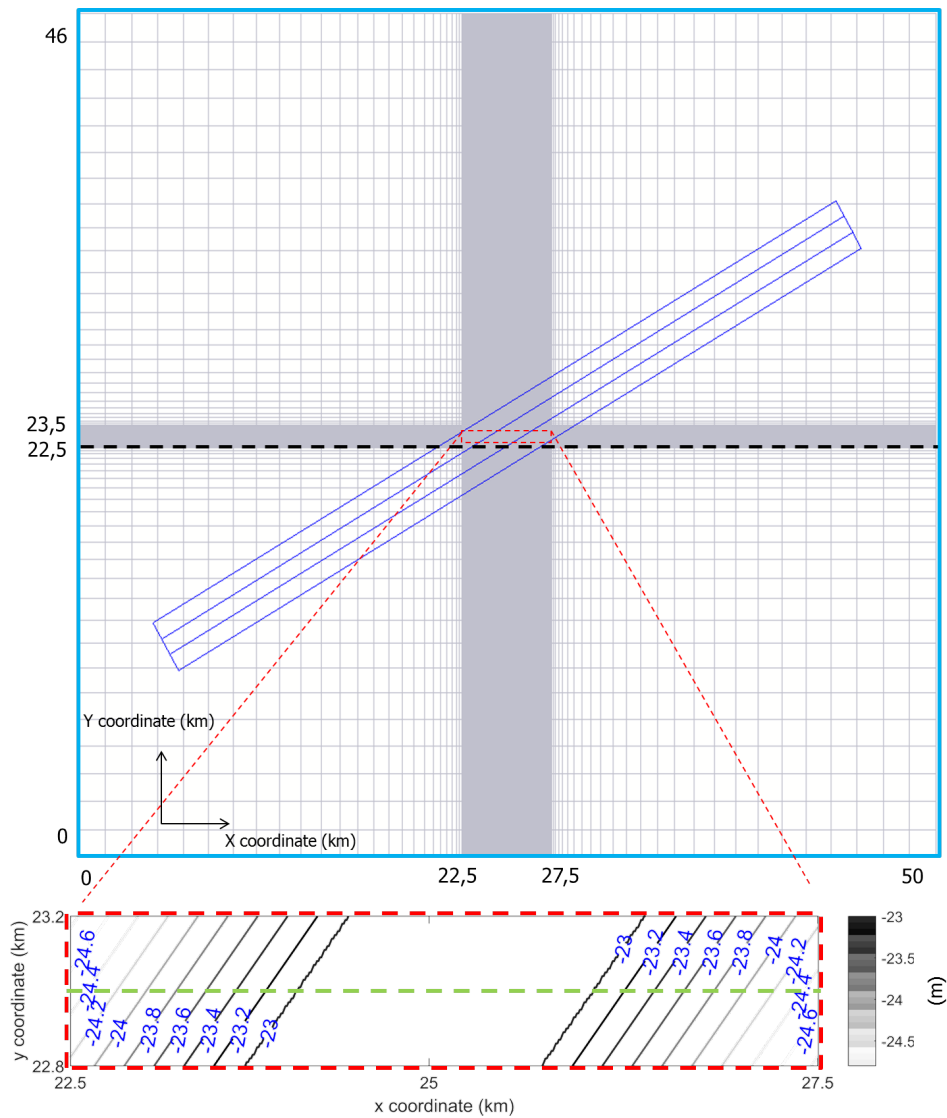


Figure 4.2.: Topview computational domain, red rectangle area considered in results

4.2.2. Model set-up

The model has a horizontal dimension in the x-direction of 50 km and in the y-direction of 46 km, in both directions the horizontal grid resolution is variable. The refined area has horizontal dimensions of 5 km in the x-direction and 1 km in the y-direction. In this area the grid resolution is 10 by 10 m. In both horizontal directions this grid size increase exponentially to 1500 meter (fig. 4.2). In the vertical dimension the model contains 60 layers with more refinement near the bottom. The remaining parameters are set similar to the idealized model described in Chapter 3 and are shown in table 3.1. The tidal sand bank orientation and width are taken 30 degrees and 3 km respectively. These parameters are not variable because the computational times become unrealistically long when they change. A smaller angle of the tidal sand bank result in a larger horizontal x dimension of the refined area. The increase of the width of the tidal sand bank additionally would result in a increase in the width of the refined area. Given a constant width of the tidal sand bank, the sand bank height and slope can be seen as one parameter. To distinguish the influence from the tidal sand bank and tidal deviations such as a residual current or other tidal constituents, the tide is taken symmetrical for the first set of cases. Additionally, models with a residual current on top of the S_2 -tide constituent and models with the S_4 -tide constituent included are run. The phase shift between the S_2 and S_4 -tide constituent is taken 120 degrees, to obtain an asymmetry in the ebb direction of the velocity signal. The cases considered to investigate the influence of the tidal sand bank are presented in table 4.1. Coriolis is taken into account in contrast to the idealized model with a horizontal bed. Looking only at sand waves Coriolis can be neglected (Hulscher, 1996). Tidal sand banks however, have horizontal dimensions in the order of kilometers. Therefore the Coriolis effect becomes important (Roos & Hulscher, 2003).

Table 4.1.: Parameter overview

Parameter description	Symbol	Values	Dims.			
Mean water depth	H_0	25	m			
Tidal sand bank orientation	θ_{bank}	30	degrees			
Tidal sand bank width	B_{bank}	3	km			
Include sediment (Y)es/(N)o	-	Y	-			
Initial wave amplitude	A_0	0.25	m			
Initial wave length	L_{FGM}	400	m			
Model conditions		Case I	Case II	Case III	Case IV	
Amplitude of horizontal S_2 tidal velocity	U_{S_2}	0.65	0.65	0.65	0.65	m s^{-1}
Sand bank height	H_{bank}	2	2	10	10	m
Sand bank slope	i_{bank}	1/500	1/500	1/100	1/100	-
Median grain size	D_{50}	350	200	350	200	μm
Model conditions		Case V	Case VI			
Amplitude of horizontal S_2 tidal velocity	U_{S_2}	0.65	0.65			m s^{-1}
Magnitude of horizontal S_0 tidal velocity	U_{S_0}	0.05				m s^{-1}
Amplitude of horizontal S_4 tidal velocity	U_{S_4}		0.05			m s^{-1}

Case V and VI are run with sand bank and sediment properties as Case IV

4.2.3. Fast-Fourier Transform

The red rectangle, discussed in the model modification, is displayed in three dimensions in Fig. 4.3a. A cross-section is defined along the center of the red rectangle to investigate the migration direction of the sand waves over the tidal sand bank, indicated by the green line (fig. 4.3a). Figure 4.3b represent this cross-section. The vertical black lines indicate the sand waves on the flanks of the tidal sand bank of which the migration direction is determined using the Fast-Fourier Transform¹.

¹FFT is a Matlab module which determines the complex amplitude of the sinusoidal wave form

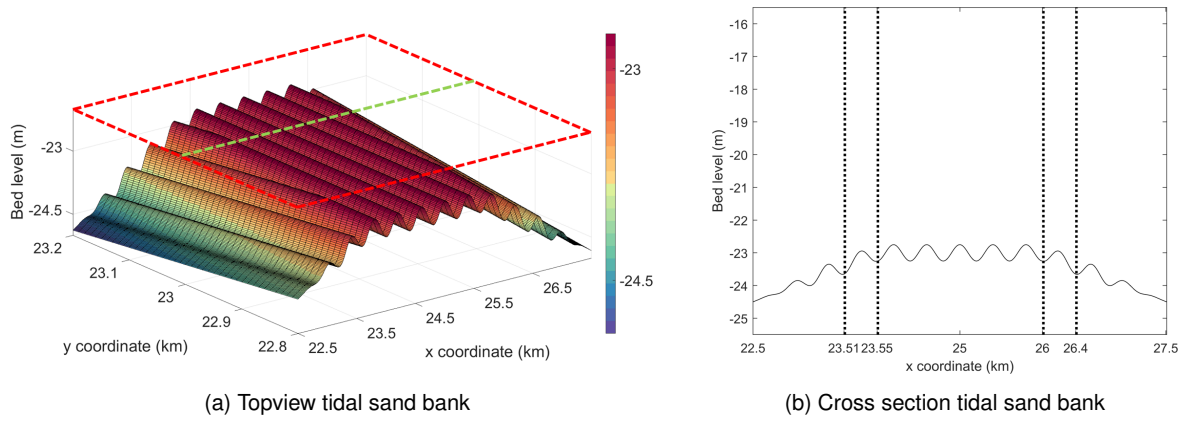


Figure 4.3.: Areas used in results

In contrast to the horizontal underlying seabed topography case the trend of the underlying tidal sand bank is extracted prior to calculating the migration direction. The remaining steps and assumptions are similar as for the flat bottom case described in subsection 3.2.3. For completeness the formula is displayed below.

$$\gamma_I = \frac{-1}{kT} \text{Im} \left\{ \log \left(\frac{A_1}{A_0} \right) \right\} \quad (4.1)$$

In which k is the topographic wave number $2\pi/L$ and T the tidal period

4.3. Results

The full horizontal x -direction of the refined area is taken into account. The tidal sand bank is modelled with an infinite extent. Processes in the refined area around the tidal sand bank are therefore constant along the tidal sand bank. A segment of 400 meter out of the 1 kilometer refined y -direction is displayed (fig. 4.3).

4.3.1. Symmetrical boundary conditions

Case I to IV have symmetrical boundary conditions and the results of these models are displayed in this subsection. The scale of the tidal sand bank (red rectangle fig. 4.3a) is used to explain the hydrodynamics around the tidal sand bank without waves on top. The hydrodynamic results on the scale of the tidal sand bank of models with sand waves are qualitatively the same and displayed in Appendix B. Subsequently models containing sand waves are used to look at the hydrodynamics on the scale of sand waves (green line fig. 4.3b). Finally the results of the models regarding sediment transport and migration direction of the sand waves are presented.

4.3.1.1. Hydrodynamic processes

To display the horizontal interaction of the tidal sand bank and the tidal flow, Fig. 4.4a shows the area concerned within the refined grid area (red rectangle). During flood flow the flow is from left to right. Towards the top of the tidal sand bank the water depth decreases and the flow accelerates, being maximum at the beginning of the top of the tidal sand bank. Over the top towards the flat bottom the flow decelerates due to a increasing water depth. The flow experience a deflecting movement by the Coriolis effect in the negative y -direction during flood flow. The two phenomena during flood flow are displayed in Fig. 4.4b. During ebb flow a similar flow pattern in opposite direction is observed. Again the flow accelerates towards the top of the tidal sand bank and decelerates moving over the top towards the flat bottom (fig. 4.4c). Since the flow during ebb flow is from left to right the flow experience again the Coriolis effect, deflecting the flow in the positive y -direction. Averaged over a tidal cycle the tidal sand bank generates a horizontal residual current as displayed in Fig. 4.4d (Roos & Hulscher, 2003). At both flanks of the tidal sand bank a parallel residual flow is observed. The strength of the horizontal tide averaged velocities are larger at the beginning of the flanks of the tidal sand bank. The results displayed in Fig. 4.4 are for a tidal sand bank with a height of 2 m. For a tidal sand bank with a height of 10 m, the magnitude of the residual flow is larger and the deflection of the flow enhanced by the Coriolis effects

is also larger, due to smaller water depths. This idealized model is based on a tidal sand bank configuration in the northern hemisphere, therefore tidal horizontal residual currents move clockwise. The same hydrodynamics would be obtained by a tidal sand bank in the southern hemisphere, the difference is the orientation of the tidal sand bank and the Coriolis effect. Resulting in a different direction of the horizontal residual current being anti clockwise (Roos & Hulscher, 2003).

The hydrodynamics on the scale of the tidal sand bank influence the hydrodynamics on the scale of sand waves. As explained in the methods sand wave migration on each flank is looked at. Therefore also the changes in hydrodynamics are investigated at these locations. Models including sand waves are used regarding the hydrodynamics on the scale of sand waves. On the left flank of the tidal sand bank, the horizontal residual flow of the tidal sand bank has a positive x -component. The recirculating cell of the sand waves is disturbed and all velocity vectors are to the right (fig. 4.5a). On the right flank the horizontal residual flow of the tidal sand bank has a negative x -component, resulting in a distortion to the left for the sand wave on the right flank (fig. 4.5b). Figures 4.5a and 4.5b represent case I and II, in which the height of the tidal sand bank is 2 m. For case III and IV the larger height of the tidal sand bank results in stronger residual currents. Although qualitatively the same, the distortion is more significant (figs. 4.5c and 4.5d).

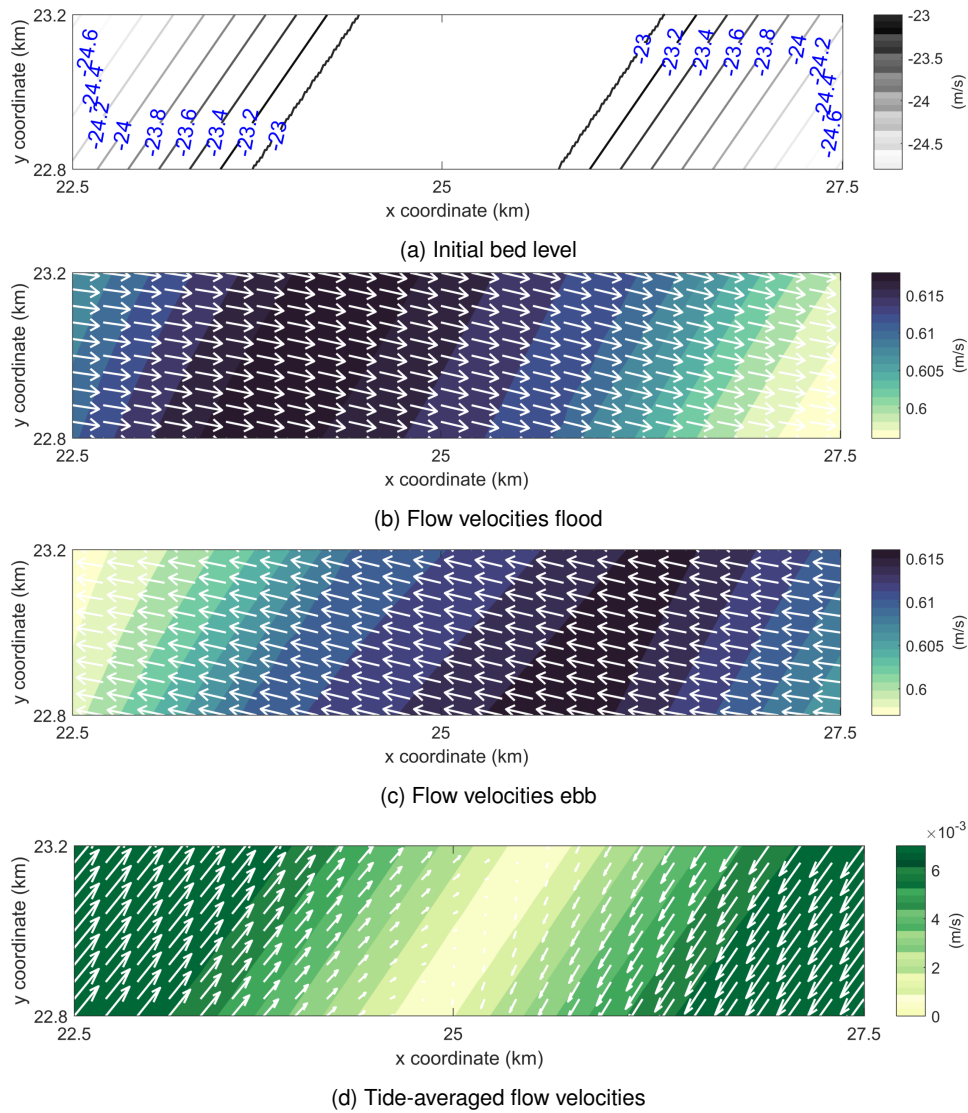


Figure 4.4.: Hydrodynamics tidal sand bank

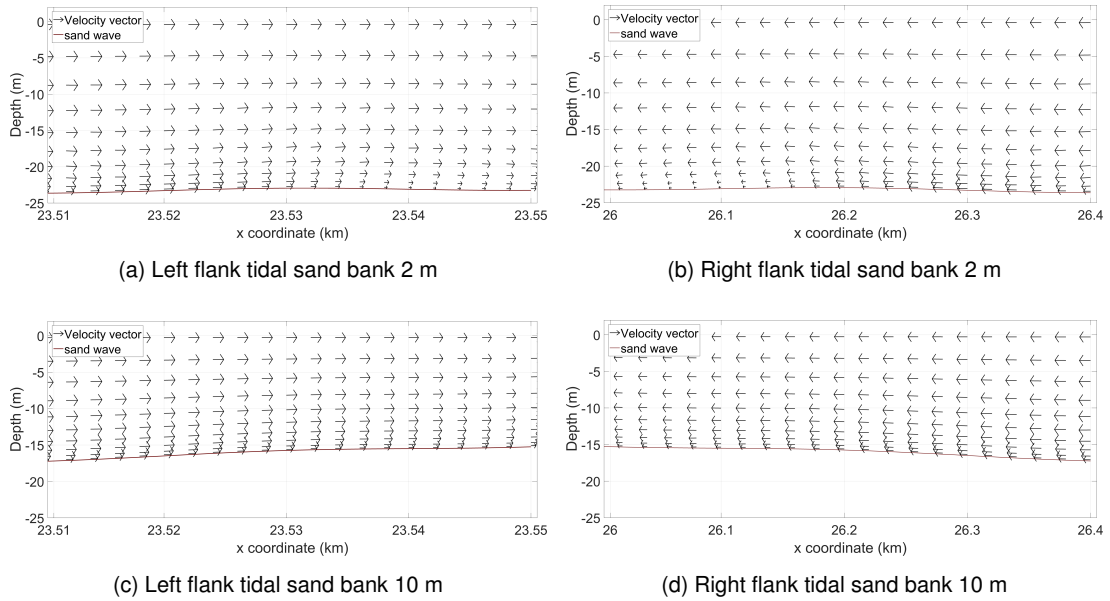


Figure 4.5.: Tide averaged flow velocities on sand wave scale

4.3.1.2. Sediment transport

Figure 5.3 shows the sediment transports for Case I. Looking at the sand wave on the left flank of the tidal sand bank (fig. 4.6c), both bed load transport and suspended load transport are directed in the positive x -direction towards the top of the tidal sand bank. Along the sand wave on the right flank (fig. 4.6d) the same is observed in opposite direction, both bed load transport and suspended load transport are directed towards the top. This can be explained by the alteration of the vertical recirculating cell of the sand waves by the horizontal residual current generated by the tidal sand bank. The phenomena can be compared to adding a residual flow to the symmetrical tidal signal for a horizontal underlying bottom in Chapter 3. For case I the sediment grain size is $350 \mu\text{m}$, therefore the bed load transport is larger compared to the suspended load transport because the sediment is mainly located at low water depths. Looking over the whole refined domain (fig. 4.6b), bed load and suspended load transports reverse from positive to negative transports on top of the tidal sand bank. Due to the stronger residual currents at the beginning of the tidal sand bank flanks, the transports here are larger for both bed load and suspended load transport.

For case II, III and IV the sediment transports over the tidal sand bank are displayed in Figs. 4.7a, 4.7c and 4.7d respectively. In addition the tidal sand bank bed level is shown in Fig. 4.7b. For case II, the smaller grain size of $200 \mu\text{m}$ result in larger suspended sediment transports compared to case I. Besides the magnitude of the suspended sediment transport load the influence of the tidal sand bank is similar resulting in sediment transport on both flanks towards the top of the tidal sand bank. For case III and IV the magnitudes of both bed and suspended sediment load transports are larger compared to case I and II. This can be explained by smaller water depths resulting in stronger horizontal residual currents for the larger tidal sand bank. Suspended load transport again is significantly larger for a smaller grain size, whereas the bed load transport only becomes a little lower.

4.3.1.3. Migration direction

The horizontal residual flow of the tidal sand bank disturbs the vertical recirculating cell of the sand wave resulting in residual currents towards the top of the tidal sand bank. Depending on the grain size and the size of the tidal sand bank the migration of sand waves is larger or smaller, but in all cases towards the top. This is because the boundary conditions are taken symmetrical so far to display the migration due to a tidal sand bank solely. Decreasing the sediment grain size for a given tidal sand bank height from $350 \mu\text{m}$ to $200 \mu\text{m}$ doubles the migration speed on both flanks. Increasing the height of the tidal sand bank from 2 to 10 meters, the migration speeds of the sand wave increases almost by a factor 10.

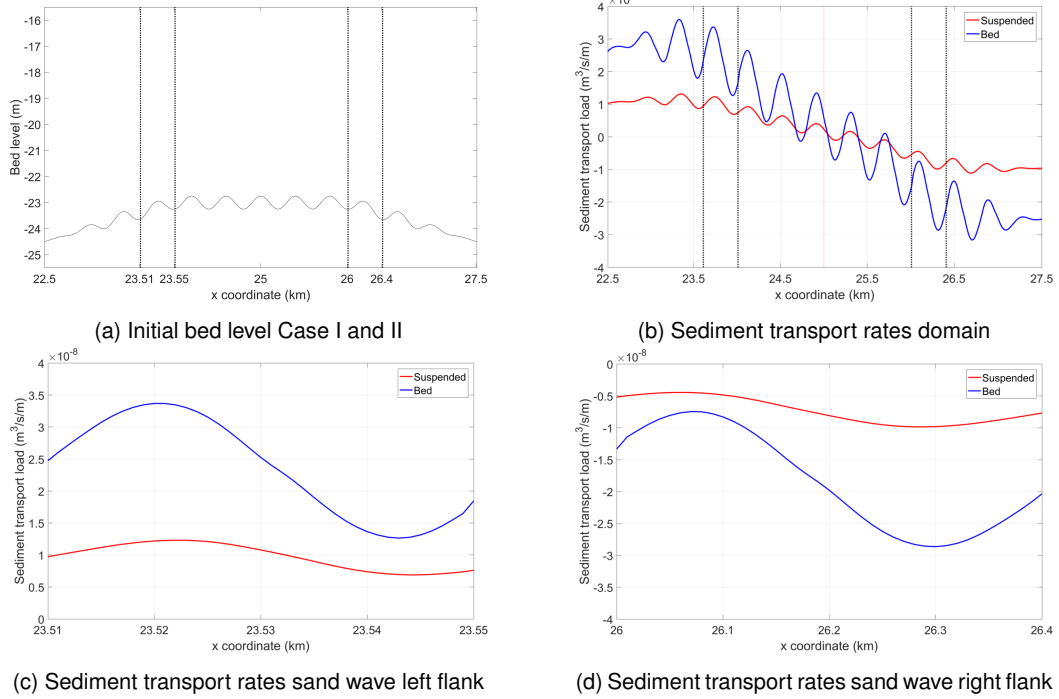


Figure 4.6.: Sediment transport case I

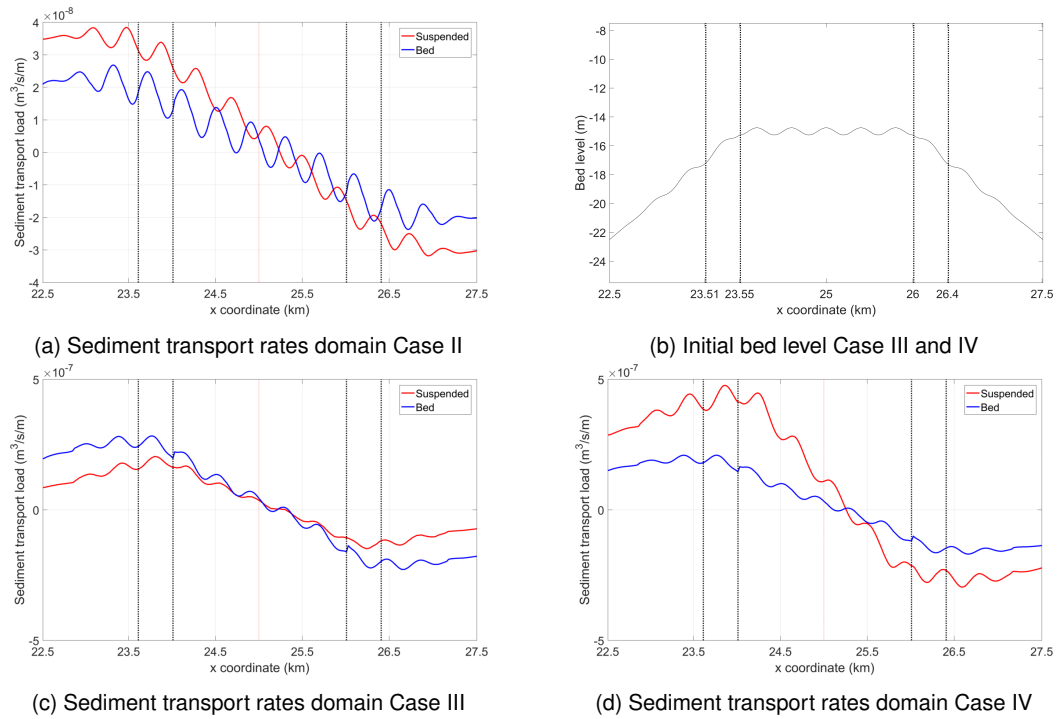


Figure 4.7.: Sediment transports case II, III and IV

4.3.2. Residual current

In case V the boundary condition is extended with a residual current of 0.05 m s^{-1} besides the S_2 -tide constituent. A tidal sand bank height of 10 meters and grain size diameter of $200 \mu\text{m}$ are taken to display the effect of a residual current on the migration direction. Firstly the hydrodynamics are discussed and secondly the sediment transports and migration directions observed.

4.3.2.1. Hydrodynamic processes

Figure 4.8a shows the initial bathymetry of case V. The residual current added in the boundary condition is in the flood direction. Therefore flood flow has a larger magnitude over the tidal sand bank (fig. 4.8b) compared to ebb flow (fig. 4.8c). The flow during flood and ebb has a larger deflection due to the Coriolis effect compared with a tidal sand bank of 2 meters. This is due to higher flow velocity caused by smaller water depths. The tide averaged horizontal residual flow over the tidal sand bank is directed in the direction of the flood flow due to the higher magnitudes of the flood flow (fig. 4.8d). The direction of the tide averaged flow is not constant over the tidal sand bank. From left to right the tide averaged velocity vectors point more in the negative y -direction. The components along the cross-section at which sand wave migration is looked at are therefore smaller on the right flank of the tidal sand bank (fig. 4.9).

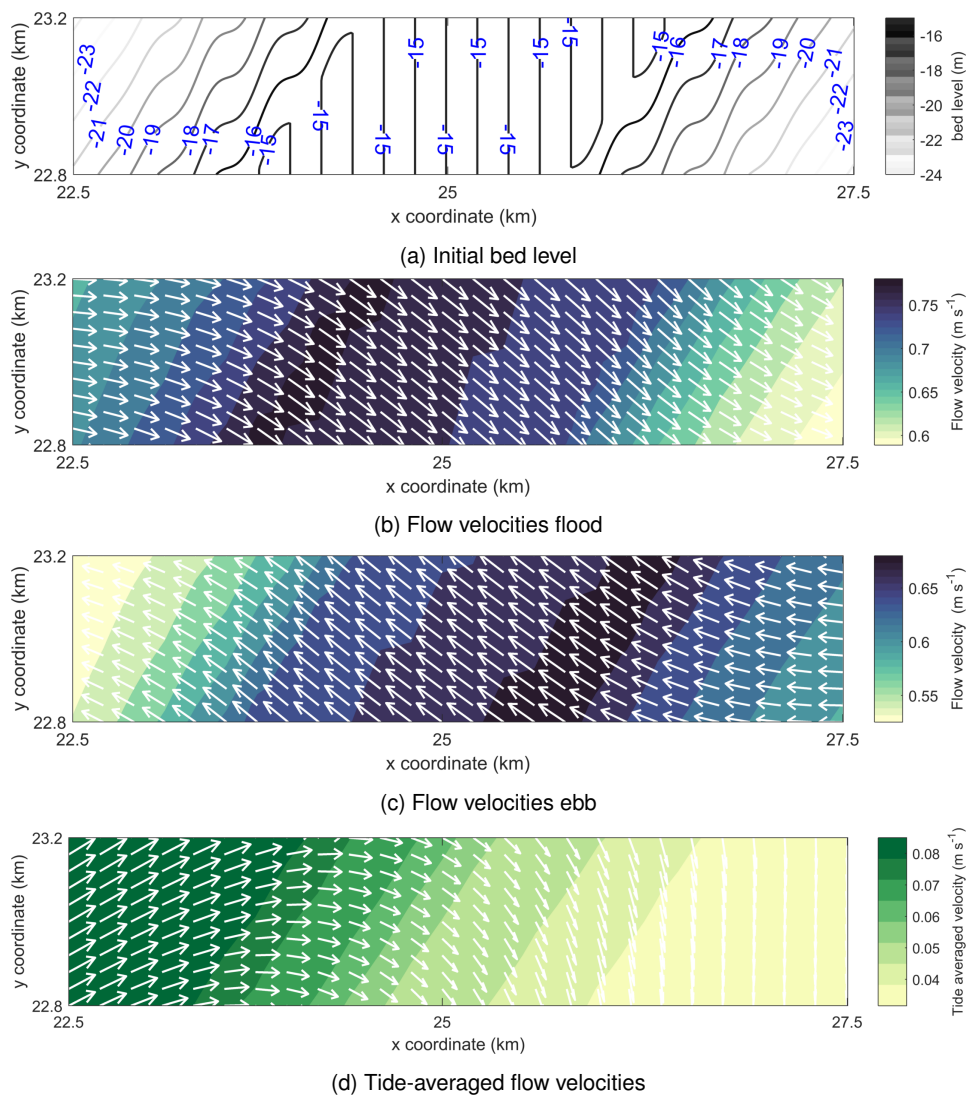


Figure 4.8.: Hydrodynamics including a residual current

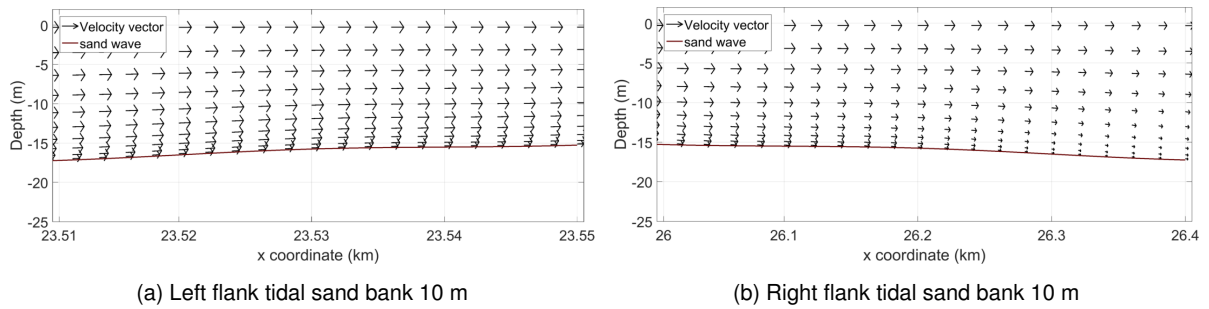


Figure 4.9.: Tide averaged flow velocities on sand wave scale

4.3.2.2. Sediment transport

Adding the residual current result in positive sediment transport loads along the domain cross-section for bed and suspended load transports (fig. 4.10b). Along the left flank of the tidal sand bank the tide averaged flow velocities have a positive component and on the right flank a negative component in the x -direction for the symmetrical case. Since the residual current is in the positive x -direction the symmetry of the tide averaged flow velocities is disturbed in this direction, resulting in the positive bed and suspended transport loads. The magnitudes of the transport loads are larger on the left flank. This can be explained by the changing direction of the tide averaged velocity vectors over the tidal sand bank (fig. 4.9).

4.3.2.3. Migration direction

The migration directions of the sand waves at both flanks of the tidal sand bank are directed in the positive x -direction. This is the result of the positive sediment transport loads over the whole domain for bed and suspended load transports caused by the residual current. The magnitude of the migration along the cross section is about 10 times larger on the left flank of the tidal sand bank. This is due to the changing direction of the tide averaged flow vectors over the tidal sand bank.

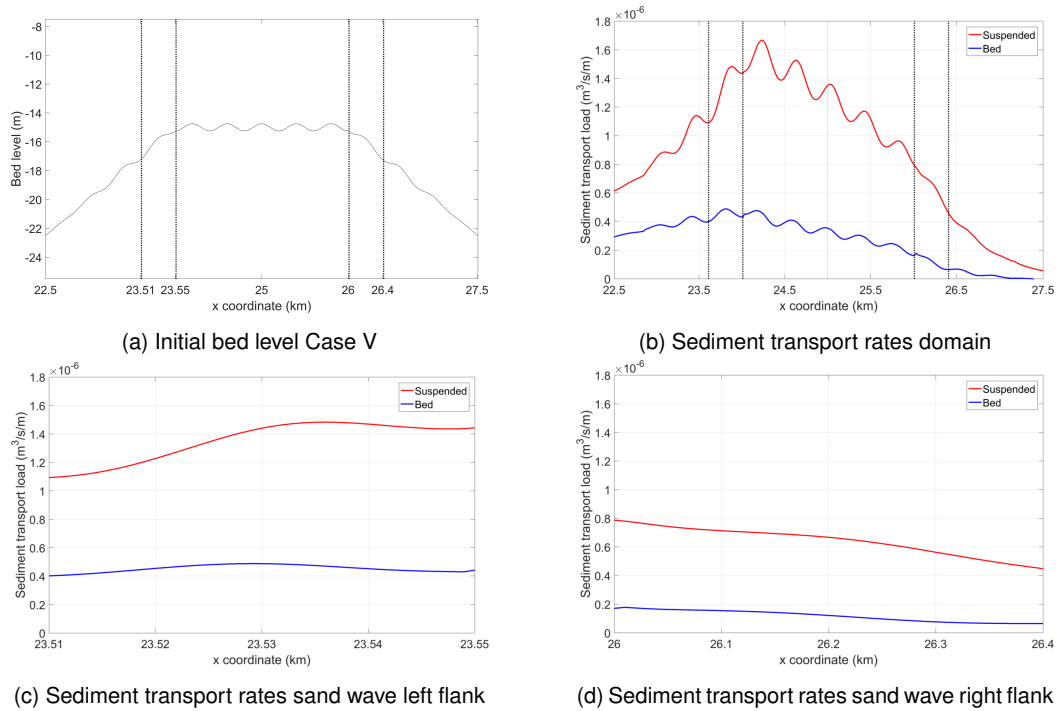


Figure 4.10.: Residual current sediment transports

4.3.3. Higher order tidal constituent

In case VI the S_4 -tide constituent is added in addition to the S_2 -tide constituent. The phase between the two tidal constituents is 120 degrees. Again the height of the tidal sand bank is 10 meters and the sediment grain size $200 \mu\text{m}$. Firstly the hydrodynamics are discussed and secondly the sediment transports and migration directions observed.

4.3.3.1. Hydrodynamic processes

The initial bed level (fig. 4.11a) is similar to case V. The flood flow (fig. 4.11b) is slightly lower compared to the ebb flow (fig. 4.11c) due to the inclusion of the S_4 tide constituent. Despite the assymetrical tidal velocity, the resulting tide averaged horizontal residual currents are observed as in the case of a symmetrical tidal signal (fig. 4.11d). This result in tide averaged flow velocities towards the top at both flanks of the tidal sand bank on the scale of the sand waves (fig. 4.12).

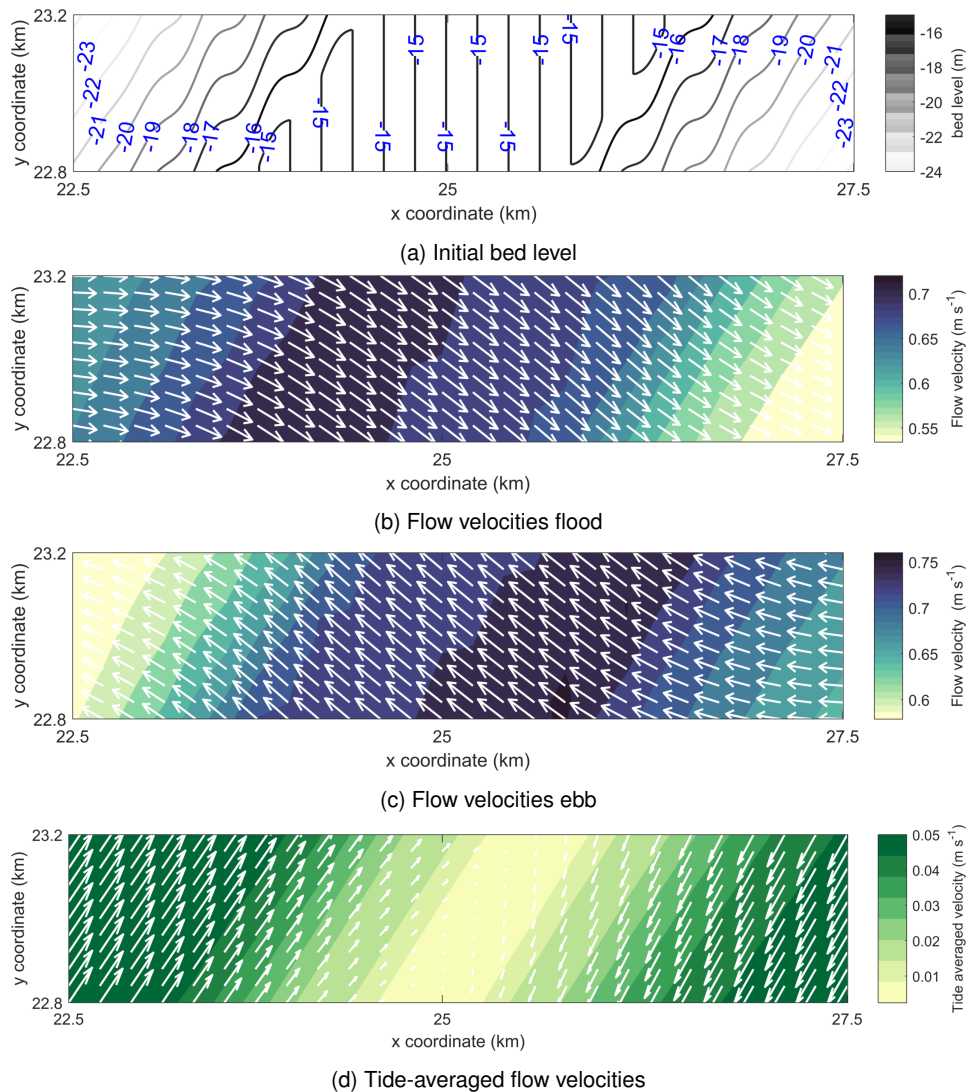


Figure 4.11.: Hydrodynamics S_2 and S_4 tide constituents

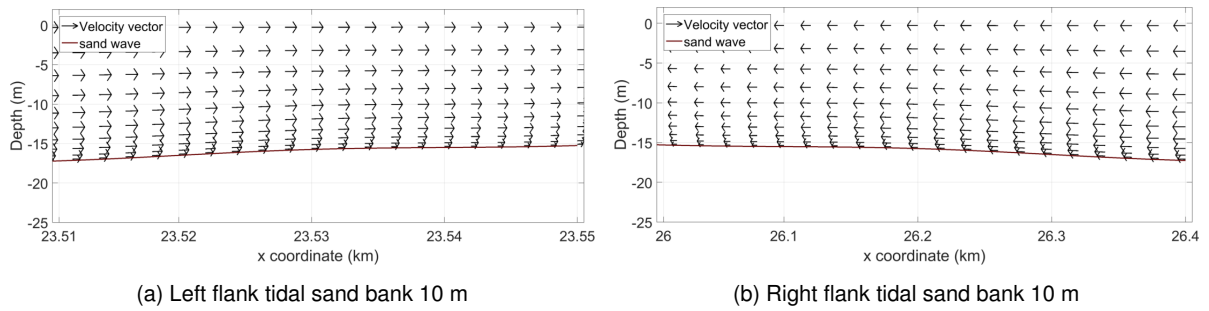


Figure 4.12.: Tide averaged flow velocities on sand wave scale

4.3.3.2. Sediment transport

Although the tide averaged horizontal residual currents are similar to case I to IV with symmetrical tidal forcing, negative sediment transport loads are observed for large part of the domain (fig. 4.13b). This is due to the asymmetrical tidal velocity signal enhancing negative sediment transport loads. Looking at the sand waves location on the left flank, the bed load transports are positive and the suspended load transport is around zero (fig. 4.13c). For the right flank of the tidal sand bank both bed and suspended load transport are negative (fig. 4.13d).

4.3.3.3. Migration direction

The migration of the sand wave on the left flank is still positive, only about half the magnitude compared with the symmetrical boundary conditions for the same tidal sand bank in case IV. On the right flank of the tidal sand bank the migration direction is in the negative x direction. Here due to the larger negative sediment transport rates, the magnitude is larger compared to case IV.

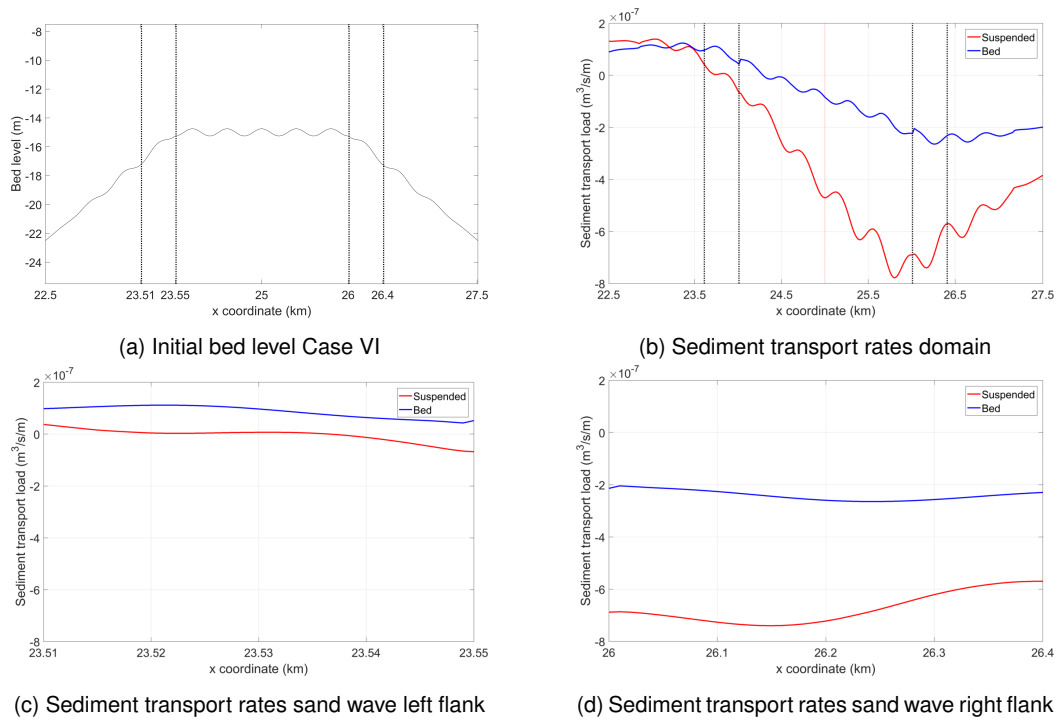


Figure 4.13.: sediment transport S_2 and S_4 -tide constituents

5 | Case study Borssele

5.1. Introduction

In this chapter an existing 2DH Delft3D-FLOW model developed by Deltares for Borssele wind farm zone (hereafter: BWFZ) (Deltares, 2015b) is used and modified to investigate sand wave migration behaviour in a realistic case study. The BWFZ is located in the southern part of the Dutch North Sea (fig. 5.1). The configuration of the original and modified model are presented in this chapter. In section 5.2, the description of the original model, the modifications made and the set-up of the model are presented. Additionally in subsection 5.2.4 the method regarding approaching the migration direction in the model is discussed and in subsection 5.2.5 migration directions derived from data are presented. Finally in section 5.3 the results of the model are shown. Model results are compared with migration data to see if the influence of underlying bed forms can be seen as in the idealized model.

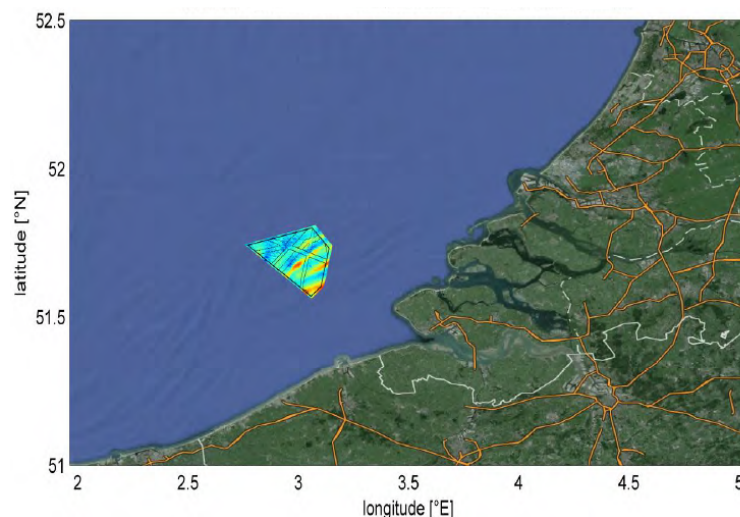


Figure 5.1.: Location Borssele Wind Farm Zone in the southern part of the Dutch North Sea (Deltares, 2015b)

5.2. Methods

5.2.1. Model description

In the original model by Deltares, four sub domains are coupled using two model techniques (fig. 5.2a). This is done to be able to model large-scale processes of the entire North Sea (Dutch continental Shelf Model (DCSM)), and link these to smaller domains covering the southern part of the North Sea and BWFZ in which smaller-scale processes are important (Regio, DD600 and DD200). Offline nesting is used to derive boundary conditions from the DCSM for the Regio domain. The Regio, DD600 and DD200 domains are coupled using *domain decomposition*. In this model technique the domains are simulated online, meaning that the boundary conditions defined at the outer boundaries of the Regio model are transmitted to the smaller domains in the same computation. The models Regio, DD600 and DD200 are used as a starting point for the model modifica-

tion in the case study of BWFZ (fig. 5.2a). The DCSM model is not considered in this study, only the boundary conditions are applied. The results in the domains for the original model are validated and hind-cast modelled for currents and water levels (Deltares, 2015b). When the modified model represents the flow as in the original model, it is assumed that the model can be used to investigate the migration direction behaviour of sand waves.

5.2.2. Model modification

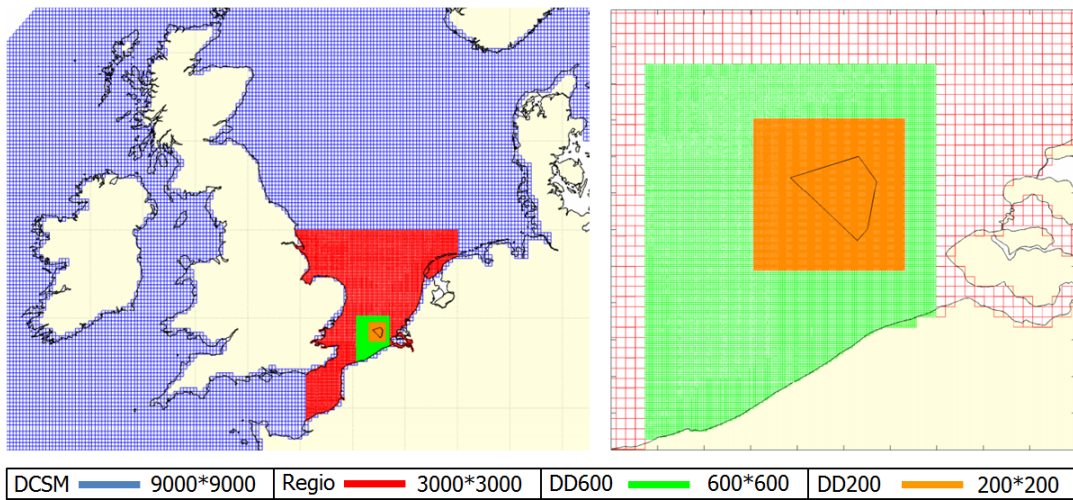
To model the processes regarding the migration direction of sand waves an additional refinement is required in the horizontal and vertical direction. The details of the various domains are displayed in Fig. 5.2b. Initially the aim was to apply a vertical and horizontal resolution in the area of interest equally to the idealized model with underlying seabed topography (horizontal resolution 10 m and 60 vertical layers). Due to a contradiction between grid refinement and computational time of the model this was not possible. The idealized model is tested with less vertical layers, to check if the important processes still are modelled as found in the idealized model including underlying seabed topography. A solution is found at 20 layers, for which the processes are modelled in idealized form correctly and the domain decomposition model has ending computational times. However the computational time still was unrealistic long. This is due to the fact that the DD model technique run sub domains in a parallel matter. When one sub domain contains the largest amount of computational cells the other sub domains have to wait until one computational time step is computed, and large computational times are the result. In the original configuration the finest model contained 90 percent of the computational cells. Therefore the computational grid with the finest resolution is divided into four sub domains (fig. 5.2b). The model decisions shortly addressed above, are more extensively discussed in Appendix C. The horizontal refinement is made such that the underlying bed form present in BWFZ lies within the domains with the finest resolution (fig. 5.2c). The location indicated by the black square, is presented in the report, since here the underlying bed form is largest (fig. 5.2d). The same method of domain decomposition is applied to other locations (black dashed lines fig. 5.2c), the results regarding the remaining locations are shown in Appendix D.

5.2.3. Model set-up

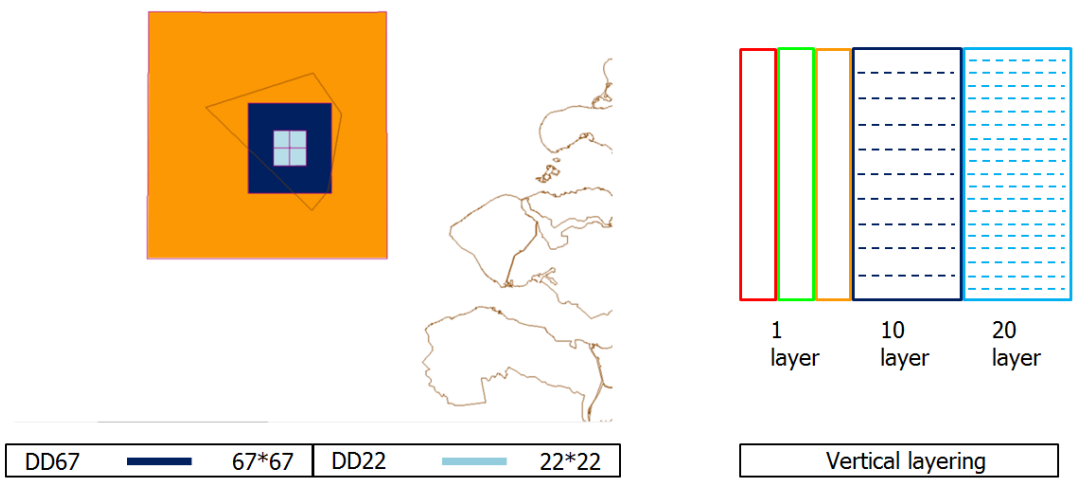
The model is run in spherical co-ordinate system. The Regio, DD600 and DD200 domain are run in 2D mode. A 3D approach is applied for the DD67 and DD22 domains. The computational grids of the DD67 and DD22 domain, have a horizontal resolution of 66.67 m and 22.33 m and a vertical resolution of 10 and 20 layers respectively. The finest domains covers the area in which the underlying bed form is present under the sand wave field. A water level time-series is defined at the boundary of the Regio model. The boundary conditions obtained for the Regio model are generated by tidal motion defined at the open boundaries of the DCSM. The tidal motion within the finer domains in this study is therefore representative for a set of 11 tidal constituents, including M2, S2, N2, K2, O1 and K1 (Deltares, 2015b). The model is run for 3 days. The first two days are used for spin-up. During the last day output is generated to investigate the sediment transport over a tidal cycle. The bottom is not updated during the computation. In all the domains sediment is present with a grain size diameter of 350 μm , which is equal to a medium grain size for North Sea areas where sand waves are present. The roughness in the new domains is assumed equal to the finest domain of the original model. The parameters used in the case study are presented in table 5.1.

Table 5.1.: Parameter overview

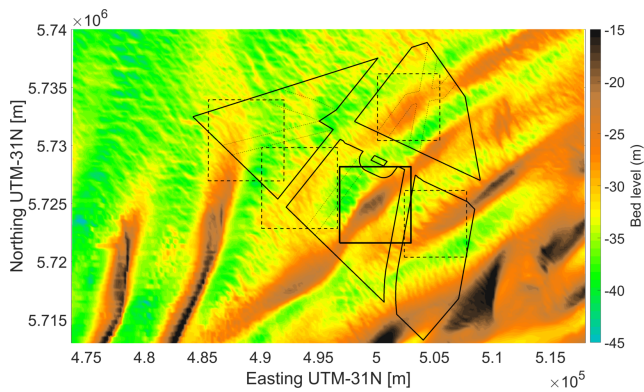
Model domain		Regio	DD600	DD200	DD67	DD22	
Parameter description	Symbol						Dimension
Mode	-	2D	2D	2D	3D	3D	-
Grid size x & y	Δx & Δy	3000	600	200	71.33	23.33	m
Layers	-	1	1	1	10	20	-
Time step	Δt			6			sec
Horizontal eddy viscosity	μ_h	10	10	2	1	1	$m^2 s^{-1}$
Vertical eddy viscosity	ν_v	-	-	-	$k - \epsilon$	$k - \epsilon$	$m^2 s^{-1}$
Roughness (Manning)	k_s	0.03	0.03	0.026	0.026	0.026	$m^{1/3} s^{-1}$
Sediment grain size	D_{50}	350	350	350	350	350	μm



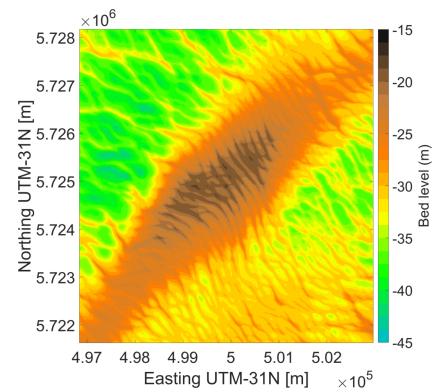
(a) Grid domains (name + resolution (m)) original model (Deltares, 2015b)



(b) Grid domains (name + resolution (m)) (left) and vertical resolution model modification (right)



(c) Bathymetry BWFZ



(d) Bathymetry location investigated

Figure 5.2.: Overview grid domains and bathymetry case study model

5.2.4. Migration direction derived from model results

The model output contains sediment transports, the seabed level is however kept constant during the computation. To compare the migration direction of sand waves derived from data discussed in subsection 5.2.5 with the model results, an assumption regarding the migration direction based on the model results is required. When looking over the transect of a sand wave, the tide-averaged sediment transport can be directed in one direction over the whole sand wave length. When in addition the maximum sediment transport is located at the sand wave crest, the tide-averaged sediment transport graph is obtained as displayed in Fig. 5.3a over the length of a sand wave. To the left of the sand wave crest, the tide-averaged sediment transport increases. From the crest to the right the tide-averaged sediment transport decreases. Converting this into a sediment balance, erosion on the left flank of the sand wave and accretion on the right flank is the result (fig. 5.3b). Assuming that the tide-averaged sediment transport within a spring-neap period differs in magnitude per tidal cycle but is the same in direction, migration in the direction of the positive tide-averaged transport is obtained (fig. 5.3b). This means that for the model results, areas with tide-averaged transports in the same direction and with the maximum at the sand wave crest indicate migration of sand waves in that direction.

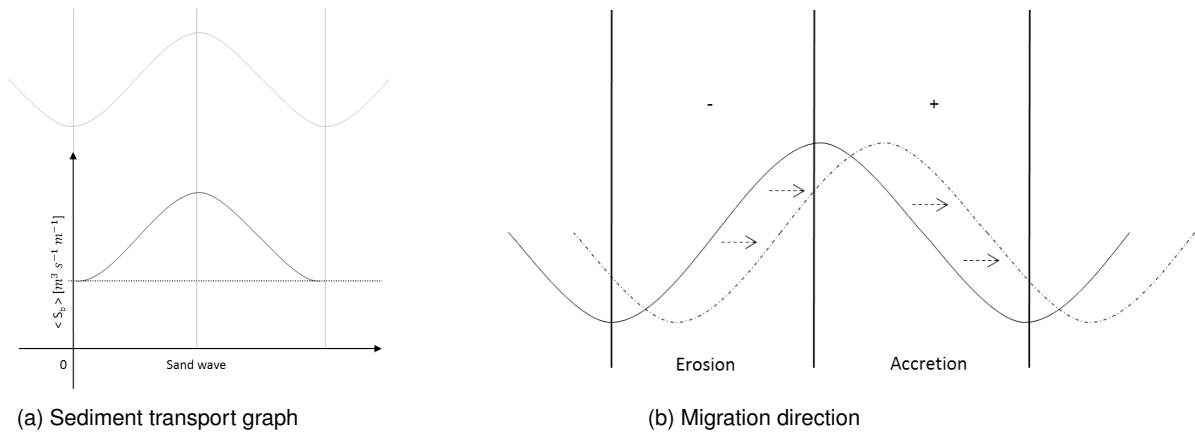


Figure 5.3.: Migration assumption model results

5.2.5. Migration direction derived from data-driven analyses

In-house data from Deltares is presented in this section for a comparison between the migration direction derived from model results and derived from data-driven analyses. The migration direction of sand waves is based on historical bathymetrical surveys of BWFZ from the year 2010 and 2015. The migration direction and speeds are derived using the gradient method and subsequently a cross-correlation technique (Deltares, 2016a, 2016b). The gradient method is based on the general shape and migration of sand waves. A mild sloping stoss side and a steeper lee side in the direction of migration are normally characteristic for migrating

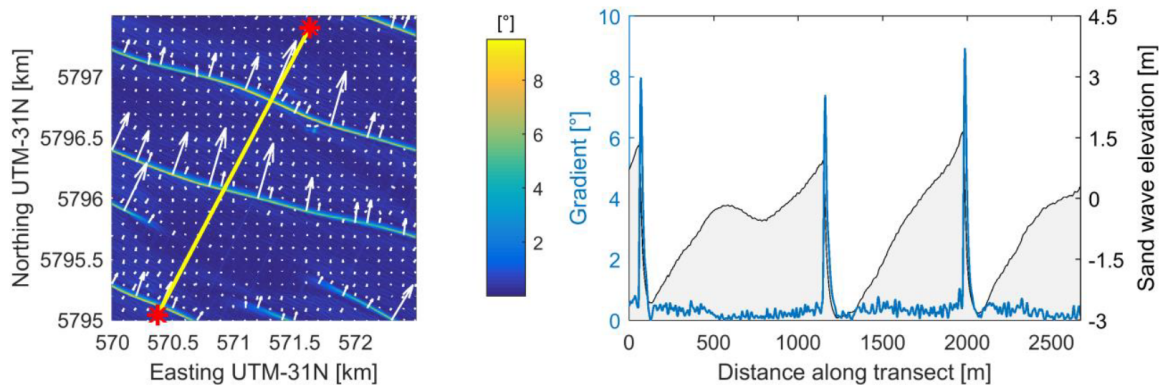


Figure 5.4.: Gradient method (Deltares, 2016b)

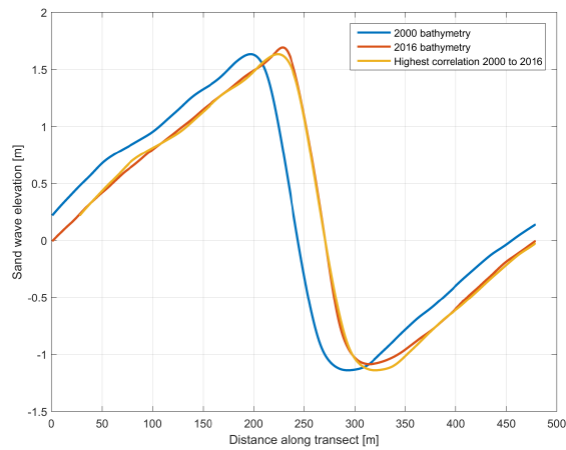


Figure 5.5.: Example cross correlation technique executed for all the transects defined (Deltares, 2016b)

sand waves. In addition the migration direction of sand waves is roughly perpendicular to the sand wave crest. Using this property one bathymetrical bed survey can be used to derive transects along which sand waves tend to migrate, known as the gradient method (Deltares, 2016a). The gradient method is illustrated in Fig. 5.4. Along the direction perpendicular to the crest, it can be seen that the crest has a significant larger gradient compared to the surrounding bathymetry. Besides the larger gradient at the crest in the perpendicular direction, sand waves also tend to migrate in this direction. The migration direction can therefore be approximated by the direction of the steepest gradient. The transects obtained from the bathymetry surveys of 2010 and 2015 are averaged to obtain the final transects along which the cross correlation technique is used to find the migration speed. By artificially shifting a transect derived from one bed survey data set towards a transect derived from the second bed survey data set the offset between the two data sets can be determined. The offset for which the correlation between both transects is highest is considered as the sand wave migration distance over the period considered (fig. 5.5) (Deltares, 2016b). The same methods as described above are used to determine the migration transects and speed within BWFZ. The transects found using the gradient method have an angle between North and 80 degrees clockwise relative to North (fig. 5.6a). Comparing subsequently the bathymetrical surveys of 2010 and 2015, the migration speeds shown in Fig. 5.6b are found. Red colors indicate migration towards the South-West and blue colors indicate migration to the North-East.

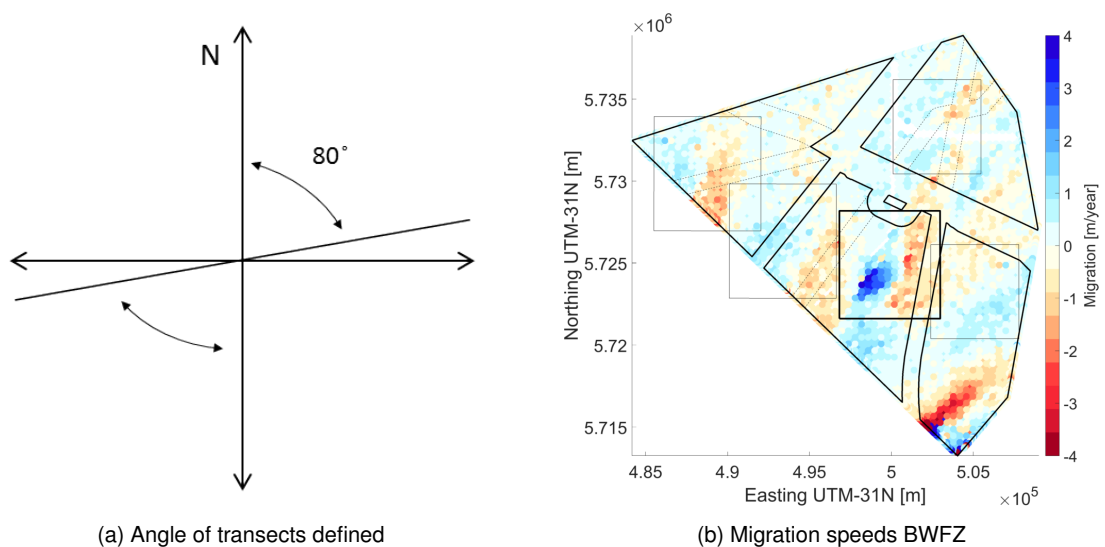


Figure 5.6.: Migration determined from data surveys between 2010 and 2015

5.3. Results

5.3.1. Model modification

To check if the hydrodynamics in the southern part of the Dutch North Sea around the BWFZ are modelled correctly, the original model is compared with the modified model during ebb and flood flow. In Figs. 5.7a and 5.7b the bathymetries and domains are shown of the original model and the modified model, which are similar. However, since the modified model domains, DD67 and DD22, have higher resolutions the bed forms are represented more accurately in the modified model. Moreover the data used to construct the bathymetry of the DD200 domain of the modified model has a higher resolution, resulting in a more accurate representation of the bed forms. When looking at flood and ebb flow in Figs. 5.8 and 5.9, the modified model represents the flow without producing large errors. During flood flow the connection between the DD200 and DD67 domains introduces an error at the left top corner due to the direction of the flow. This not holds for the whole computation as can be seen for ebb flow in which no large errors are present. In addition this corner is several kilometers away from the area of interest (DD22), and not considered to influence the model results used to investigate the migration direction of sand waves. The variation over the DD200 domain in the original model is related to the complex bathymetry of the area formed by the underlying bed forms and considered modelled correctly by the modified model domains.

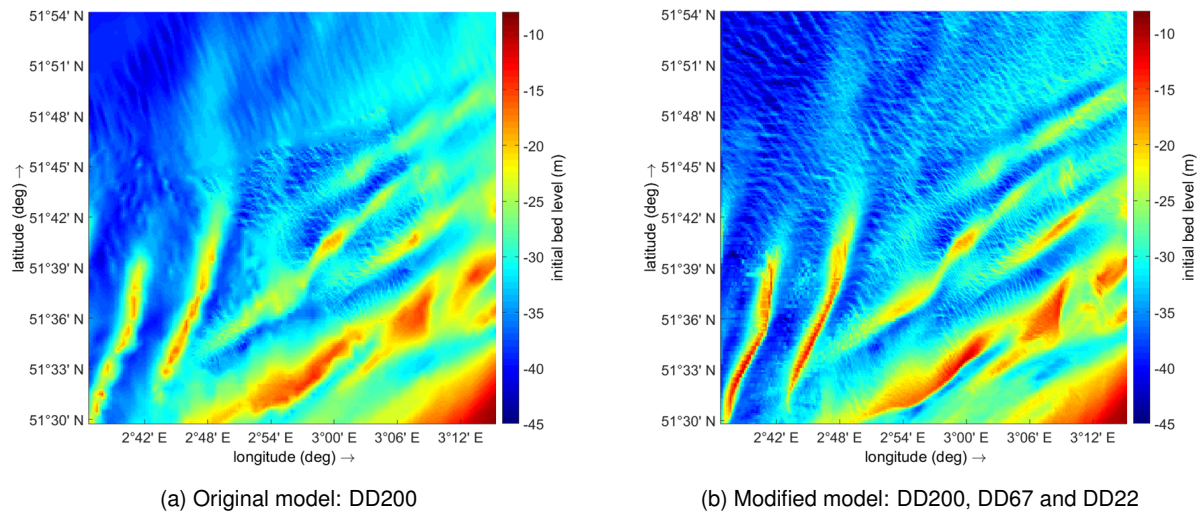


Figure 5.7.: Bathymetry original and modified model

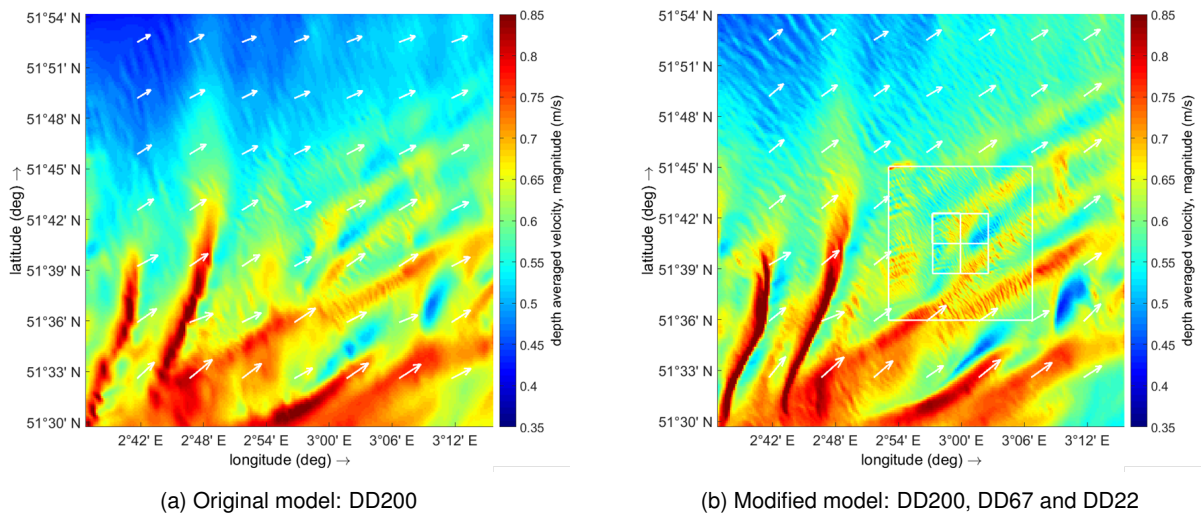


Figure 5.8.: Flood flow original and modified model

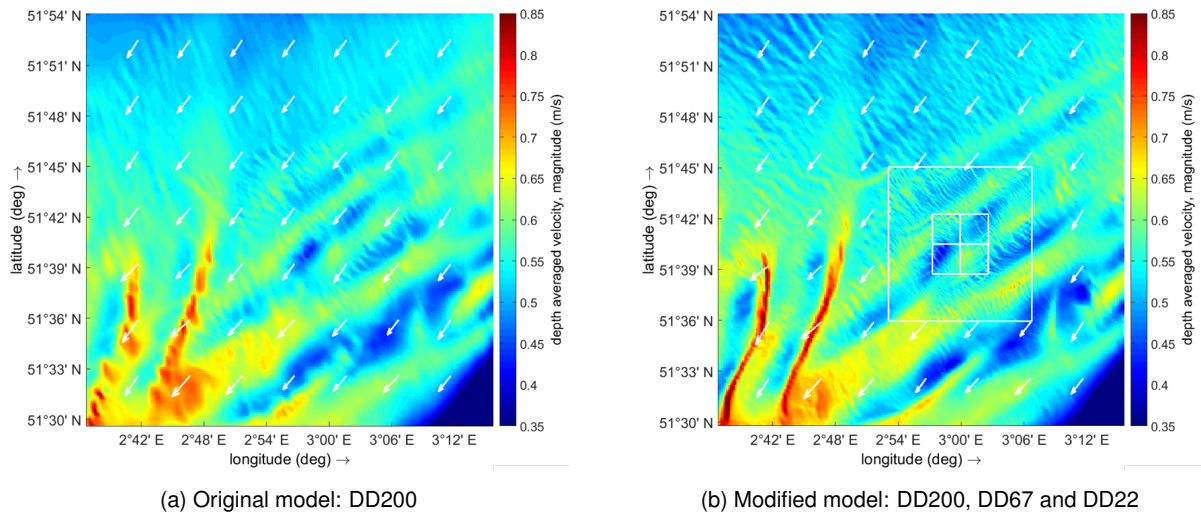


Figure 5.9.: Ebb flow original and modified model

5.3.2. Hydrodynamic processes

Figure 5.10a displays the bathymetry of the finest domains (DD22). The underlying tidal sand bank is present along the diagonal of the domain. On both sides deeper swales are present. Over this underlying seabed topography sand waves are present, and the hydrodynamics influencing the migration direction of these sand waves are discussed in this subsection. In the figures presenting the flood flow, ebb flow and the tide-averaged flow, the black line represent a depth of 30 m, being the transition between the top of the tidal sand bank and the deeper swales. Flood flow (fig. 5.10b) is directed towards the North-East, whereas the ebb flow is directed to the South-West (fig. 5.10c). The magnitudes during flood flow are higher compared with ebb flow, showing the asymmetry of the tidal signal in the domain. During flood flow the flow accelerates towards the top and decelerates from the top over the tidal sand bank, resulting in an area with low velocities behind the tidal sand bank in the direction of the flow. Furthermore the flow is directed around the tidal sand bank, which result in higher velocities around the top of the tidal sand bank. During ebb flow the same processes are observed only with lower velocity magnitudes. In addition, the higher flow velocities are not present on top of the tidal sand bank, only along the deeper swales. The flood and ebb flow result in tide-averaged flow directed in the ebb direction (fig. 5.10d). The colors indicate the magnitude of the tide-averaged velocities, distinguishing areas in which the flood flow and ebb flow are dominantly present. Low tide-averaged flow velocities are observed in areas where the asymmetry of the flood flow is relatively large and the flood flow is dominantly present (blue areas). Areas in which the ebb flow is dominantly present have relatively large magnitudes during ebb flow, resulting in tide-averaged flow velocities of around 5 mm/s (red areas). Due to the Coriolis effect the flow is deflected during flood and ebb flow to the right, enhanced by the presence of the tidal sand bank. The direction of the tide-averaged flow varies over the tidal sand bank.

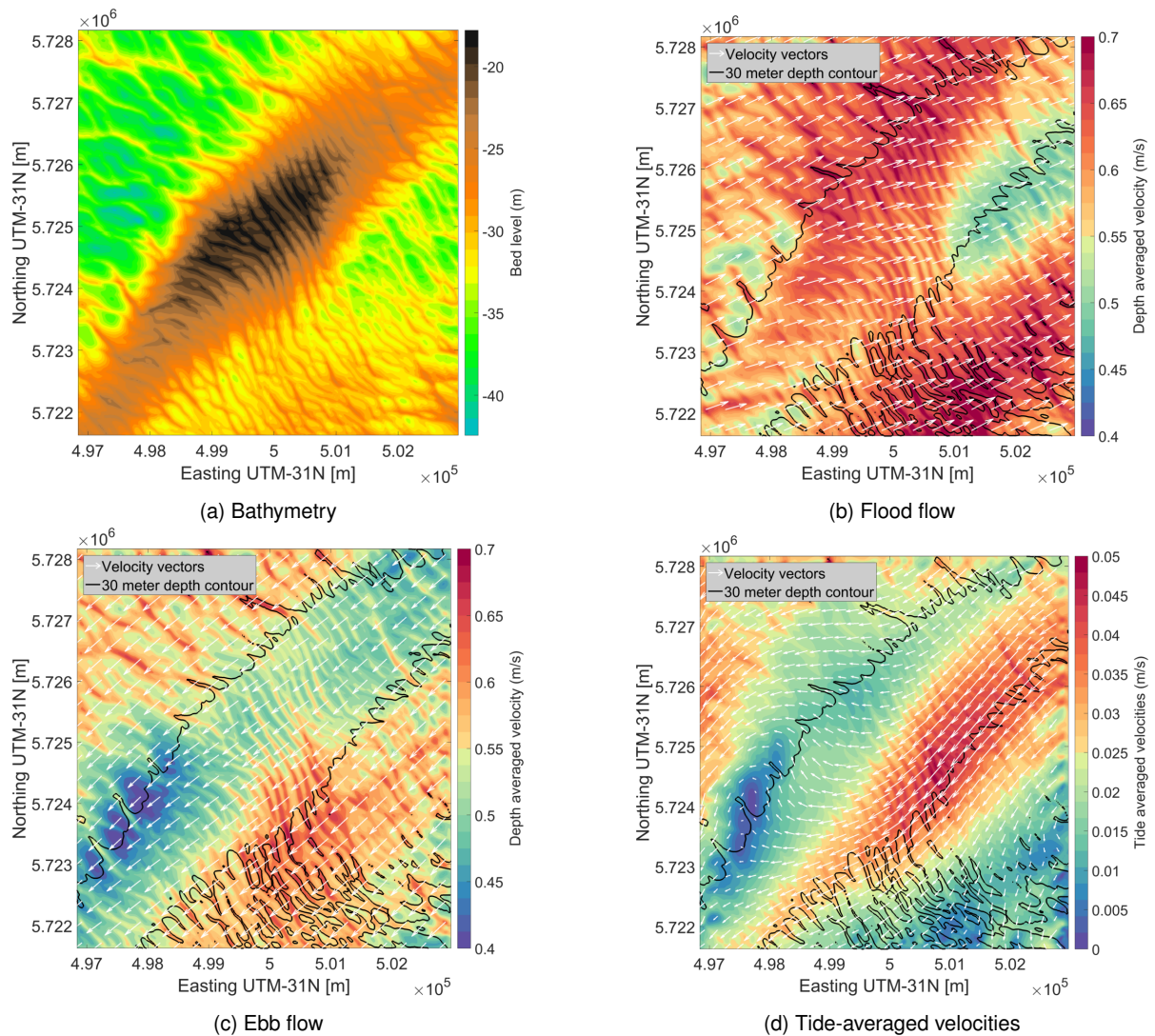


Figure 5.10.: Hydrodynamic processes

5.3.3. Sediment transports

In Figs. 5.11a and 5.11b, the tide-averaged sediment transport load magnitudes are shown for bed load and suspended load respectively. A variation in sediment load magnitudes is observed on the scale of sand waves and on the scale of the tidal sand bank. For sand waves, the magnitudes are higher at the sand wave crest compared to the trough of the sand wave. This is observed both on top of the tidal sand bank and in the deeper swales. For tide-averaged suspended load transport the magnitudes are also larger at the sand wave crest compared to the trough. However this is only observed for sand waves on top of the tidal sand bank. The magnitudes are very low in deeper parts of the swales. On the scale of the tidal sand bank the variation in magnitudes is related to areas in which the flood flow or ebb flow is dominantly present. For areas in which the flood flow is dominantly present, the flood flow has high magnitudes compared to the ebb flow. This results in high tide-averaged bed and suspended load transports and is observed at the left side of the tidal sand bank and the shallow part of the right swale. For the areas in which the ebb flow has relatively large magnitudes, the asymmetry is smaller and tide-averaged bed and suspended load transport have lower magnitudes.

When looking at the direction of the tide-averaged bed and suspended load transport vectors (figs. 5.11c and 5.11d), the influence of the tidal sand bank is again observed. Areas in which the direction is towards the North-East and areas in which the direction is towards the South-West can be distinguished. These areas can be related to the magnitude of the tide-averaged velocities and the interaction between the flood flow, ebb flow and the presence of the tidal sand bank. For areas in which the vector direction is in the direction of the

flood flow, the asymmetry of the tidal signal enhances sediment transport in this direction. Areas with vector directions in the ebb direction have higher tide-averaged velocities, indicating a higher ebb flow relative to the flood flow. Together with the longer duration of the ebb flow this result in tide-averaged sediment transport in the ebb direction. Within the area with bed load transport vectors approximately towards the South-West, a variation can be seen of the direction over the sand waves. At the crest the direction is towards 225 degrees (yellow patches), but in the troughs of the sand waves the light blue patches indicate transports towards approximately 150 degrees.

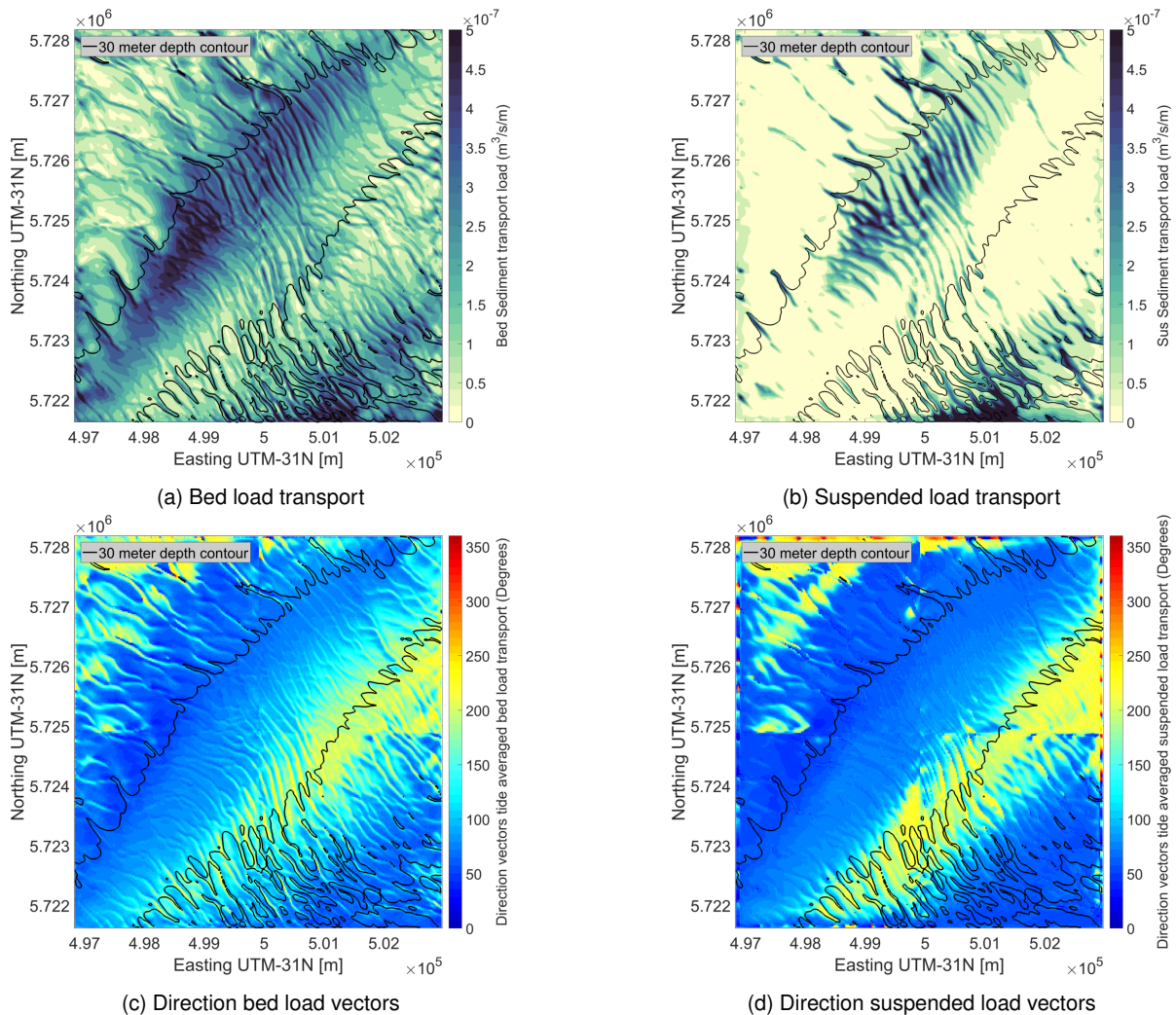


Figure 5.11.: Sediment transport and direction

5.3.4. Migration direction

In Fig. 5.12 the migration of sand waves is displayed, derived from the bed survey data from 2010 and 2015 by Deltares as explained in subsection 5.2.5. A transition between positive and negative migration direction is observed over the tidal sand bank. The transition is defined along a line directing towards the North over the tidal sand bank. Positive migration (blue) is defined as migration approximately towards the North-East and negative migration (red) approximately towards the South-West. It can be observed that over large part of the domain the migration speeds per year are small, indicated by the light blue and red color. This means that the tide-averaged sediment transports will be very small if only one tidal cycle is considered. To compare migration directions from the model results and from the data, areas in which the migration speed is higher compared to 1 m/year are distinguished. This is used in Fig. 5.13, to illustrate the transition in migration direction over the tidal sand bank.

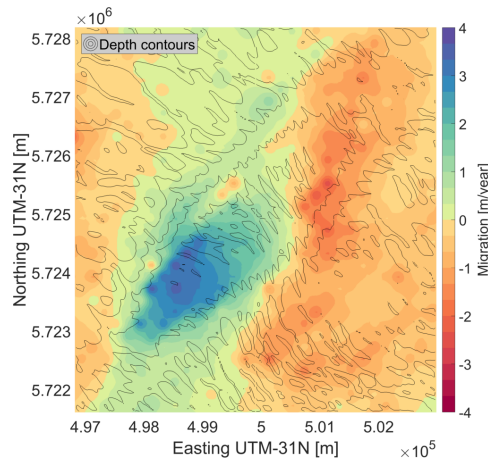


Figure 5.12.: Migration directions from data

Within the areas displayed with the black lines in Fig. 5.13 the migration is 1 m/year or higher, as explained above. In addition the vector magnitudes of the tide-averaged bed load and suspended load transport are plotted (figs. 5.13a and 5.13b). Within the contour lines showing positive migration from data towards the North-East, the magnitudes of the direction vectors are approximately 60 degrees, indicated by the dark blue color. For the contour line representing negative migration from data towards the South-West, the magnitudes of the direction vectors are approximately 220 degrees, indicated by the yellow color. This means that the tide-averaged bed and suspended load transport show a transition in direction over the tidal sand bank. Together with the maximum of the tide-averaged sediment transports at the sand wave crests presented in the subsection 5.3.3, the assumption can be applied explained in subsection 5.2.4. For the left side of the tidal sand bank the direction of the tide-averaged sediment vectors are directed towards the North-East, this indicate migration towards the North-East. With a similar reasoning migration towards the South-West is indicated at the right flank of the tidal sand bank in the model. The contour lines of the absolute migration speeds indicate a similar transition over the tidal sand bank.

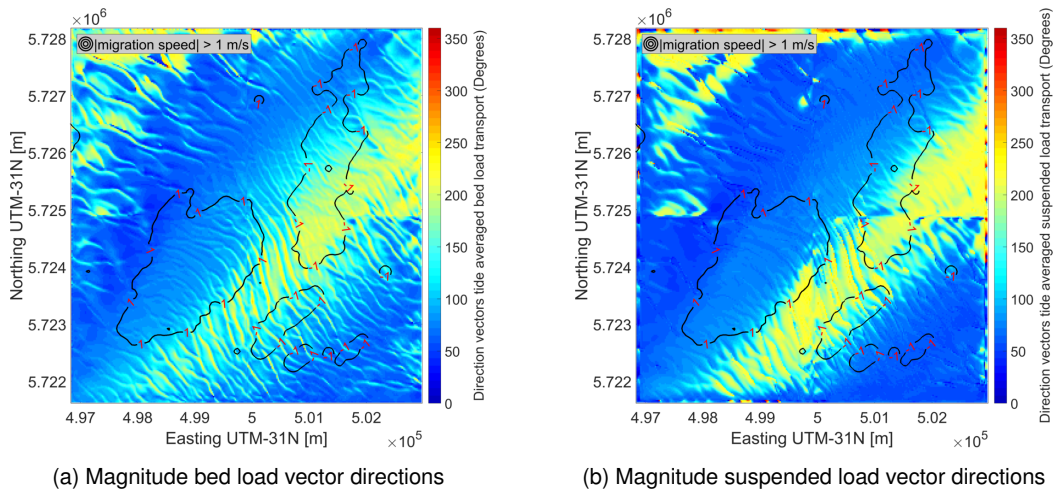


Figure 5.13.: Comparison migration direction model results and data

6 | Discussion

In this thesis the influence of underlying seabed topography on the migration direction of sand waves is showed in an idealized model. Finally a comparison with field data showed that also in a realistic model the transition of the indicative migration direction by the presence of a tidal sand bank is observed. In this chapter first the assumption regarding the model modification and inaccuracies of the idealized model are discussed. Secondly, the model technique *Domain Decomposition*, revealed some important aspects to take into account when modelling sand wave field dynamics in practice.

6.1. Assumptions and inaccuracy idealized model including underlying seabed topography

- **Sand wave length chosen equal to the Fastest Growing Mode**

As explained in the literature study, in complex numerical models the initial bed configuration is based on the assumption that sand waves are self organizational phenomenon under a certain forcing with a prevailing characteristic length scale known as the fastest growing mode. Depended on the initial deviation from the fastest growing mode and the randomized bathymetry the timescale of the consolidating process is up to 80 years. Because of the long computational time to model this phenomena this self organizational property is mimicked by running models with the same forcing and wave height but many different initial sand wave lengths, which reveal the fastest growing mode of that forcing situation. In the idealized model in chapter 4 the same wave length is used as in chapter 3, based on the fastest growing mode found in [Borsje et al. \(2014\)](#). This FGM is correct for a forcing situation with a depth of 25 m, sediment grain size of 350 μm , tidal velocity amplitude of 0.65 m/s and a sand wave height of 0.5 m. However in the idealized model with underlying seabed topography, it is expected that the varying water depth over the tidal sand bank result in different fastest growing modes over the tidal sand bank. Therefore if one is interested in the exact sand wave length over the tidal sand bank, a randomized initial bathymetry over the tidal sand bank should be imposed and run for a long period. In this way the fastest growing modes over the tidal sand bank prevail in the model. Since this required long computational times (up to 80 years), this is left out of consideration. The influence of the tidal sand bank however is expected to be the same, because the recirculating cell of sand wave is disturbed towards the top independent of the length of a sand wave.

- **Infinite long tidal sand bank**

The model modification showed in subsection 4.2.1, is based on the literature of a tidal sand bank of infinite extent. In this way the refined computational area around the tidal sand bank could be minimized, because the processes along the tidal sand bank of infinite extent are constant. However, due to the fact that the processes along the tidal sand bank are constant, three dimensional processes around a tidal sand bank are left out of consideration. Another possibility to mimick the tidal sand bank, is a tidal sand bank of finite extent. In both directions the finite tidal sand bank has an ending length within the area of consideration. This means that more insight is gained in the three dimensional processes around a tidal sand bank. This configuration of the tidal sand bank gives a more comparable situation with respect to reality. In this way a more realistic comparison can be made between the idealized model and a case study. The tidal sand bank of finite extent however demands large computational efforts and is therefore not considered in this study.

- **Fast-Fourier Transform along unidirectional transect defined for migration**

The idealized model with underlying seabed topography updates the bottom after one tidal cycle. In this way the amplitude of the sand waves on the tidal sand bank could be compared, using a Fast-Fourier Transform along a transect. This required short computational times because only one tidal cycle had to be modelled after spin-up of the model. However this approach disregards the three dimensional aspect of sand wave migration seen in the realistic case study. Also in the idealized case of adding a residual current on top of the tidal velocity signal, three dimensional properties of the tide-averaged flow are observed over the tidal sand bank. Therefore it is expected that after a long period migration direction also show three dimensional properties. Running for a long period gives insight in the three dimensional properties of sand wave migration over the tidal sand bank and therefore is a recommendation.

- **Asymmetry in the tide-averaged sediment transports over the tidal sand bank**

The tide-averaged sediment transports for the cases with symmetrical tidal boundary conditions are not exactly zero in the middle of the transect, along which the migration of sand waves is considered. This indicates an asymmetry around the tidal sand bank. The origin of the asymmetry in the tide-averaged sediment transports, can be found in an asymmetry in the tide-averaged flow pattern around the tidal sand bank. Apparently the flood and ebb flow are not exactly the same causing the tide averaged flow velocity in the flood direction to be larger compared to the tide-averaged flow velocities in the ebb direction. This could be a numerical error caused by an asymmetrical set-up of the initial bathymetry, or an influence of the assumed infinite far boundary conditions in combination with the Coriolis effect. The goal of the idealized model with underlying seabed topography however was to show that it is possible to have opposite migration directions of sand waves caused by the presence of a tidal sand bank. Because this inaccuracy does not influence the final conclusions of this thesis the exact reason of this asymmetry in the tide-averaged sediment transports is not investigated in more detail. Furthermore, if the tide-averaged sediment transport is exact zero in the middle of the transect, sand waves still migrate towards the top on both flanks of the tidal sand bank.

6.2. The step from idealized modelling to a field case

The most important shortcomings of the *Domain Decomposition* (hereafter:DD) model technique, revealed during this thesis, are the combination between computational errors and computational time. They are discussed separately below, more background on the modelling steps regarding DD is given in appendix C. Additionally the sediment grain size used and the direction of the sediment vectors are discussed.

- **Computational errors**

The transitions between the sub-domains in the modified model, result in grid refinement in the vertical and horizontal direction. Computational errors at the boundaries of the sub-domains are introduced due to this refinements in the model, regarding hydrodynamics and sediment transports. Regarding the hydrodynamics, a locally enlarged viscosity at the sub-domain boundaries reduced the hydrodynamic errors as explained in appendix C. The errors which are still present in the current model are outside the area of interest or small enough to assume that the hydrodynamics of the BWFZ are modelled correctly, subsection 5.3.1. The errors introduced regarding sediment transport, showed in appendix C, are unavoidable using the *Domain Decomposition* technique. The solution to exclude these errors, is to place the transition between the sub-domains well outside the area of interest. In the current model this is not possible because the computational effort is already very large and placing the boundaries of the finest model domain further away would result in a larger finest domain. A larger finest domain lead to unrealistic computational times. The errors in the sediment transport are mainly present in the magnitude close to the boundary between the DD67 and DD22 domain. Therefore it is assumed that the transition in migration direction over the tidal sand bank is not influenced by these boundary errors. However, for future research on sand waves field dynamics, these errors are an argument to consider other model techniques, such as Delft3D Flexible Mesh, to investigate sand waves.

- **Computational time**

The *domain decomposition* model technique runs the sub-domains in a parallel matter. This means that computational capacity of one virtual computer is used, and divided over the sub-domains defined. The domain decomposition model is not able to simulate on different virtual computers, and the efficiency of the model is thus determined by the distribution of the computational cells over the sub-domains. In the

modified model, the goal was to refine the resolution in the area of interest to a comparable resolution as the idealized model. This meant that 60 layers in the vertical and a horizontal resolution of 10 meter is aimed for. The amount of computational cells in the finest sub-domain covered 90 percent of the total amount of cells in all sub-domains in that situation. Because of this reason the DD computation became very inefficient, and a new horizontal and vertical resolution were necessary. To obtain simulation times in the order of days, the maximum time period considered in this thesis is 3 days.

- **Migration from data**

The in-house migration data of Deltares presented in this thesis, represents the mean value of the migration magnitudes found based on the bed surveys of the year 2010 and 2015. Apart from the mean migration value, maximum and minimum migration magnitudes are derived from the comparison of the same bed surveys. These maximum and minimum migration magnitudes show different transitions in the migration direction over the tidal sand bank compared with the transition presented in subsection 5.3.4. These maximum and minimum migration magnitudes are disregarded in the thesis, because the goal of the comparison was to show the presence of the transition. The exact migration direction of sand waves over the tidal sand bank is therefore not considered in this thesis.

- **Varying sediment grain size diameter over Borssele Wind Farm Zone**

The sediment grain size is variable over Borssele Wind Farm Zone. In general smaller water depths are accompanied by smaller sediment grain sizes of approximately 200 μm , larger sediment grain size of approximately 350 μm occur in larger water depths. In the current model one uniform grain size diameter of 350 μm , is assumed for all the sub-domains. To investigate the influence on the result for the DD model, a computation with one uniform value of 200 μm is run. The results obtained are similar. A model in which the sediment grain size diameter is varying over the area of interest is not investigated in this thesis.

- **Varying tide-averaged sediment transport vectors over the length of sand waves**

The assumption regarding the migration direction of sand waves in subsection 5.2.4 assumed sediment transports in one direction over the length of a sand wave. In the results of the model, areas in which the tide-averaged sediment vectors are directed towards the North-East and areas with tide-averaged sediment vectors towards the South-West are distinguished. However when looked in detail at tide-averaged bed load transport vectors, the vectors vary over the length of the sand waves for the area with the direction towards the South-West. In the trough of the sand wave the direction is approximately 150 degrees indicated by the light blue color. At the sand wave crest the yellow color indicate a direction of approximately 220 degrees. This variation is not taken into account determining the migration direction of sand waves in this thesis.

6.3. The domain decomposition model as engineering tool

When morphodynamic studies are executed for the design of an offshore wind farm, the model presented in this study is too computationally demanding to function as support in the sense of an engineering tool. In this section some aspects of consideration and opportunities are discussed with respect to this matter. A comparison is made between the model presented in chapter 5 and a depth averaged version of this model.

In the situation of designing an offshore wind farm, at least one bathymetric survey is assumed to be available, since in real projects this is expected to be always the case. Prior to modelling with the domain decomposition technique presented in this research the characteristics of the sand waves and possible additional bed forms (mega ripples and tidal sand banks), can be extracted from the bathymetry survey. Subsequently a model with a similar composition as the model presented in this thesis can provide insight in the net sediment transports and thereby indicative migration directions within an offshore wind farm location. However due to the many vertical layers, large computational efforts are required for relative short computational duration. In this way only a very small spatial model is possible which is not suitable for engineering applications.

A way to model for a longer duration would be to run the model depth averaged. In this way larger spatial scales and longer time periods can be considered. However it is the question whether the results are still correct. Therefore the model from chapter 5 is run in depth average mode. The model results are presented in appendix E.

The model results showed a similar transition in the net sediment transport and thereby indicative migration direction over the tidal sand bank. As a first indication of transitions in migration directions of sand waves a depth averaged model using the configuration presented in this thesis can therefore be used for a first indication over an offshore wind farm.

7 | Conclusions

In this research the migration direction of offshore sand waves is investigated to understand the hydro- and morphodynamic processes regarding the migration direction of offshore sand waves including underlying seabed topography. This resulted in the research questions introduced in the introduction and answered in this chapter. The first research question represents the migration direction over horizontal underlying seabed topography based on literature. Subsequently the main focus of this research is the inclusion of underlying seabed topography. Finally the gained knowledge is used to explain the obtained migration directions in the field case study.

7.1. Migration direction over horizontal underlying seabed topography

How do the strength, direction and phase shift of different tidal constituents relate to the migration direction of sand waves over a horizontal underlying bottom?

Symmetrical boundary conditions No migration is observed for a tidal boundary condition consisting solely of the S_2 -tide constituent. This can be explained by the symmetrical tide-averaged flow velocities with respect to the sand waves crest.

Asymmetrical boundary conditions Adding a residual current additional to a symmetrical tidal boundary condition, results in sand wave migration in the direction of the residual current. Due to the distortion of the recirculating cells of sand waves, the tide-averaged flow velocities are in the direction of the residual current over the entire sand wave.

Inclusion of the S_4 -tide constituent additional to the S_2 -tide constituent with a phase shift of 120 degrees results in an asymmetrical tidal velocity signal. The asymmetry of the tidal velocity signal results in larger horizontal velocities in one direction compared to the other one. Sediment transports are enhanced in that direction, due to a nonlinear relation between the flow velocity and sediment transport. The migration direction observed is in the direction with larger horizontal velocities. An additional tidal constituent, with a magnitude and phase shift, would result in a different asymmetry of the tidal velocity signal. The migration direction depends on the enhancement of sediment transports in a direction due to the asymmetry of the tidal velocity signal.

7.2. Migration direction over underlying seabed topography

What is the influence of underlying bed forms on the migration direction of sand waves?

Symmetrical boundary conditions The inclusion of a tidal sand bank in the idealized model, results in different tide-averaged horizontal flow patterns compared to the models with horizontal underlying bottom. Due to continuity and the deflection enhanced by the Coriolis effect of the tidal flow, a horizontal tide-averaged flow pattern around the tidal sand bank is generated. Parallel flow along both flanks of the tidal sand bank in opposite direction is observed. This results in tide-averaged flow components towards the top of the tidal sand bank on the scale of sand waves. Due to the disruption of the vertical recirculating cells of sand waves, the migration direction of sand waves is directed towards the top of the tidal sand bank for symmetrical tidal boundary conditions. Increasing the height of the tidal sand bank from 2 to 10 meters, resulted in a migration magnitude of almost a factor 10 higher. Decreasing the sediment grain size from 350 μm to 200 μm doubled the migration

magnitude. In all cases migration towards the top is observed.

Asymmetrical boundary conditions The horizontal tide-averaged flow pattern around the tidal sand bank is disturbed by the inclusion of a residual current. The tide-averaged flow on the scale of sand waves is in the direction of the residual current. Including a residual current results in migration of sand waves on both flanks of the tidal sand bank in the direction of the residual current. Depending on the flank looked at, the migration magnitude is different. On one flank the residual current is in the same direction as the tide-averaged flow for the symmetrical case, resulting in larger tide-averaged sediment transports and migration magnitudes. On the other flank of the tidal sand bank, the residual current is in the opposite direction compared to the tide-averaged flow in the symmetrical case, resulting in lower sediment transports and migration magnitudes.

Including the S_4 -tide constituent does not disturb the tide-averaged horizontal flow pattern around the tidal sand bank. On both flanks, the tide-averaged flow velocities are towards the top of the tidal sand bank. However due to the asymmetrical tidal velocity signal, horizontal velocities in one direction are larger. The nonlinear relation between the flow velocity and sediment transport enhances the sediment transports in that direction. Migration on the right side of the tidal sand bank has a larger magnitude towards the top of the tidal sand bank compared with migration for the symmetrical tidal velocity signal. The positive migration on the left flank is lowered due to the asymmetrical tidal velocity signal.

7.3. Borssele migration direction

How can the migration direction of sand waves observed in Borssele Wind Farm Zone be explained, using the case study of Borssele?

The tidal velocity signal is asymmetrical in the flood direction. Furthermore the ebb flow has a longer duration compared to flood flow. The flow is directed around the tidal sand bank through the deeper swales, resulting in higher flow velocities around the tidal sand bank during both flood and ebb flow compared to the top and the back side of the tidal sand bank. Due to the asymmetry in the flood direction, larger parts of the tidal sand bank have higher flow velocities during flood compared to ebb flow. In both direction the acceleration and deceleration of the flow, due to the presence of the tidal sand bank, result in areas with lower flow velocities behind the tidal sand bank. In general this interaction between flood flow, ebb flow and the tidal sand bank, result in tide-averaged flow velocities in the ebb direction with a varying angle over the tidal sand bank. Areas differ in magnitude of the tide-averaged flow velocities due to the asymmetry in the tidal velocity signal.

The areas in which the ebb flow is dominantly present, result in tide-averaged sediment transport and vector directions in the ebb direction, indicating migration of offshore sand waves towards the South-East. Areas in which the asymmetry of the tidal signal in the flood direction is dominant, result in tide-averaged sediment transport and vector directions in the flood direction indicating migration of offshore sand waves towards the North-West.

The transition of the indicative migration direction of offshore sand waves from the model result can be linked to the presence of the tidal sand bank in the domain as seen for the idealized model with underlying seabed topography. The presence of the tidal sand bank influence the hydrodynamics by creating areas in which the tide-averaged sediment transport in the ebb direction are enhanced and areas in which the tide-averaged sediment transports in the flood direction are enhanced. In this way a transition in the migration direction over the tidal sand bank is observed. The migration directions from the model results and migration direction from data show a comparable transition over the tidal sand bank.

8 | Recommendations

Based on the discussion and conclusions presented in Chapters 6 and 7 respectively, recommendations are made regarding modelling the migration direction of sand waves and future research.

8.1. Idealized model underlying seabed topography

- **Spring-neap** The idealized model results in this thesis are based on output of one tidal cycle. Forcing the model with typical spring-neap cycles is expected to give more insight in sand wave migration behaviour over a spring-neap cycle. In this way a step can be made towards understanding the long term sand wave migration in idealized form.
- **Tidal sand bank of finite extent** The tidal sand bank mimicked in this thesis is the tidal sand bank of infinite extent. Modelling a tidal sand bank of finite extent gives more insight into three-dimensional processes around tidal sand banks. Also the possibility to model multiple tidal sand banks in idealized form becomes relevant choosing the tidal sand bank of finite extent.

8.2. Modelling sand wave migration direction in practice

- **Long term migration direction**
In this study the migration direction of sand waves is based on the tide-averaged sediment transport over one tidal cycle. During the computation the bottom is not updated. Furthermore the morphodynamic changes are not multiplied by a factor, known as a MORFAC (morphodynamic factor). Modelling with typical spring-neap cycles together with the use of a MORFAC and bottom updates, is expected to provide the step from an indicative migration direction towards migration direction determined by movement of the bottom.
- **Comparison data and results**
To investigate the migration direction in practice, longer computational times are required. Furthermore a similar post-processing technique as the in-house data study from Deltares have to be developed for the model results. In this way migration directions from model results can accurately be compared with the migration directions from data-driven analysis.
- **Variation tide-averaged sediment transport vector direction**
It is recommended to investigate the period and processes of the variation of the tide-averaged sediment transport direction over sand waves. This is a reason why the indicative migration direction was hard to determine for the additional locations investigated within BWFZ (appendix D). Knowing the period of these variations, a duration can be determined over which sand waves have to be modelled. In this way sediment transports can be averaged to obtain the migration direction in which the variation of sediment transport are taken into account.

- **Surface gravity waves**

In the current model set up, surface gravity waves are not taken into account. Surface gravity waves in the form of storms influence the sediment transports at the time of occurrence. When surface gravity waves (storms) only occur during a certain period of a spring-neap cycle, the sediment transports at that moment are influenced. It is expected that the tide-averaged sediment transport are influenced, because the sediment transports are only enhanced for a certain period. In this way certain directions during the tidal cycle experience relatively larger sediment transports. It is recommended to investigate the influence of typical storm events (direction, duration) on the migration direction of sand waves.

8.3. Future Research

Summarizing, the next step in investigating the migration direction of sand waves is modelling for a longer period with bottom updates. For post-processing, a technique is required to accurately compare migration direction from the model with migration direction obtained from data analyses. Alternative modelling techniques might be considerable when modelling larger areas for longer periods. The discussion with respect to the computational errors and time are arguments to consider alternative modelling techniques. A requirement for the model technique is that large scale processes of the entire North Sea can be coupled to smaller scale processes to model sand wave migration while preserving one computational grid. In this way the computation can be computed by many different virtual computers and longer computation (spring-neap cycle) become realistic. Delft3D Flexible Mesh is expected to be a solution to do this. However currently the morphodynamic module is not yet fully integrated.

References

- Bagnold, R. A. (1956). The flow of cohesionless grains in fluids. *Philosophical Transactions of the Royal Society of London. Series A, Mathematical and Physical Sciences*, 235–297.
- Besio, G., Blondeaux, P., Brocchini, M., Hulscher, S. J., Idier, D., Knaapen, M., . . . Vittori, G. (2008). The morphodynamics of tidal sand waves: a model overview. *Coastal engineering*, 55(7-8), 657–670.
- Besio, G., Blondeaux, P., Brocchini, M., & Vittori, G. (2003b). Migrating sand waves. *Ocean Dynamics*, 53(3), 232–238.
- Besio, G., Blondeaux, P., Brocchini, M., & Vittori, G. (2004). On the modeling of sand wave migration. *Journal of Geophysical Research: Oceans*, 109(C4).
- Besio, G., Blondeaux, P., & Frisina, P. (2003a). A note on tidally generated sand waves. *Journal of Fluid Mechanics*, 485, 171–190.
- Besio, G., Blondeaux, P., & Vittori, G. (2006). On the formation of sand waves and sand banks. *Journal of Fluid Mechanics*, 557, 1–27.
- Blondeaux, P., & Vittori, G. (2005a). Flow and sediment transport induced by tide propagation: 1. the flat bottom case. *Journal of Geophysical Research: Oceans*, 110(C7).
- Blondeaux, P., & Vittori, G. (2005b). Flow and sediment transport induced by tide propagation: 2. the wavy bottom case. *Journal of Geophysical Research: Oceans*, 110(C8).
- Blondeaux, P., & Vittori, G. (2016a). A model to predict the migration of sand waves in shallow tidal seas. *Continental Shelf Research*, 112, 31–45.
- Blondeaux, P., Vittori, G., & Mazzuoli, M. (2016b). Pattern formation in a thin layer of sediment. *Marine Geology*, 376, 39–50.
- Borsje, B. W., de Vries, M. B., Bouma, T. J., Besio, G., Hulscher, S. J., & Herman, P. M. (2009). Modeling bio-geomorphological influences for offshore sandwaves. *Continental Shelf Research*, 29(9), 1289–1301.
- Borsje, B. W., Kranenburg, W., Roos, P. C., Matthieu, J., & Hulscher, S. J. (2014). The role of suspended load transport in the occurrence of tidal sand waves. *Journal of Geophysical Research: Earth Surface*, 119(4), 701–716.
- Borsje, B. W., Roos, P. C., Kranenburg, W., & Hulscher, S. J. (2013). Modeling tidal sand wave formation in a numerical shallow water model: The role of turbulence formulation. *Continental shelf research*, 60, 17–27.
- Campmans, G. H. P., Roos, P. C., de Vriend, H. J., & Hulscher, S. J. (2017). Modeling the influence of storms on sand wave formation: A linear stability approach. *Continental shelf research*, 137, 103–116.
- Cherlet, J., Besio, G., Blondeaux, P., Van Lancker, V., Verfaillie, E., & Vittori, G. (2007). Modeling sand wave characteristics on the Belgian Continental Shelf and in the Calais-Dover Strait. *Journal of Geophysical Research: Oceans*, 112(C6).
- Choy, D. Y. (2015). Numerical modelling of the growth of offshore sand waves: a delft3d study (master of science thesis).

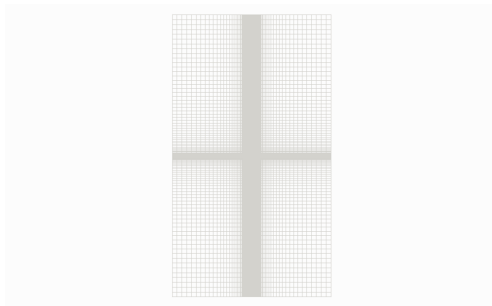
- Deltares. (2008). *Sand waves dynamics Bligh Bank* (Tech. Rep. No. H5239). Delft:Deltares.
- Deltares. (2015a). *Morphodynamics of Belwind ii offshore wind farm* (Tech. Rep. No. 1210493-00-HYE-0006). Delft:Deltares.
- Deltares. (2015b). *Site studies wind farm zone borssele, metocean study for borssele wind farm zone site 1* (Tech. Rep. No. 1210467-000-HYE010). Delft:Deltares.
- Deltares. (2016a). *Morphodynamics of borssele wind farm zone wfs-iii, wfs-iv and wfs-v update version january 25th, 2016* (Tech. Rep. No. 1210520-000-HYE-0012). Delft:Deltares.
- Deltares. (2016b). *Morphodynamics of Hollandse Kust (zuid) wind farm zone* (Tech. Rep. No. 1230851-000-HYE-0003). Delft:Deltares.
- Deltares. (2017). Simulation of multi-dimensional hydrodynamic flows and transport phenomena, including sediments. user manual. [Computer software manual]. (Version 3.15)
- Dodd, N., Blondeaux, P., Calvete, D., De Swart, H. E., Falqués, A., Hulscher, S. J., ... Vittori, G. (2003). Understanding coastal morphodynamics using stability methods. *Journal of coastal research*, 849–865.
- Energieonderzoek Centrum Nederland. (2017). Nationale energieverkenning 2017.
- Gerkema, T. (2000). A linear stability analysis of tidally generated sand waves. *Journal of Fluid Mechanics*, 417, 303–322.
- Hulscher, S. J. (1996). Tidal-induced large-scale regular bed form patterns in a three-dimensional shallow water model. *Journal of Geophysical Research: Oceans*, 101(C9), 20727–20744.
- Huthnance, J. M. (1982). On one mechanism forming linear sand banks. *Estuarine, Coastal and Shelf Science*, 14(1), 79–99.
- Knaapen, M. A., Hulscher, S. J., Vriend, H. J., & Stolk, A. (2001). A new type of sea bed waves. *Geophysical Research Letters*, 28(7), 1323–1326.
- Komarova, N. L., & Hulscher, S. J. (2000). Linear instability mechanisms for sand wave formation. *Journal of Fluid Mechanics*, 413, 219–246.
- Lesser, G., Roelvink, J., Van Kester, J., & Stelling, G. (2004). Development and validation of a three-dimensional morphological model. *Coastal engineering*, 51(8), 883–915.
- Matthieu, J., Borsje, B. W., Raaijmakers, T., Hasselaar, R. W., & Hulscher, S. J. M. H. (2013). *Self-organizational properties of tidal sand wave fields*. (Deltares)
- Matthieu, J., & Raaijmakers, T. (2012). Interaction between offshore pipelines and migrating sand waves. In *Asme 2012 31st international conference on ocean, offshore and arctic engineering* (pp. 203–209).
- Morelissen, R., Hulscher, S. J., Knaapen, M. A., Németh, A. A., & Bijker, R. (2003). Mathematical modelling of sand wave migration and the interaction with pipelines. *Coastal Engineering*, 48(3), 197–209.
- Németh, A., Hulscher, S. J., & Van Damme, R. M. (2006). Simulating offshore sand waves. *Coastal Engineering*, 53(2-3), 265–275.
- Németh, A. A., Hulscher, S. J., & de Vriend, H. J. (2002). Modelling sand wave migration in shallow shelf seas. *Continental Shelf Research*, 22(18), 2795–2806.
- Netherlands Enterprise Agency. (2015). Offshore wind energy in the Netherlands the roadmap from 1,000 to 4,500 MW offshore wind capacity.
- Roos, P. C., & Hulscher, S. J. (2003). Large-scale seabed dynamics in offshore morphology: Modeling human intervention. *Reviews of geophysics*, 41(2).
- Sekine, M., & Parker, G. (1992). Bed-load transport on transverse slope. i. *Journal of Hydraulic Engineering*, 118(4), 513–535.

- Sterlini-van der Meer, F. M. (2009). *Modelling sand wave variation*. University of Twente.
- Tonnon, P., Van Rijn, L., & Walstra, D. (2007). The morphodynamic modelling of tidal sand waves on the shoreface. *Coastal Engineering*, 54(4), 279–296.
- van den Berg, J., Sterlini, F., Hulscher, S. J., & Van Damme, R. (2012). Non-linear process based modelling of offshore sand waves. *Continental shelf research*, 37, 26–35.
- Van Gerwen, W. (2016). *Modelling the equilibrium height of offshore sand waves* (master of science thesis).
- van Gerwen, W., Borsje, B. W., Damveld, J. H., & Hulscher, S. J. (2018). Modelling the effect of suspended load transport and tidal asymmetry on the equilibrium tidal sand wave height. *Coastal Engineering*, 136, 56–64.
- Van Oyen, T., & Blondeaux, P. (2009a). Grain sorting effects on the formation of tidal sand waves. *Journal of Fluid Mechanics*, 629, 311–342.
- Van Oyen, T., & Blondeaux, P. (2009b). Tidal sand wave formation: Influence of graded suspended sediment transport. *Journal of Geophysical Research: Oceans*, 114(C7).
- Van Rijn, L., Walstra, D., & Van Ormondt, M. (2004). Description of transpor 2004 (tr2004) and implementation in delft3d online, rep. Z3748, *Delft Hydraulics, Delft, The Netherlands*.
- van Rijn, L. C. (2007). Unified view of sediment transport by currents and waves. ii: Suspended transport. *Journal of Hydraulic Engineering*, 133(6), 668-689. doi: 10.1061/(ASCE)0733-9429(2007)133:6(668)
- Verboom, G. K., & Slob, A. (1984). Weakly-reflective boundary conditions for two-dimensional shallow water flow problems. In *Finite elements in water resources* (pp. 621–633). Springer.
- Walstra, D., Van Rijn, L., Van Ormondt, M., Brière, C., & Talmon, A. (2007). The effects of bed slope and wave skewness on sediment transport and morphology. In *Coastal sediments' 07* (pp. 137–150).
- Wen-Bin, J., & Mian, L. (2011). Application of grid-nesting technique to sandwave migration simulation i-ultra-high resolution 3d current simulation. *Chinese Journal of Geophysics*, 54(5), 712–724.
- Wen-Bin, J., Mian, L., Yong, L., Feng-Xin, F., & Jun, Y. (2014). Application of grid-nesting technique on sandwaves migration simulation iisandwaves migration in northern South China sea. *Chinese Journal of Geophysics*, 57(3), 355–368.

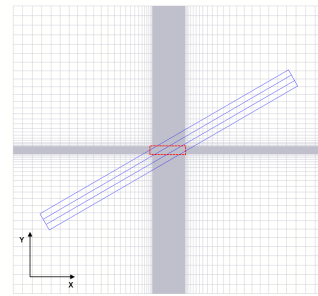
Appendices

A | Grid study tidal sand bank

For an equal sand bank length, an extra expansion in the y-direction of 22.5 kilometer is tested. The total width outside of the refined area is in this case 45 kilometers (fig. A.1a). The hydrodynamic results obtained stay the same compared with an expansion of 22.5 kilometers at both sides of the refined area (fig. A.1b). Therefore to keep the computational times in the order of 12-15 hours, the grid width is 22.5 kilometers extra in the y-direction at both sides of the refined grid area. Furthermore different tidal sand bank lengths are tested with the 22.5 kilometer expansion (fig. A.2). The initial bed level is not accurate for the long tidal sand bank compared to the middle length, because the long tidal sand bank reaches the very large computational cells far outside the refined area (fig. A.2 c). The short length (fig. A.2 a) showed large deviations in the tide-averaged velocity compared with the longest tidal sand bank representation. The middle long tidal sand wave is chosen in this thesis based on accurate initial bed level representation and small changes in hydrodynamic results compared with the very long tidal sand bank. (0.05 mm/s difference with respect to total magnitude of 5 mm/s for tide-averaged flow velocities)

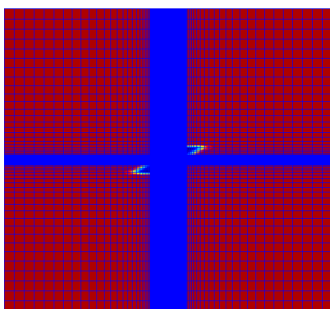


(a) Topview grid with expansion y-direction of 45 km at both sides refined area

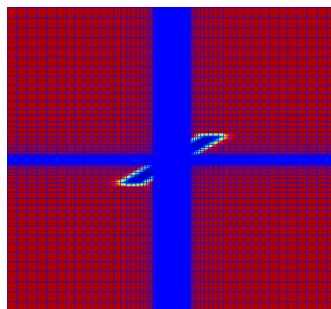


(b) Topview grid with expansion y-direction of 22.5km at both sides refined area

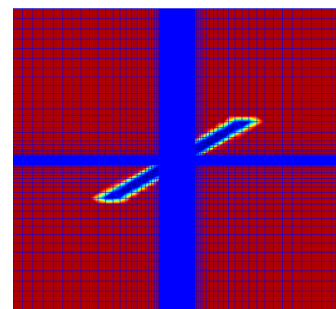
Figure A.1.: Grid aspect y-direction expansion



(a) Short length tidal sand bank



(b) Middle length tidal sand bank



(c) Long length tidal sand bank

Figure A.2.: Different tidal sand bank lengths

B | Hydrodynamics Case I,II,III and IV

B.1. Case I

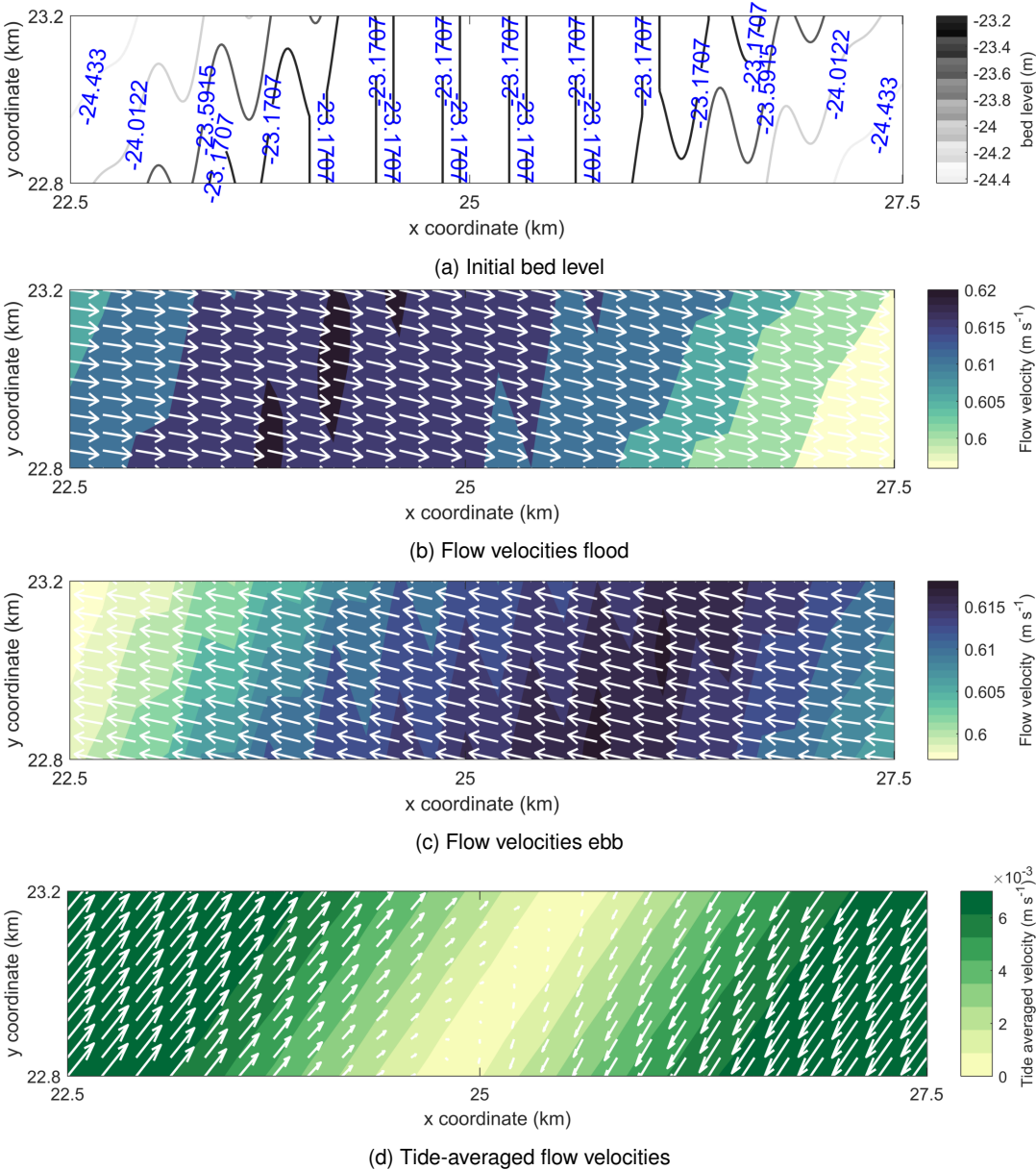


Figure B.1.: Hydrodynamics Case I

B.2. Case II

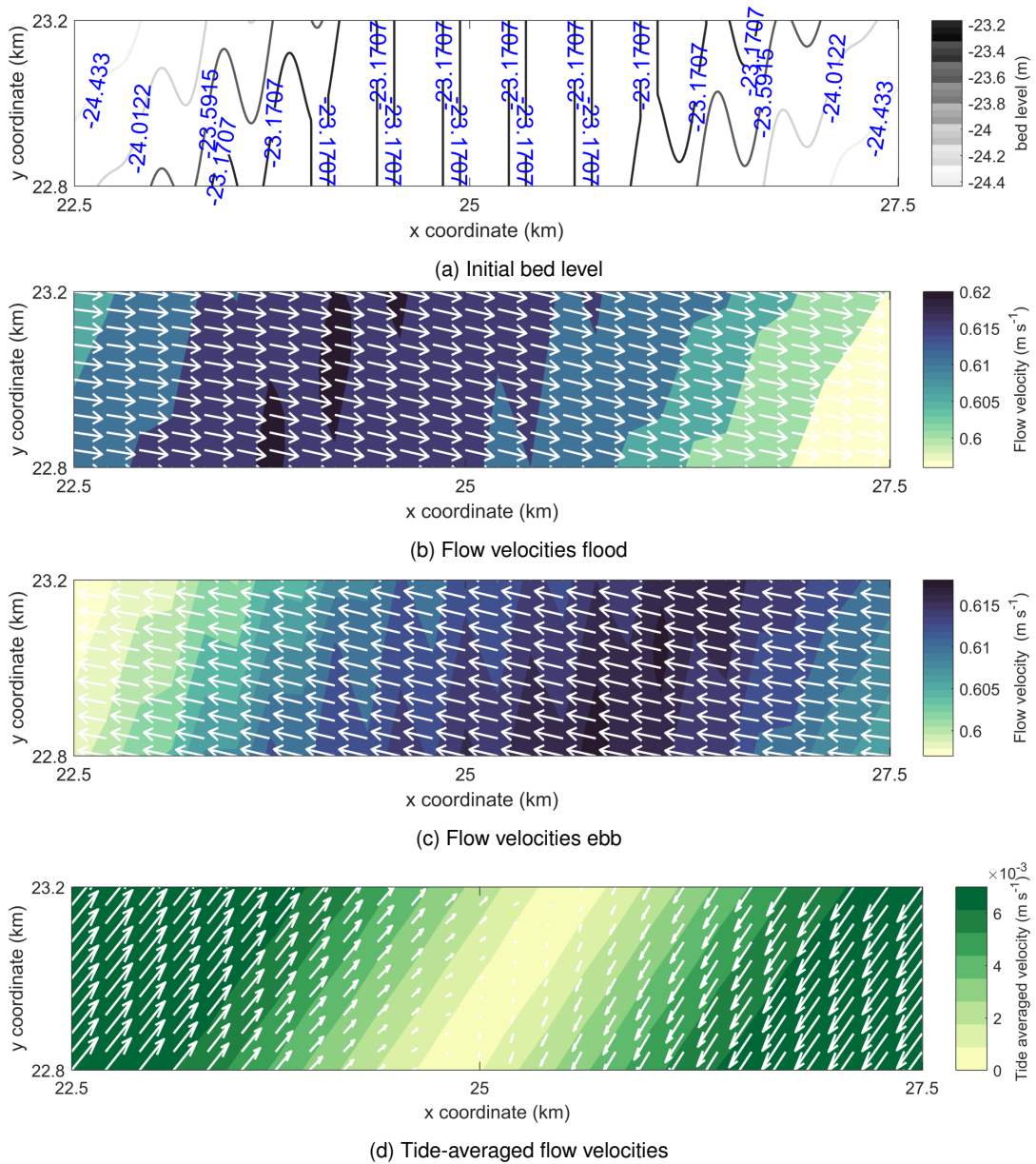


Figure B.2.: Hydrodynamics Case II

B.3. Case III

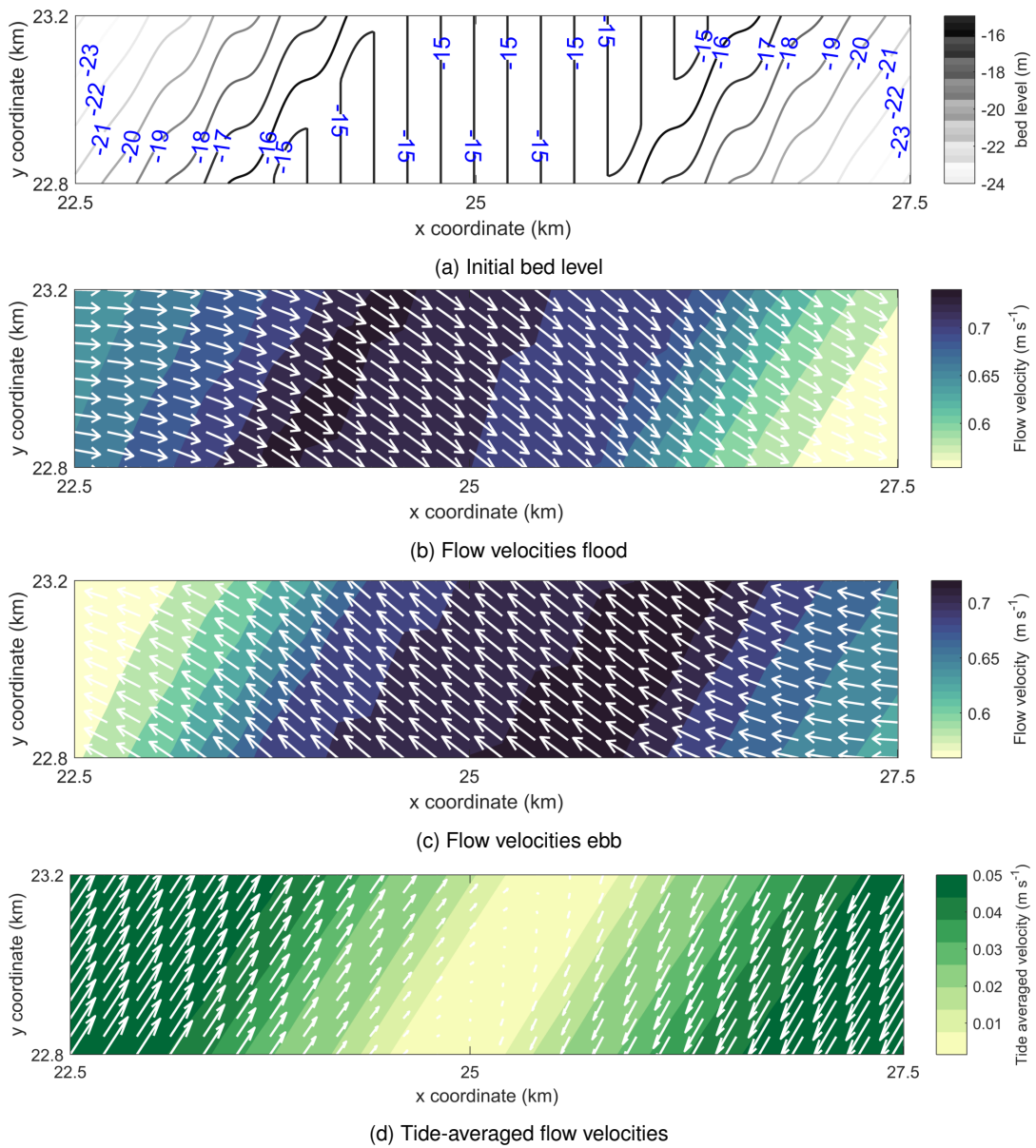


Figure B.3.: Hydrodynamics Case III

B.4. Case IV

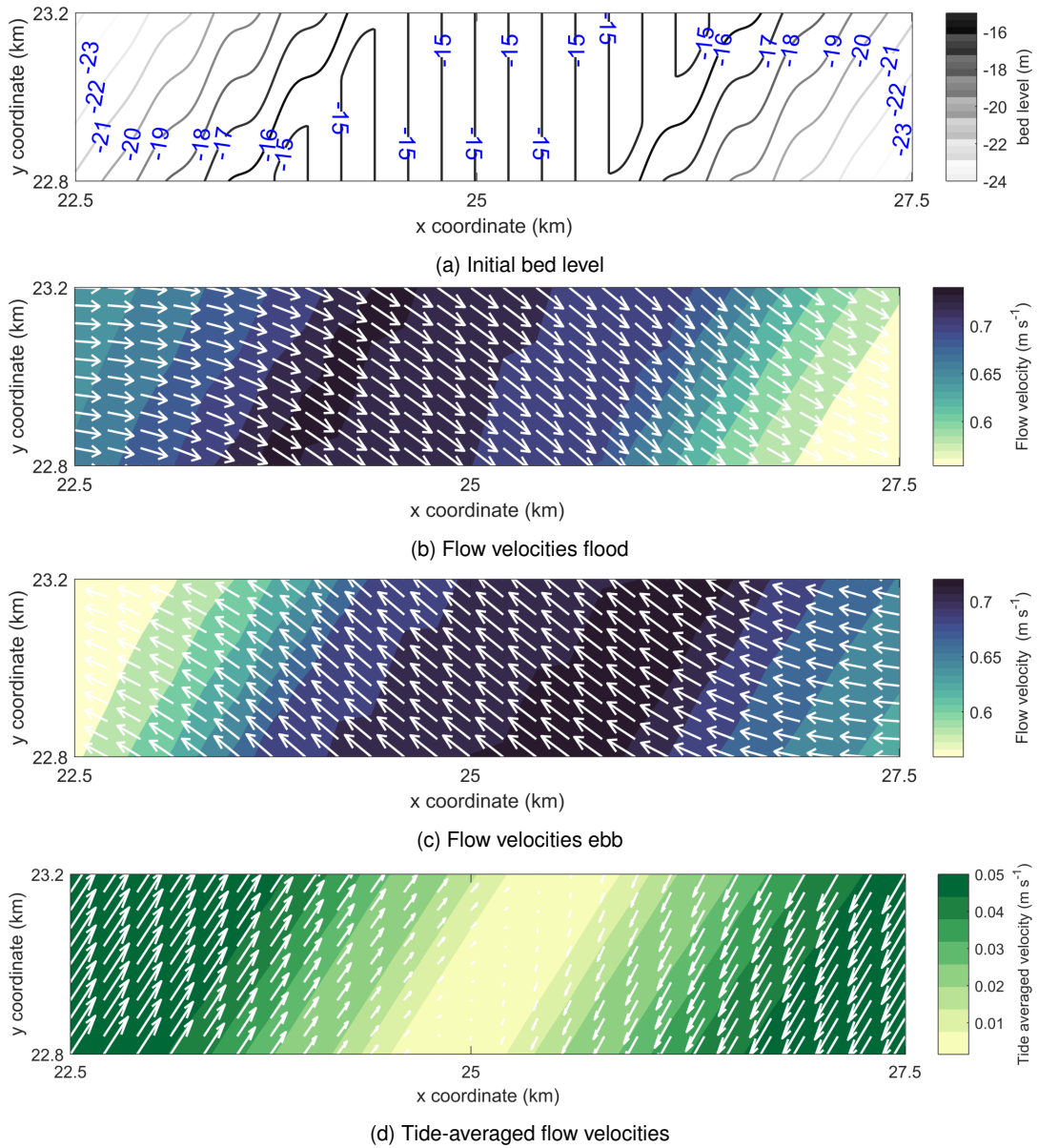


Figure B.4.: Hydrodynamics Case IV

C | Discussion Domain Decomposition

Regarding the set-up of the domain decomposition model several decisions are made, explained in this appendix. Furthermore some side notes on the results of the domain decomposition model are important interpreting the results.

- Increased viscosity on domain boundaries for hydrodynamic results influencing the model resolution
- Subdividing finest domain
- New vertical resolution
- Sediment concentration over domain decomposition boundaries

Increased viscosity on domain boundaries for hydrodynamic results influencing the model resolution

In the original model the viscosity on the domain boundaries is increased to avoid hydrodynamic errors to pass along the domain decomposition boundaries. In the new model this numerical approach is also applied fig. C.1. The enlargement of the viscosity locally at the domain decomposition boundaries required a small time step. In the first model set-up with the same resolution as the idealized model with underlying seabed topography (10 m horizontally and 60 vertical layers), this resulted in unrealistic simulation times of around one month. To be able to apply the numerical approach and a small enough time step, a reduced resolution in the horizontal direction was required. Therefore the resolution of DD67 and DD22 are chosen.

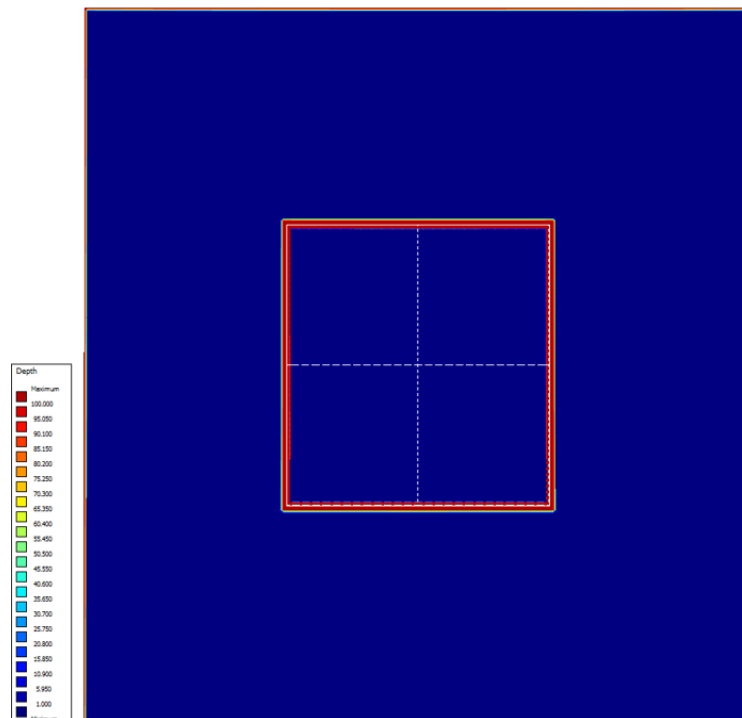


Figure C.1.: Enlarged viscosity domain decomposition boundaries

Subdividing finest domain

With the new horizontal resolution, the computational times were still in the order of half a month. The reason is that domain decomposition makes use of a parallel modelling approach of the sub domains. Therefore it is not possible to run the model on multiple cores. This can be explained by the fact that the parallel approach is already encoded in the domain decomposition model technique and an additional parallel approach is not possible. The solution to reduce the computational time, is to divide the computational effort over more sub domains, in this way the parallel approach is mimicked. Therefore the finest domain is divided into four sub domains.

New vertical resolution

With the new horizontal resolution and the four sub domains in the finest model domain, the computational times were still in the order of 1 week, which is not desirable. Therefore it was checked and shown that the important processes are still modelled in the idealized model with less vertical layers (fig. C.2). In the final configuration of the DD model therefore 20 vertical layers are applied.

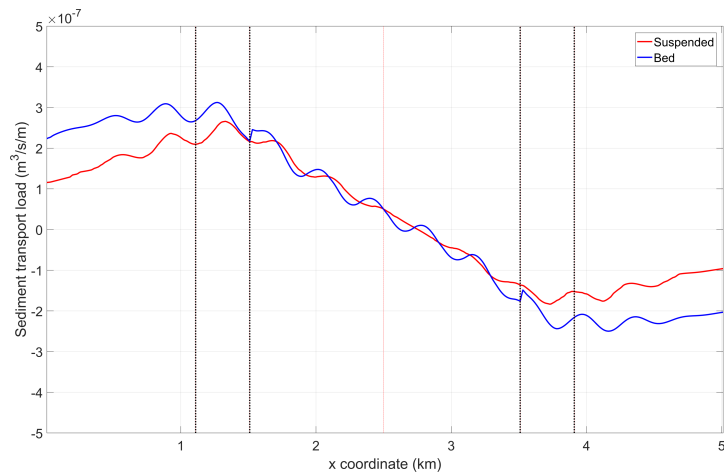


Figure C.2.: Sediment transport rates domain 20 layers

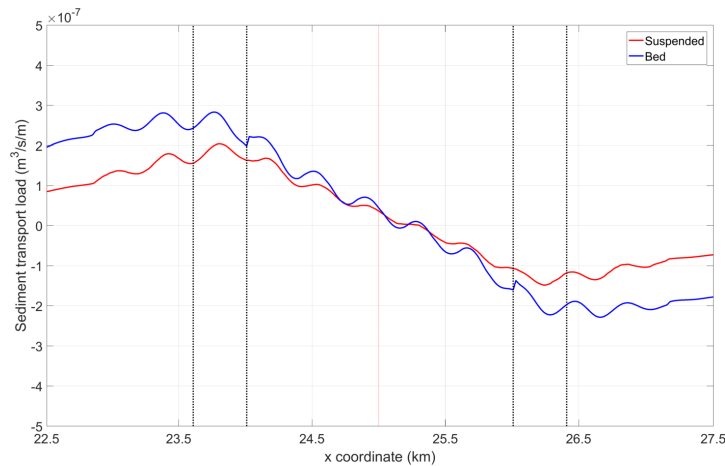


Figure C.3.: Sediment transport rates domain 60 layers

Sediment concentration over domain decomposition boundaries

The sediment concentration during flood flow and ebb flow are shown in figs. C.4 and C.5 respectively. The layer near the bottom of the DD67 and the DD22 are shown, which have a different vertical dimension because the DD67 domain has 10 layers and the DD22 domain has 20 layers. So the comparison is not at the same water depth, however it shows that the sediment concentrations are not smoothly transmitted between the two finest domains. This introduces errors in the sediment transports at the boundaries, which have to be kept in mind interpreting the results.

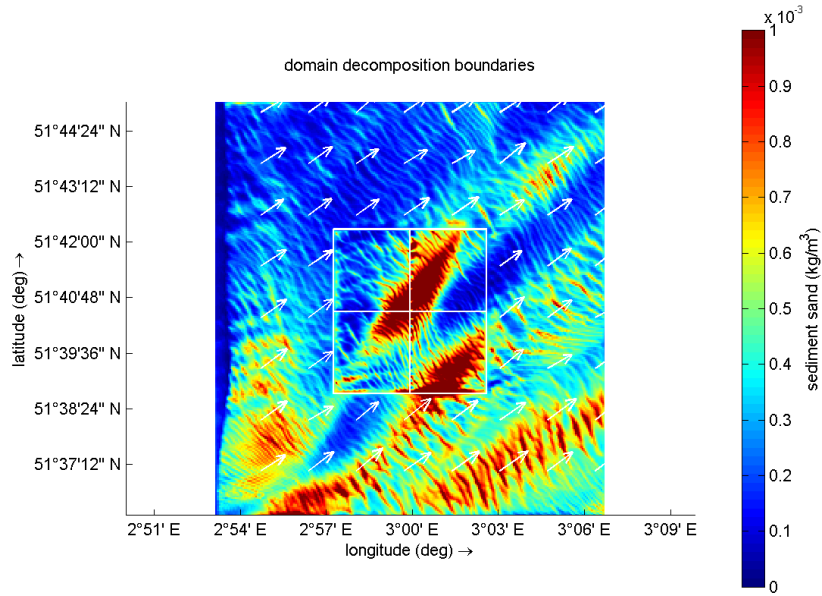


Figure C.4.: Sediment concentrations during flood flow

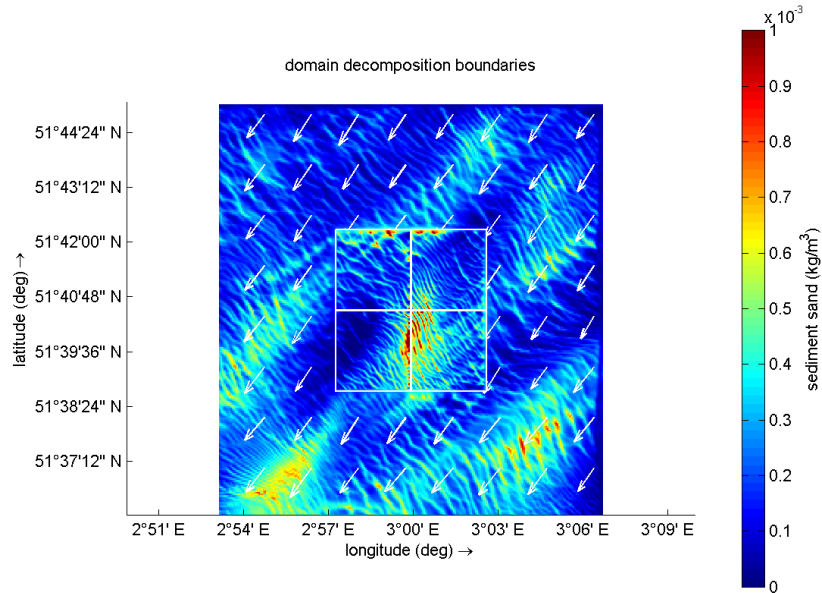


Figure C.5.: Sediment concentrations during ebb flow

D | Results other locations

On the next pages the results regarding the other locations within Borsselle Wind Farm Zone are presented. The influence of underlying bed forms can be seen in the magnitudes of the tide-averaged velocities. Areas in which the flood flow is dominant can be distinguished from areas in which the ebb flow is dominant. The transition in tide-averaged velocities show good comparison with the transitions observed in the migration directions from data. However conclusions regarding the migration direction of sand waves within the other locations are difficult to make. The magnitudes of the direction vectors show a larger variation over the areas. Therefore the assumption regarding indicative migration direction is not valid. The boundaries of the sub-domains furthermore show a larger influence on the sediment vector direction magnitudes compared with the location presented in the main report. The reason for the variation of the vector magnitudes over the area may be the less significant height of the underlying seabed topography.

An additional effect which makes it difficult to draw a conclusion within the other locations is the fact that the underlying bed forms are not entirely present within the area with finest resolution. The finest sub-domain becomes too large when these underlying bed forms are included fully, resulting in too high computational efforts. Summarizing, The influences of the underlying bed forms is noticed in the other location within BWFZ. However conclusions regarding the migration direction of sand waves are difficult to draw because the underlying bed forms are less significant in height and not entirely present within the finest domain. Additionally some of the underlying seabed topography is located outside BWFZ where no migration data is available. A comparison between migration direction based on modelling and migration direction based on data is therefore not possible.

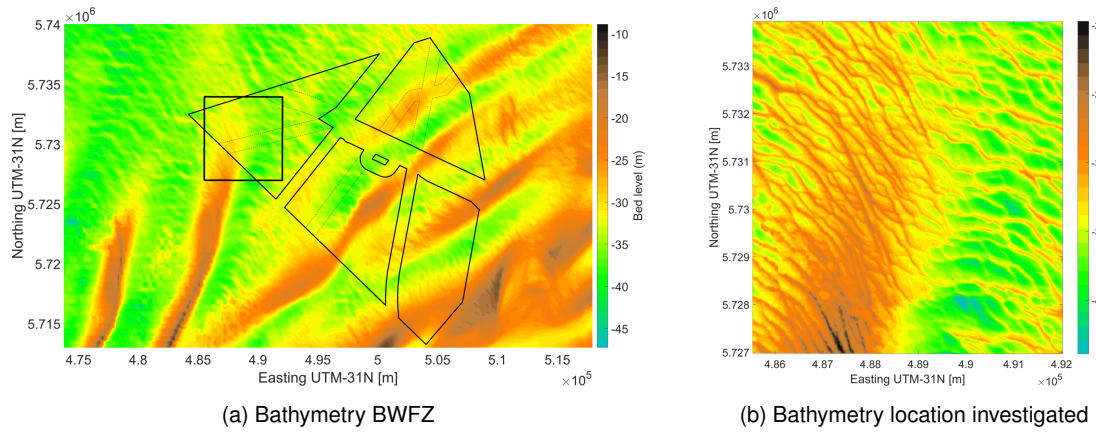


Figure D.1.: Overview grid bathymetry

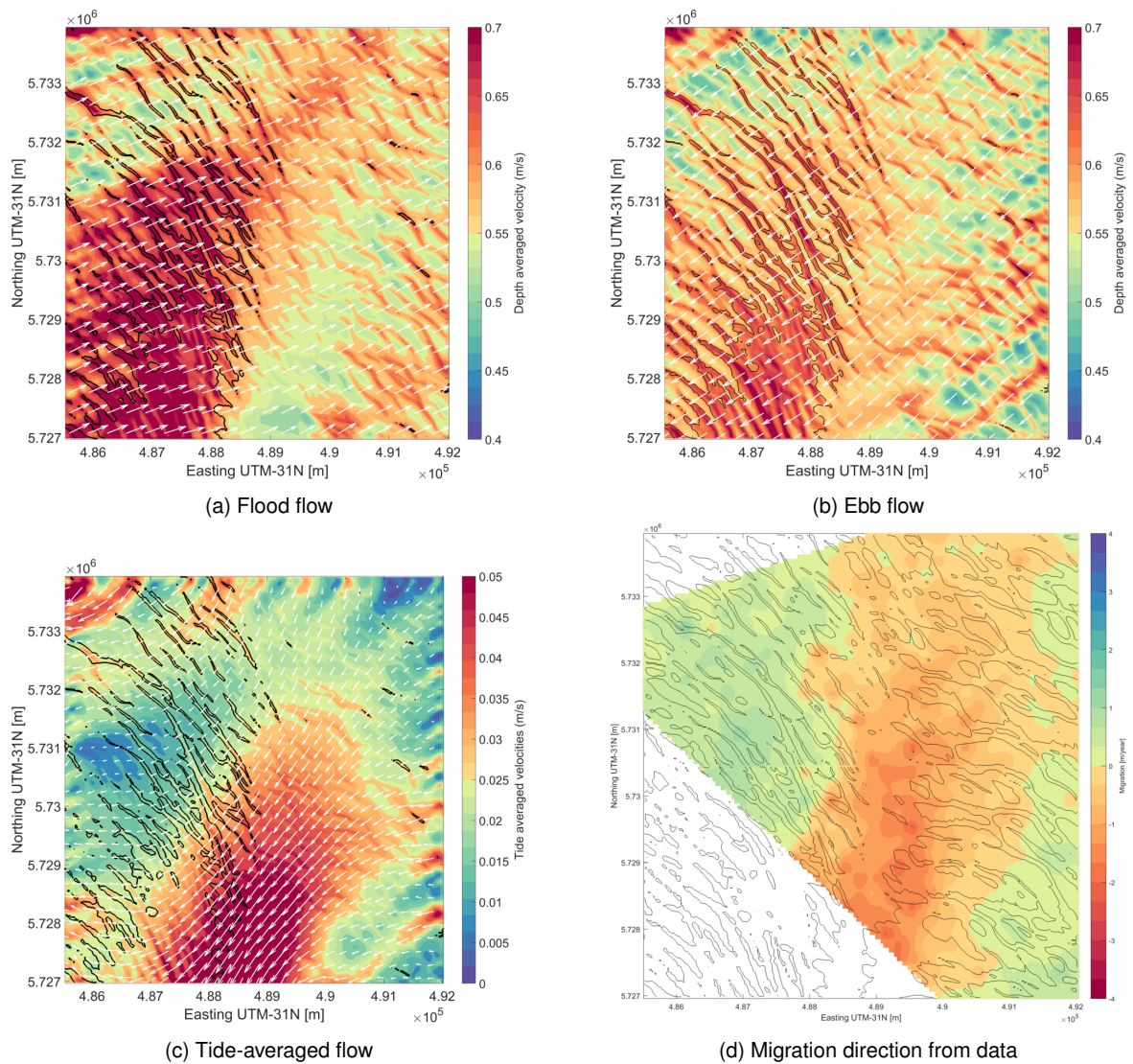
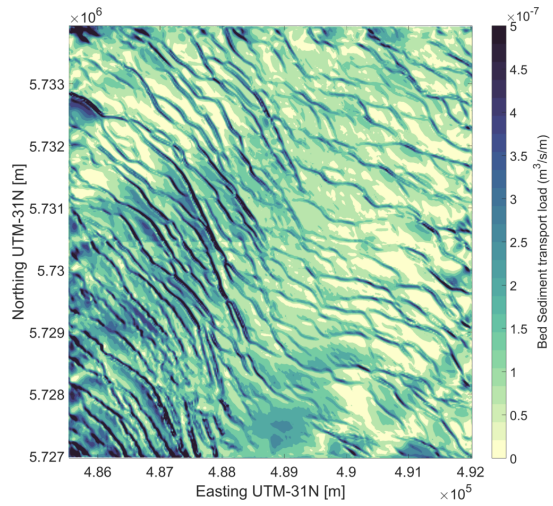
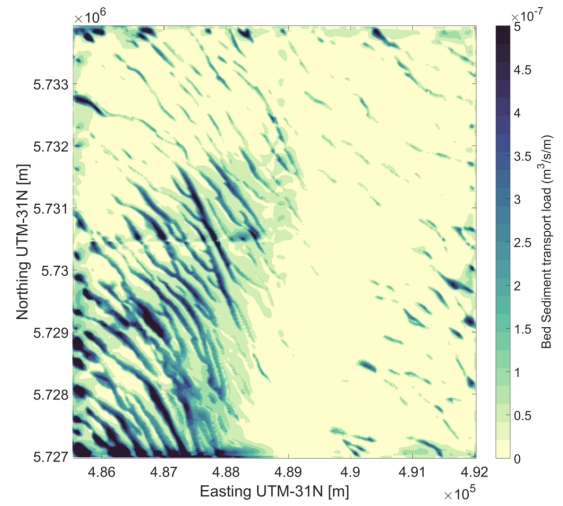


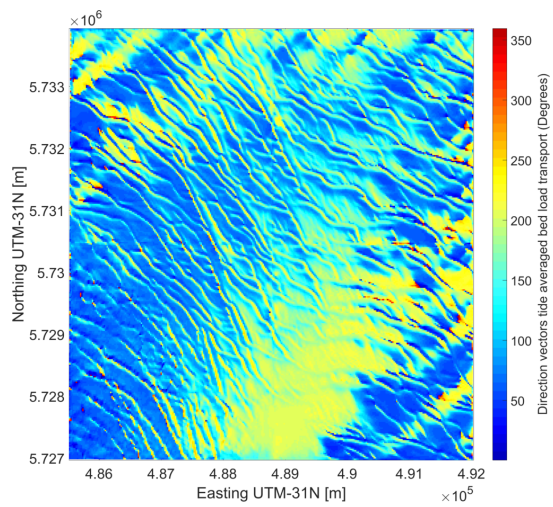
Figure D.2.: Hydrodynamic processes



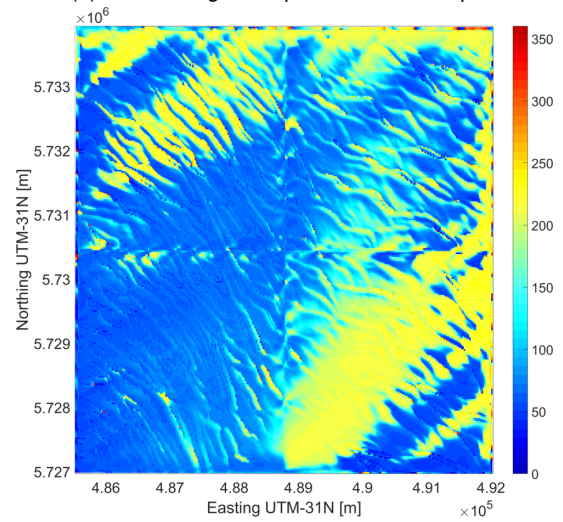
(a) Tide-averaged bed load transport



(b) Tide-averaged suspended load transport



(c) Vector directions bed load



(d) Vector direction suspended load

Figure D.3.: Sediment transport and direction

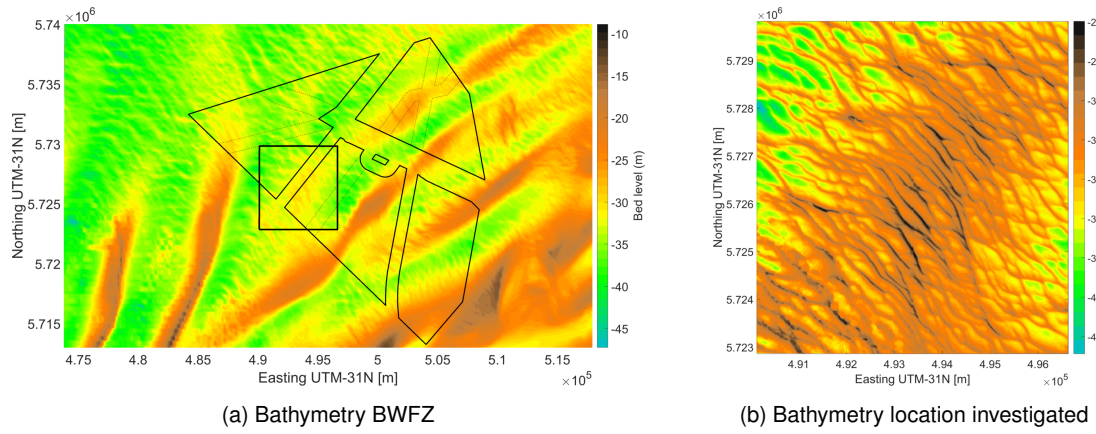


Figure D.4.: Overview grid bathymetry

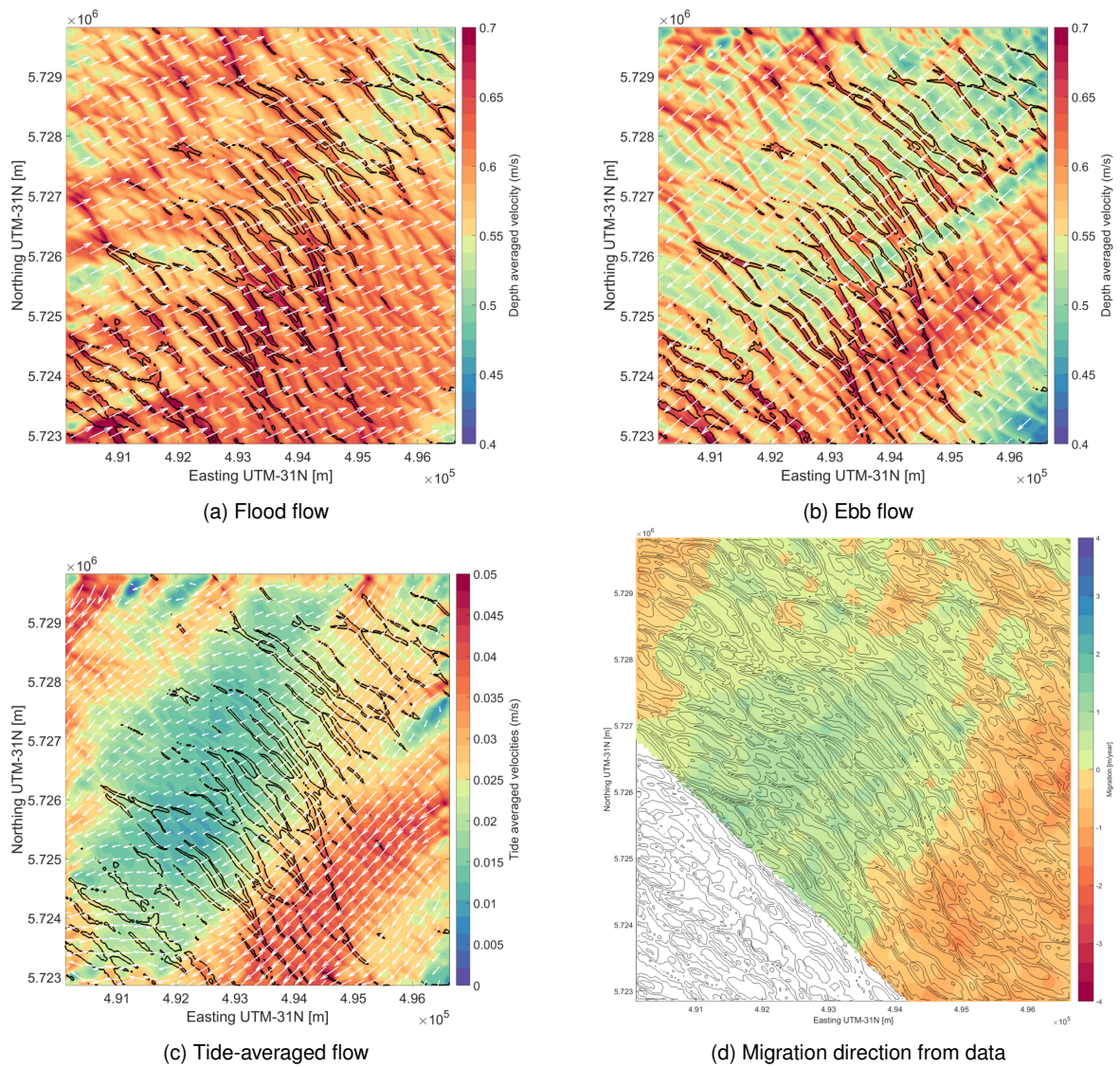
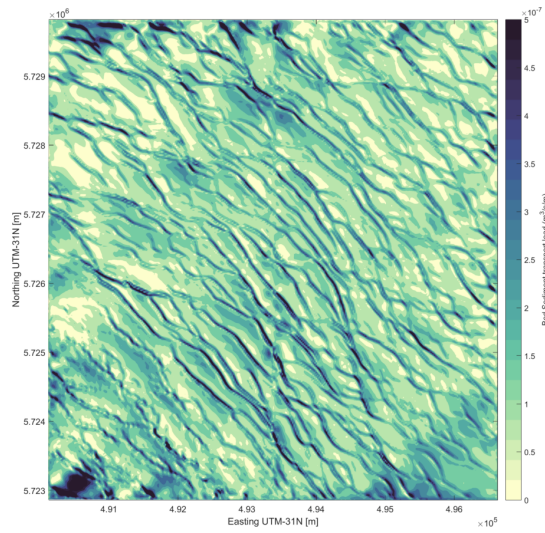
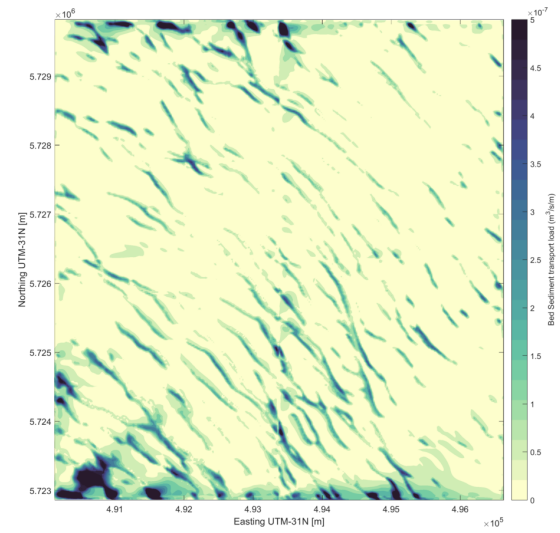


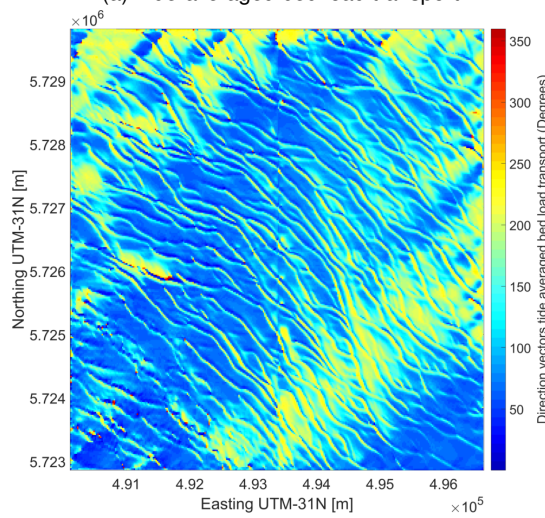
Figure D.5.: Hydrodynamic processes and data



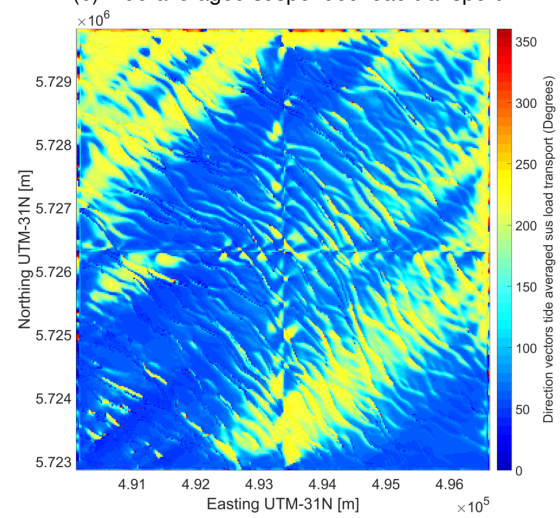
(a) Tide-averaged bed load transport



(b) Tide-averaged suspended load transport



(c) Vector directions bed load



(d) Vector direction suspended load

Figure D.6.: Sediment transport and direction

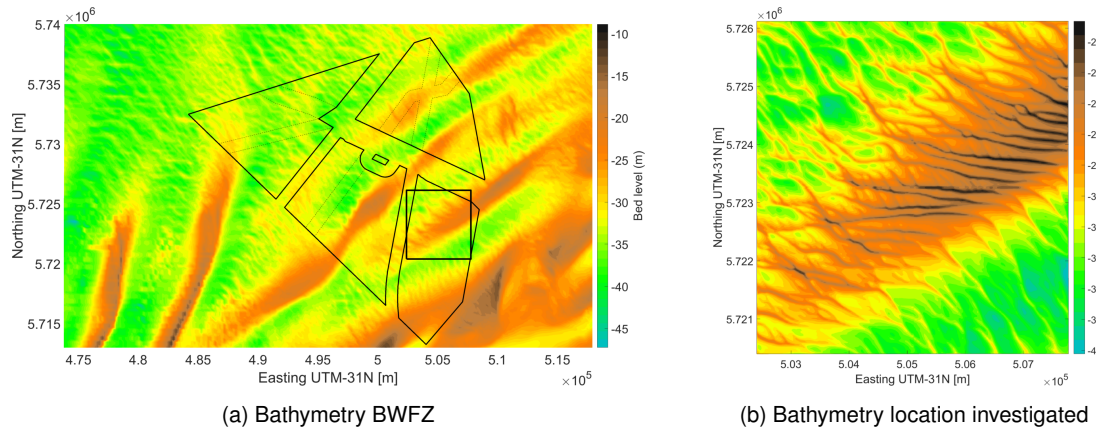


Figure D.7.: Overview grid bathymetry

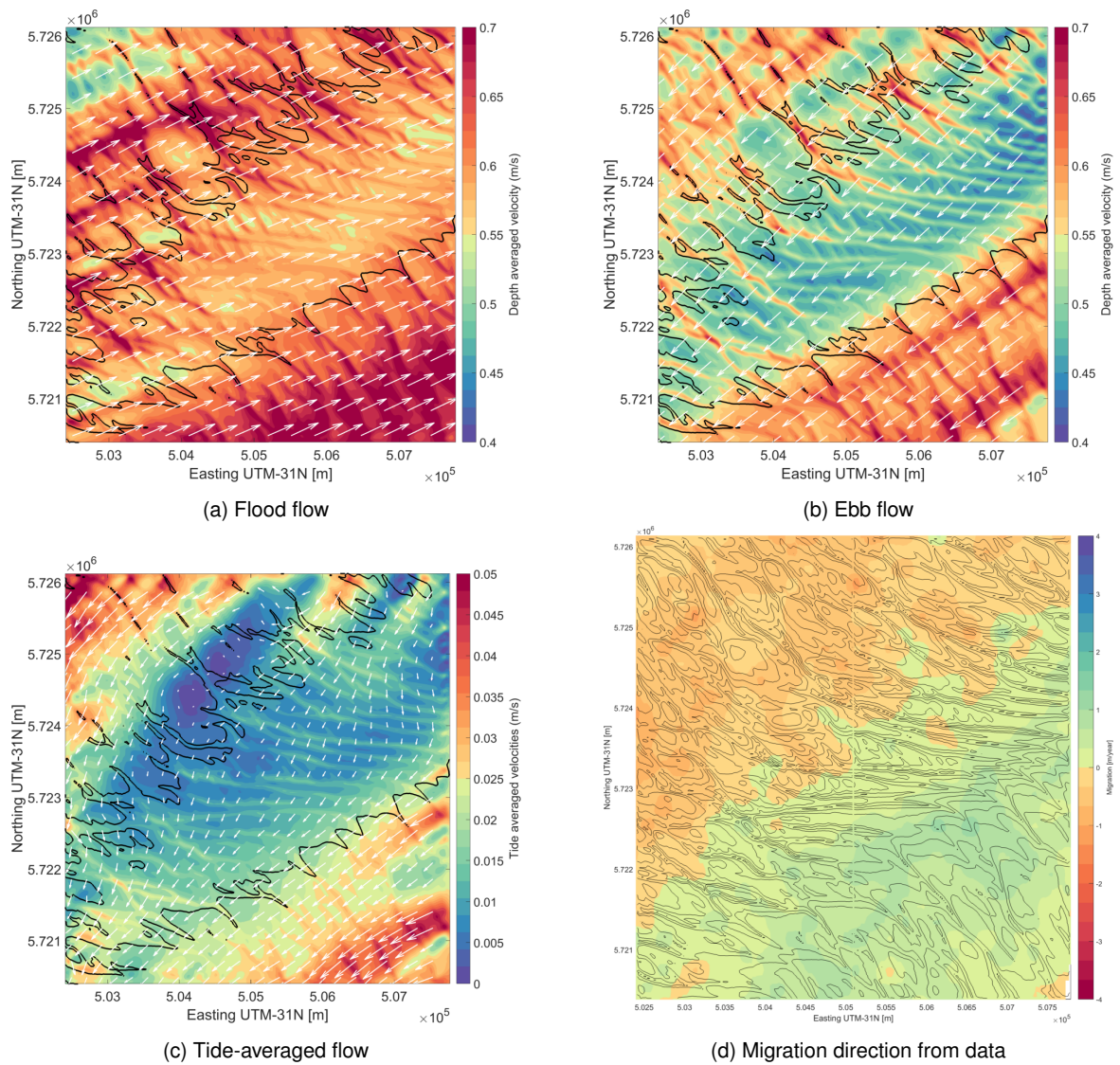
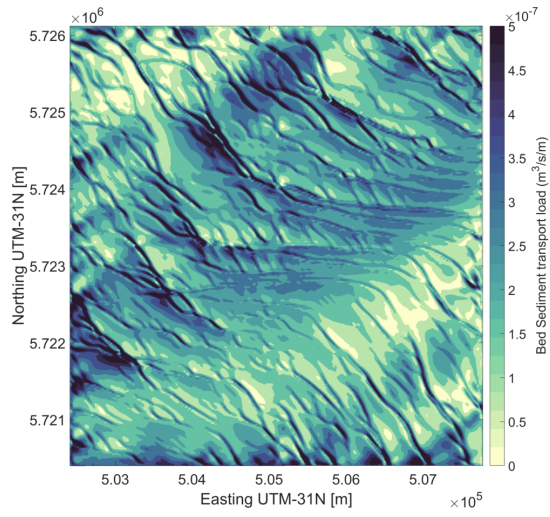
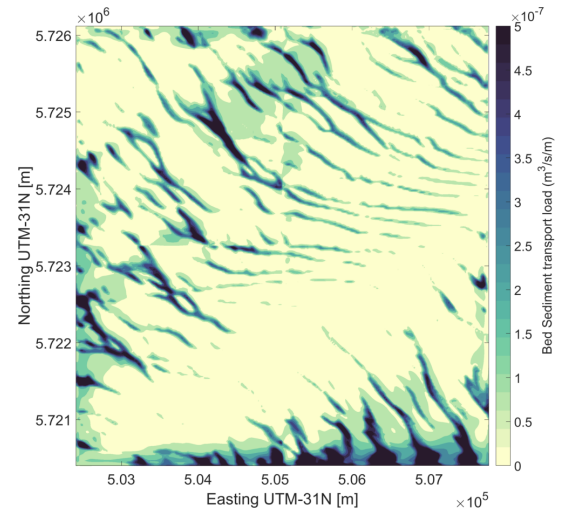


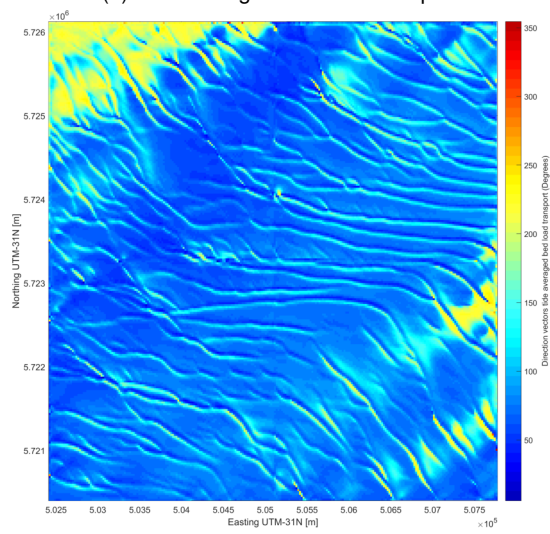
Figure D.8.: Hydrodynamic processes and data



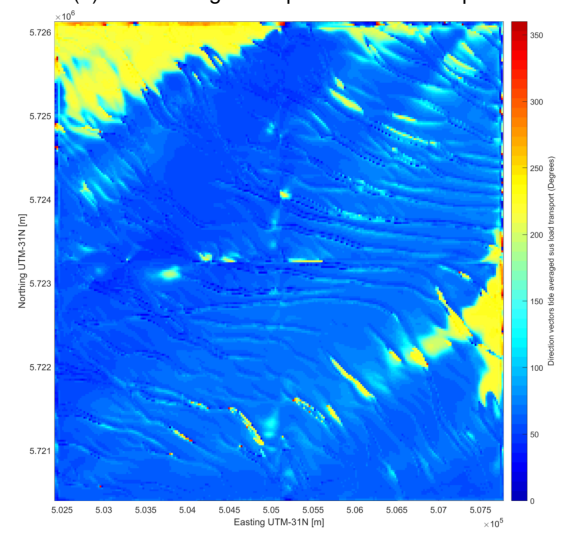
(a) Tide-averaged bed load transport



(b) Tide-averaged suspended load transport



(c) Vector directions bed load



(d) Vector direction suspended load

Figure D.9.: Sediment transport and direction

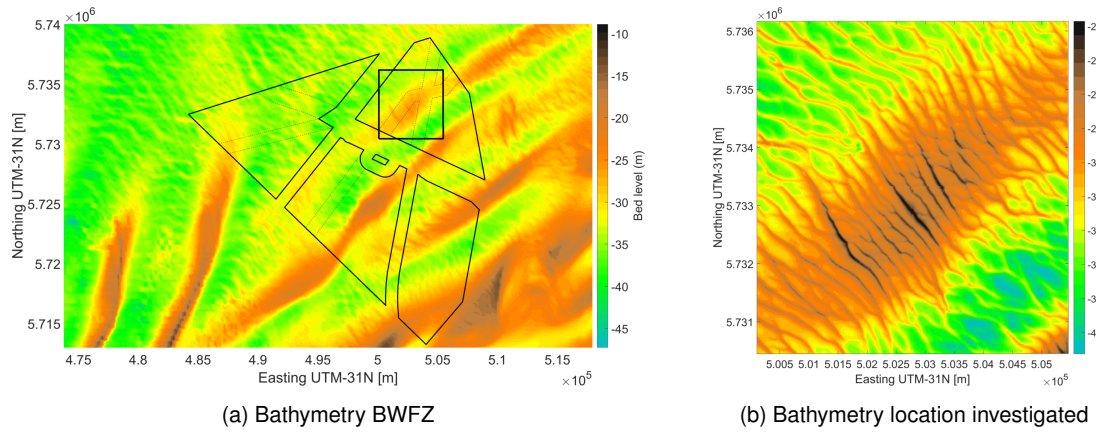


Figure D.10.: Overview grid bathymetry

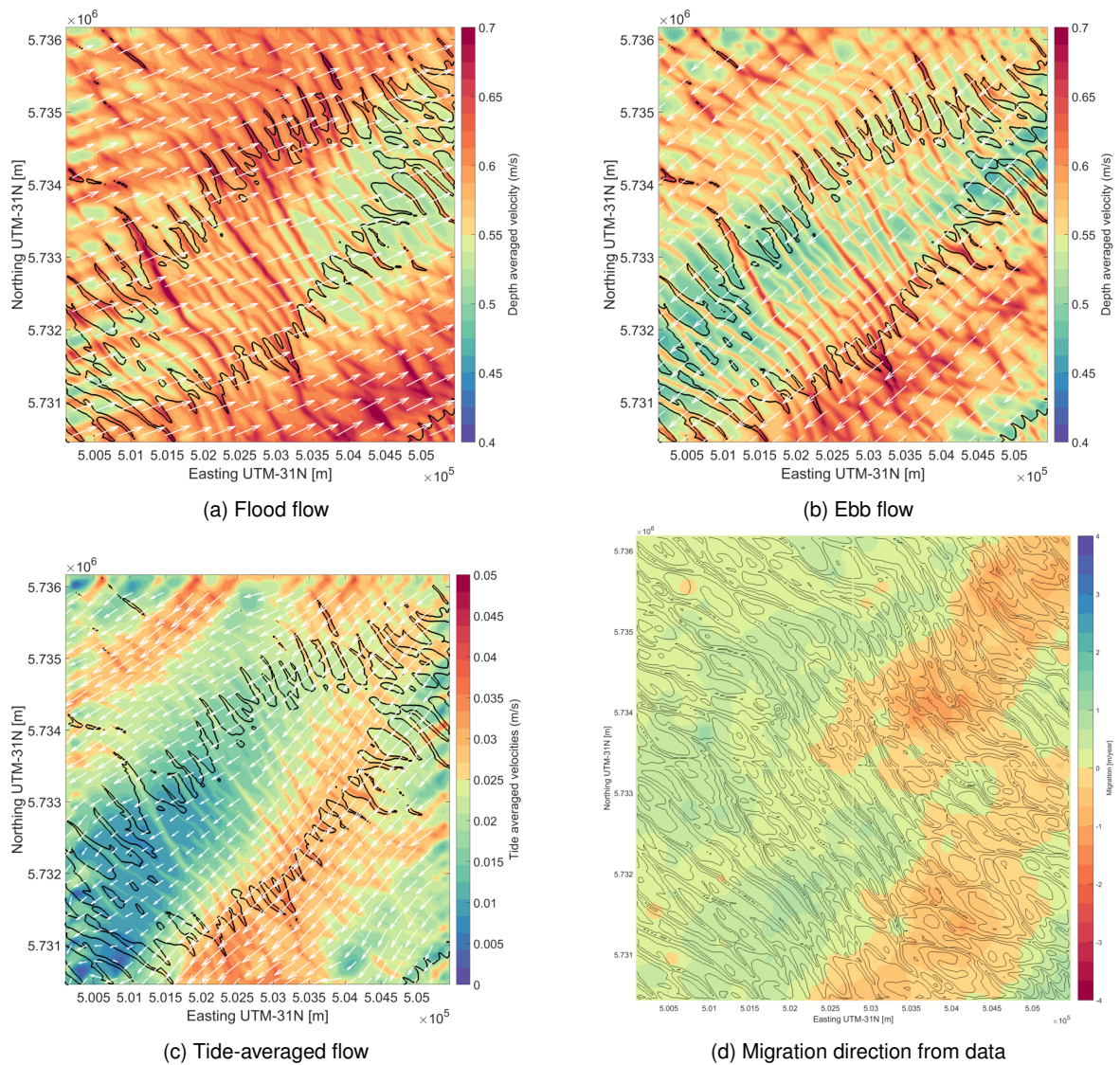
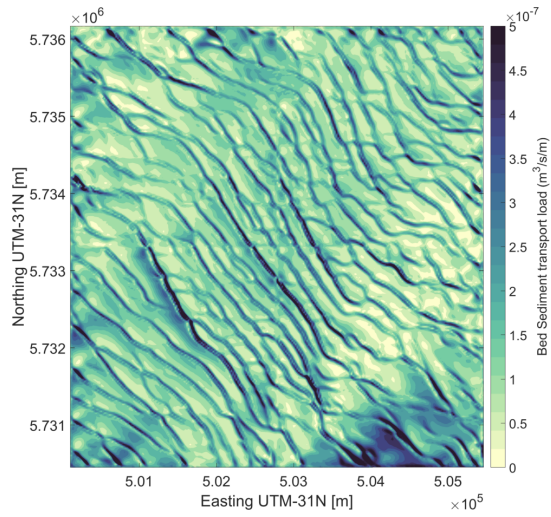
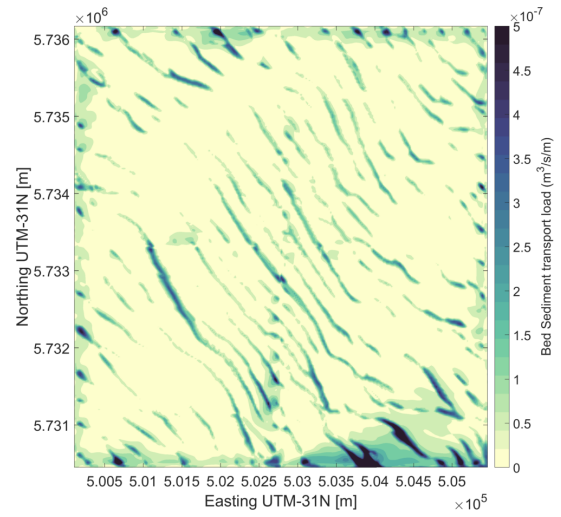


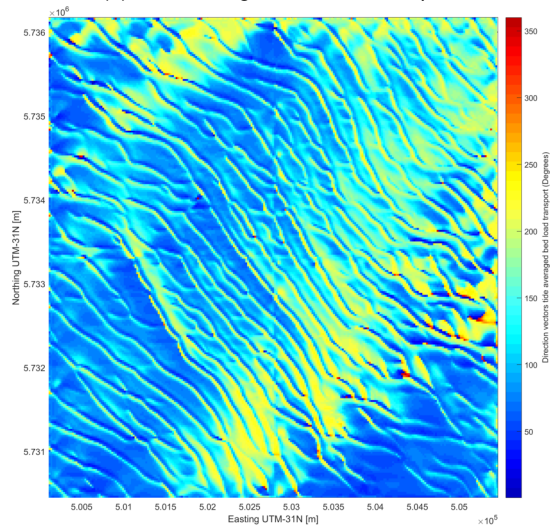
Figure D.11.: Hydrodynamic processes and data



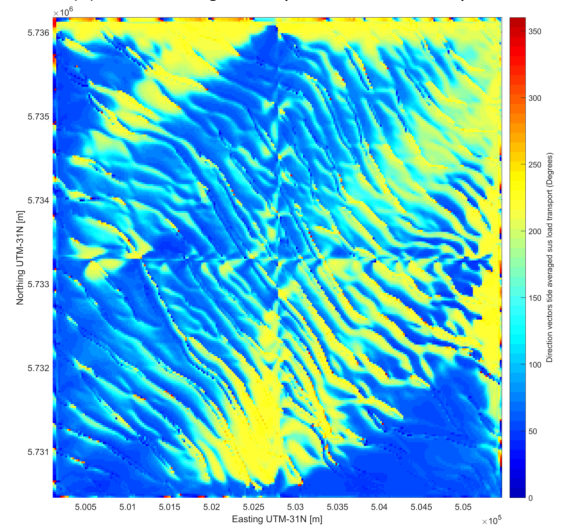
(a) Tide-averaged bed load transport



(b) Tide-averaged suspended load transport



(c) Vector directions bed load



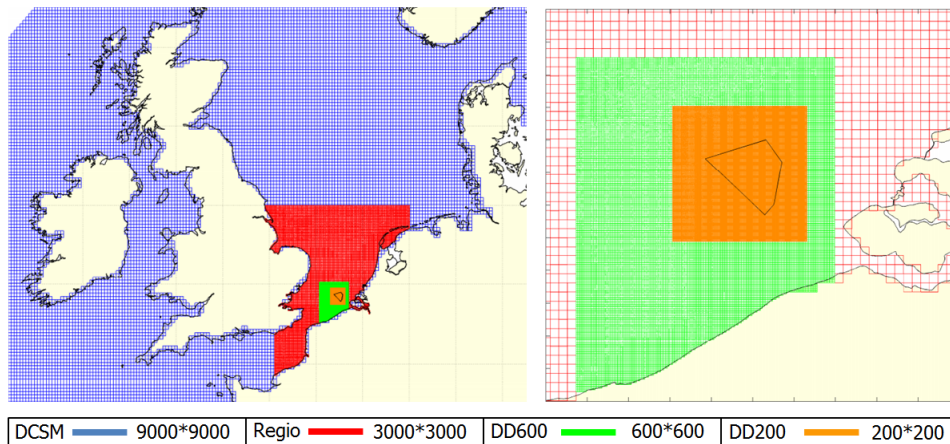
(d) Vector direction suspended load

Figure D.12.: Sediment transport and direction

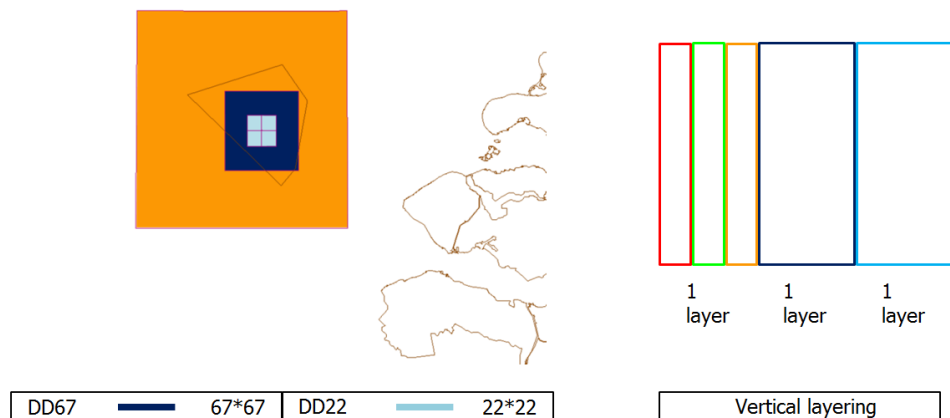
E | Domain decomposition model as engineering tool

DD model chapter 5, depth averaged

The horizontal model resolution and the area considered are the same as in chapter 5 (figs. E.1a and E.2). However, the model is run depth averaged in this case (fig. E.1b). The model show a comparable transition in tide-averaged sediment transports and directions and thereby the indicative migration direction over the tidal sand bank (fig. E.3). A depth averaged model configuration can therefore be set up to look at larger horizontal scales for new offshore wind farms. In this way a first indication of the possibility of transitions in migration directions can be made.



(a) Grid domains (name + resolution (m)) original model (Deltares, 2015b)



(b) Grid domains (name + resolution (m)) (left) and vertical resolution depth averaged model modification (right)

Figure E.1.: Overview grid domains depth averaged test

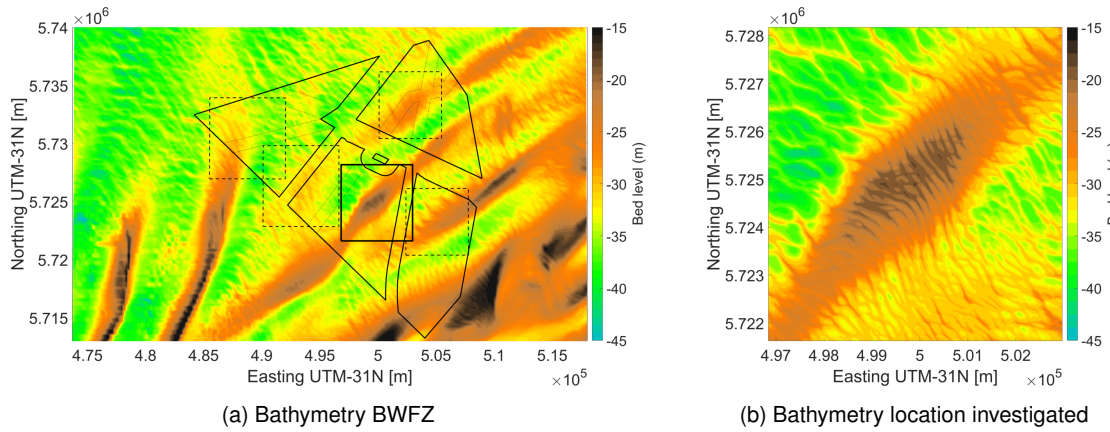


Figure E.2.: Overview bathymetry depth averaged test

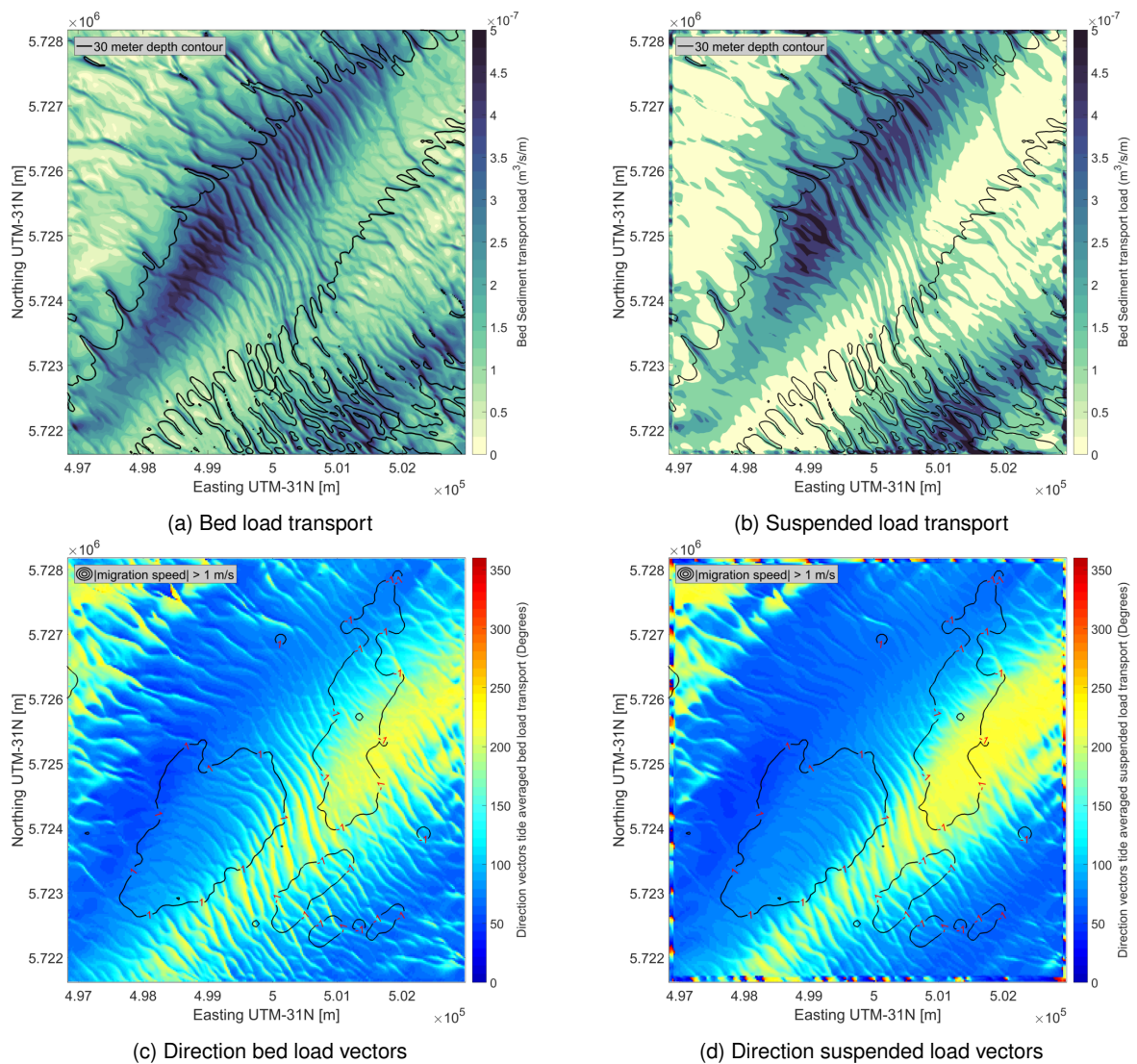


Figure E.3.: Sediment transport and direction